REFERENCE ONLY

UNIVERSITY OF LONDON THESIS

Degree PhD Year 2005 Name of Author CHADDERTON, R.T.

COPYRIGHT

This is a thesis accepted for a Higher Degree of the University of London. It is an unpublished typescript and the copyright is held by the author. All persons consulting the thesis must read and abide by the Copyright Declaration below.

COPYRIGHT DECLARATION

I recognise that the copyright of the above-described thesis rests with the author and that no quotation from it or information derived from it may be published without the prior written consent of the author.

LOANS

Theses may not be lent to individuals, but the Senate House Library may lend a copy to approved libraries within the United Kingdom, for consultation solely on the premises of those libraries. Application should be made to: Inter-Library Loans, Senate House Library, Senate House, Malet Street, London WC1E 7HU.

REPRODUCTION

University of London theses may not be reproduced without explicit written permission from the Senate House Library. Enquiries should be addressed to the Theses Section of the Library. Regulations concerning reproduction vary according to the date of acceptance of the thesis and are listed below as guidelines.

A. Before 1962. Permission granted only upon the prior written consent of the author. (The Senate House Library will provide addresses where possible).

B. 1962 - 1974. In many cases the author has agreed to permit copying upon completion of a Copyright Declaration.

C. 1975 - 1988. Most theses may be copied upon completion of a Copyright Declaration.

D. 1989 onwards. Most theses may be copied.

This thesis comes within category D.

☑ This copy has been deposited in the Library of UCL

☐ This copy has been deposited in the Senate House Library, Senate House, Malet Street, London WC1E 7HU.

SENSORY INTEGRATION IN SINGLE NEURONS OF THE CEREBELLAR CORTEX

Thesis submitted for the degree of
Doctor of Philosophy of London University

Paul Chadderton

Department of Physiology & Wolfson Institute for Biomedical Research

UNIVERSITY COLLEGE LONDON

2005

ProQuest LLC
789 East Eisenhower Parkway
P.O. Box 1346
Ann Arbor, MI 48106-1346

ABSTRACT

To understand the computations performed by the neurons within cortical structures it is essential to determine the relationship between sensory-evoked synaptic input and the resulting pattern of output spikes. In the cerebellum, granule cells constitute the input layer, translating mossy fibre signals into parallel fibre input to Purkinje cells. Until now their small size and dense packing have precluded recordings from individual granule cells *in vivo*. Here I use whole-cell patch-clamp recordings to show the relationship between mossy fibre synaptic currents evoked by somatosensory stimulation and the resulting granule cell output patterns. Granule cells exhibited low ongoing firing rates, due in part to dampening of excitability by a tonic inhibitory conductance mediated by γ-aminobutyric acid type A ($GABA_A$) receptors. Sensory stimulation produced bursts of mossy fibre excitatory postsynaptic currents that summate and trigger bursts of spikes. Remarkably, burst responses were evoked by only a few quantal excitatory postsynaptic currents. Recordings from putative mossy fibre terminals suggest that sensory-evoked granule cell spiking may result from high frequency activation of single mossy fibres. These results reveal that the input layer of the cerebellum balances exquisite sensitivity with a high signal-to-noise ratio. Granule cell bursts are optimally suited to trigger glutamate receptor activation and plasticity at downstream synapses, providing a link between input representation and memory storage in the cerebellum.

Purkinje cells integrate inputs from other neurons in the cerebellar cortex to provide the sole output of the cerebellar cortex. Using whole-cell and cell-attached recordings, I describe a profound and robust bistability of spike

output and membrane potential in these cells. Membrane potential toggles between a hyperpolarised down state and an active up state, in a complex spike-dependent manner. Sensory-evoked complex spikes reliably induced state transitions in both directions, indicating that bistability may be relevant for sensory processing in the cerebellum.

Acknowledgements

First of all, thanks to Mike Häusser, my boss, who has built an environment filled with brilliant people and state-of–the-art equipment. He has always been tolerant and supportive, and managed to push me to do things that I would never have done otherwise.

Troy Margrie taught me the all the technical and attitudinal skills necessary to do these experiments, and deserves special recognition for consistently getting me to work hard through a campaign of psychological and physical abuse.

Bartlett Mel, Mickey London, Arnd Roth and Julian Jack allowed me to pick up some important theoretical principles by osmosis.

Beverley Clark, Mark Farrant and Jonathan Ashmore have always been approachable and made me feel positive about my work.

Wolfgang Mittmann, Jenny Davie, Sévérine Mahon and Ede Rancz have kept me entertained with important arguments/discussions about neuroscience and celebrity gossip.

And everybody else...

Thank you!

CONTENTS

Chapter 1: INTRODUCTION

Neurons exist within sophisticated networks, receiving and providing numerous and diverse connections with other neurons. If we are to understand how the nervous system performs its functions, it is necessary to determine the role performed by individual neurons within their networks. With recent technical advances, it has become possible to address this issue. In the cerebellar cortex, the connectivity of the neural circuit has been established for almost 50 years. However, the computations performed by neurons within the cerebellar cortex are largely unknown. In this thesis, I will describe observations made from the study of single cells within the cerebellum *in vivo*. By studying the signals received and generated within different components of the cerebellar cortex, it has been possible to gain insight into the function of the network as a whole.

1.1 SENSORY PROCESSING

The nervous system affords a means by which organisms can detect and respond to changes in the physical world. Specially tailored sensory organs extract information about the surrounding environment. The sensors contained within these organs often operate at the physical limits of detection (Shepherd & Corey, 1992), thus providing the nervous system with detailed sensory information. This information is subsequently processed in such a way as to produce or modulate motor behaviour. Thus, the elementary task of the nervous system is simple – to drive movement. However, the means by

which sensory information is transformed to achieve this task is yet to be established.

1.1.1 General principles

Signals collected at the periphery are processed as they move through the nervous system. Many of the principles thought to underlie sensory processing were first revealed through the groundbreaking work by Hubel and Wiesel. They made microelectrode recordings of neuronal activity from various neural structures involved in visual processing in the cat, using visual stimuli to characterise the receptive fields of neurons in different areas of the brain (Hubel & Wiesel, 1959, 1962). A hierarchical organisation was revealed in visual processing, where neurons at each successive stage of sensory processing respond to increasingly precise and abstract stimulus features. In the case of visual stimuli, neurons from the retina and lateral geniculate nucleus exhibit simple centre-surround on-off receptive fields. Within visual cortex, receptive fields become larger, corresponding to specific features of orientation and direction. This increasing complexity is thought to result from the interaction feed-forward and recurrent connections between neurons within different cortical layers.

A further feature of sensory processing in many brain regions is its precise spatial organisation. Neural representation of parts of the body is such that the surfaces with the smallest receptive fields are highly over-represented. However, the spatial arrangements of receptive fields with respect to each other are preserved as a precise somatotopic representation.

This is beautifully demonstrated in the rodent whisker system: characteristic groups of neurons cluster to form cylinders that lie perpendicularly within the cortex. These clusters, termed barrels due to their shape, are consistently organised within five rows. These rows correspond exactly with the rows of whiskers on the face (Woolsey & Van der Loos, 1970). Electrical recordings from neurons within individual barrels confirm that these barrels functionally segregate inputs from each whisker, whilst the spatial layout of the whisker pad is maintained (Welker, 1976; Simons & Woolsey, 1979; Brecht & Sakmann, 2002). Across all sensory modalities, receptive fields are organised in this manner: primary visual cortex is arranged retinotopically, whilst primary auditory cortex has a tonotopic distribution. Primary motor cortex shows a similar spatial organisation. It is important to highlight, however, that such precise topographic organisation is less prevalent in the cerebellar cortex, and is less commonly observed in non-primary sensory areas of the cerebral cortex. The significance of cerebellar 'fractured' topography will be discussed in detail later.

Spatial organisation within cortical areas is also found in the radial axis. Both the neocortex and the cerebellum possess a columnar organisation. Microelectrode penetrations perpendicular to the neocortical surface have revealed that neurons share many of their receptive field properties with other neurons above and below in the same track. This was first found to be the case in primary somatosensory cortex, where, in one example, all the neurons encountered in one penetration are driven by light touch applied to the same small area of skin (Powell & Mountcastle, 1959). The same principle has been found to hold for orientation selectivity in visual cortex (Hubel & Wiesel, 1962),

and frequency-selectivity in auditory cortex (Redies *et al.*, 1989). More recently, and perhaps surprisingly, vertical organisation of tactile receptive fields has been demonstrated in the cerebellar cortex (Bower & Woolston, 1983).

1.1.2 Patterns of neural activity

The question of how features from the outside world are represented within neural networks remains a major source of contention. At the simplest level, that of a single neuron, changes in firing rate are commonly observed following the presentation of salient stimuli (Rieke *et al.*, 1997). Stimulus presentation can cause both transient and prolonged changes in neuronal firing rates. However, a frequently observed property of neuronal receptive fields, particularly at higher levels of processing, is that they tend to be rather broadly tuned, favouring responses to a range of stimuli. Secondly, stimulus-evoked spiking responses show a high degree of trial-to-trial variability (Rieke *et al.*, 1997). Together, these findings strongly indicate that single neurons, particularly at early stages of cortical processing, may only provide very general information about a stimulus. As a result, one commonly held assumption is that the neural representation of a particular stimulus involves the graded responses across a population of neurons. A single neuron is considered an 'ambiguous' descriptor, and therefore it is only the presence of very many neurons with overlapping receptive fields that enables the extraction of unambiguous details about a stimulus.

However, under these proposals, a problem arises when different stimuli evoke graded responses in overlapping groups of neurons. Of the many simultaneous neuronal firing patterns occurring in response to the sensory environment, those evoked by one particular stimulus or feature need to be distinguished and evaluated together to avoid interference with responses elicited by neighbouring features. This has been referred to as a 'binding problem' (Singer & Gray, 1995). One proposed remedy to this problem relies upon the convergence of inputs from one layer of sensory processing onto neurons of a subsequent layer (Shadlen & Newsome, 1994, 1998). The activity of a group of cells would then represent either elementary features or, at higher levels of processing, a particular set of elementary features. By introducing further stages of convergence, it might be expected that neurons could be created that would respond selectively to only single perceptual objects.

As described, evidence exists that suggests that such convergence is exploited by the nervous system to extract complex and abstract features about a stimulus (Hubel & Wiesel, 1962). However, such a scheme has several disadvantages. In particular, the number of units required to implement convergence-binding scales very unfavourably with the number of distinct patterns that can be represented. Ultimately, one cell is required for every distinguishable feature, higher-order combination, and perceptual object (Singer & Gray, 1995).

An alternative proposal has been put forward, whereby the features of a stimulus are represented by joint, synchronous activity amongst neuronal populations. Such 'assembly coding', first set down by Hebb (Hebb, 1949),

enables individual neurons to participate at different times in the representation of different patterns. Specifically, a stimulus would be represented by highly synchronised firing across a diverse population of neurons, representing the full range of features corresponding to the stimulus (Singer, 1999). Thus, it has been proposed that neuronal synchronisation may occur both locally and between spatially segregated areas of the nervous system. The use of such a scheme would be expected to substantially reduce the number of cells necessary to represent different objects.

In order to provide support for the use of 'temporal binding' during stimulus representation, experimenters have sought to find examples of transient synchronisations within neuronal populations during sensory or motor behaviour. Oscillatory field activity has been observed in many different brain areas, including the neocortex (Gray *et al.*, 1989), hippocampus (Buzsaki, 2002) and cerebellum (Adrian, 1935; Hartmann & Bower, 1998), suggesting that activity within networks can become synchronised. Unit recordings have also revealed transient increases in neuronal synchrony, both spontaneously (Harris *et al.*, 2003), during sensory stimulation (Gray *et al.*, 1989; Lampl *et al.*, 1999), and behaviour (Riehle *et al.*, 1997). It has also been reported that synchronisation if firing in sensory cortex can be modulated by attention (Steinmetz *et al.*, 2000). However, in most cases, synchrony has only been observed between small numbers of units, and is often also associated with a pure change in firing rate (Riehle *et al.*, 1997), which would be expected to increase the likelihood synchrony occurring by chance. Therefore, strong support for precise temporal synchronisation is likely to

require the study of the activity of much greater numbers of neurons simultaneously.

1.2 TECHNIQUES FOR RECORDING NEURONAL ACTIVITY

In order to understand the various aspects of brain function, it is necessary to monitor neuronal activity. Especially important is the need to study this activity within intact networks, in the presence of physiological stimuli, and during behaviour. Several techniques exist to assay neural activity, although each has its limitations. The oldest recording method is the electroencephalogram (EEG), in which voltages are recorded from an electrode placed on the surface of the brain. The EEG signal is derived from the activity of many millions of neurons, and is thus extremely difficult to analyse and interpret. More recently, techniques have been developed that allow more localised studies of neuronal activity to be performed.

1.2.1 Local field potential (LFP) and multiunit recordings

The electrical fields produced during neural activity can be very effectively recorded through the use of low-impedance microelectrodes or pipettes. Low frequency signals (typically 1-50 Hz; Castro-Alamancos, 2004) recorded in this manner constitute the LFP. It is widely accepted that the major component of the LFP results from potential changes in the dendrites and soma of neurons, and is thus likely to primarily represent synaptic activity (Ketchum & Haberly, 1993). The LFP has therefore been used to assay the

synaptic response across populations of neurons. For example, whisker stimulation evokes large negative LFP deflections within S1 of somatosensory cortex and Crus I/II of the cerebellum in both anaesthetised and awake rats (Shambes *et al.*, 1978b; Castro-Alamancos, 2004). However, the precise spatial origins of this signal are poorly established, and the contribution of single neurons to the signal cannot be determined.

Higher frequency microelectrode signals (typically 300-3000 Hz; Castro-Alamancos, 2004) constitute the multiunit response. Such signals are presumed to arise mainly from action potential activity in the region of the electrode, typically within a radius of a few hundred microns (Shoham & Nagaran, 2004). Again, it is not possible to determine the contribution of single neurons to such a signal, but multiunit activity does provide an index of population spiking activity and can also provide information concerning the degree of synchrony within neuronal populations (Castro-Alamancos, 2004).

1.2.2 Extra- and intracellular unit recordings

The spiking activity of individual neurons *in vivo* can be observed with the use of extra- and intracellular microelectrodes. An enormous amount of data has been collected using extracellular unit recordings. However, this technique suffers from two major sources of sampling bias in the determination of single cell firing rates. Firstly, since spiking is required in order to 'see' a neuron, there exists a strong recording bias towards neurons showing high spontaneous firing rates. In contrast, neurons that are silent, or active only at very low rates can easily be missed. Secondly, it is not possible

to unequivocally isolate single units with single electrodes. It is always highly possible that signals detected via extracellular electrodes constitute the summed spiking activity of several different neurons. Although several methods have been developed to sort neuronal responses on the basis of spike shape, it remains impossible to rule out the contamination of single unit recordings by neighbouring activity.

The use of multiple extracellular electrodes in close proximity has proved to be a more effective method of isolating extracellular unit activity. By correlating spike timing and waveform at multiple recordings sites, it is possible to effectively discriminate single units, particularly if spike rates are relatively low and long stretches of data can be acquired (O'Keefe & Recce, 1993; Wilson & McNaughton, 1993). Typically, a silicon 'tetrode' consists of four insulated recording sites, separated from each other by less than 50 μm.

Sharp microelectrodes have been successfully used to record intracellularly *in vivo* (Eccles *et al.*, 1967a), and have the advantage of unequivocally isolating single units. However, intracellular recordings cannot be easily applied to smaller neurons, such as interneurons.

1.2.3 Whole-cell and cell-attached patch clamp recordings

Most recently, the patch-clamp technique has been very successfully applied in the study of neuronal activity *in vivo*. Patch clamping, developed by Bert Sakmann and Erwin Neher (Neher & Sakmann, 1992), has proved to be an extremely versatile method, with a broad range of applications. Individual cells are 'sucked' onto the end of a small glass pipette, producing a very high

resistance seal onto a small area of cell membrane. Whilst attached to a neuronal membrane, single-cell spiking activity is very effectively isolated due to the high resistance of the gigaohm seal – thus 'cell-attached' patch clamp recordings afford a non-invasive means of unambiguously sampling the activity of single neurons.

Following seal formation, further suction can be applied to rupture the area of cell membrane and gain intracellular access to the neuron. It is possible to obtain very low resistances (less than 10 MΩ) between patch pipette and neuron, allowing both voltage and current to be reliably recorded and manipulated via the patch pipette. 'Whole-cell' patch clamp recordings thus reveal information about both spiking activity, i.e. neuronal 'output', and the subthreshold changes in membrane potential underlying this output. By applying this technique to neurons *in vivo*, it is possible to unequivocally study physiological patterns of spike output and synaptic input in individual neurons (Pei *et al.*, 1991; Jagadeesh *et al.*, 1992; Margrie *et al.*, 2002). This method has also been found to be suitable for recording from small cell types, such as interneurons (Margrie *et al.*, 2003), and delicate structures such as distal dendrites (Larkum & Zhu, 2002). Whole-cell and cell-attached patch clamp recordings have begun to reveal much about the contribution played by individual neurons within intact network (Jagadeesh *et al.*, 1992; Brecht *et al.*, 2004).

1.2.4 Imaging neural activity

Imaging is an additional, relatively non-invasive means by which neural activity can be monitored. Observing changes in the intrinsic fluorescence signal across a small area of brain is one such approach (Schuett *et al.*, 2002). Alternatively, dyes sensitive to voltage or concentrations of particular ions, e.g. Ca^{2+}, can be loaded into individual neurons by means of a patch pipette, or 'bulk-loaded' into many cells using membrane-permeant dyes (Stosiek *et al.*, 2003). Additionally, several means exist by which to incorporate genetically-encoded fluorescent markers, e.g. green fluorescent protein (GFP), into small numbers of neurons. Two-photon imaging now allows excellent spatial and temporal imaging of neurons at considerable depths (up to 500 μm) within the intact brain (Denk *et al.*, 1994; Helmchen *et al.*, 2001). Many of the electrophysiological methods described above can be combined with imaging to provide additional information about activity within neuronal populations, or single neurons (Grutzendler *et al.*, 2002; Trachtenberg *et al.*, 2002; Waters *et al.*, 2003). Furthermore, following the labelling of sparse cell types with GFP, two-photon imaging can be combined with patch clamp to perform 'targeted' recordings from cells that would otherwise be impossible to locate (Margrie *et al.*, 2003).

1.3 SYNAPTIC INTEGRATION

Despite coming in a wide variety of shapes and sizes, all neurons share certain characteristic properties. Synaptic inputs from other neurons are generally made onto the dendritic tree. The axon, which extends from the soma, makes synaptic contact upon other neurons. Like all cells, neurons possess a resting membrane potential, established by active ion pumps within a selectively permeable lipid bilayer. A resting leak of potassium predominates, hyperpolarizing the cell membrane to around –70 mV. A defining feature of almost all neurons is the ability to generate fast stereotyped fluctuations in their membrane potential: action potentials. Action potentials are the only signals to be transmitted down the axon, triggering synaptic release onto postsynaptic neurons. Thus action potentials represent neuronal output. The seminal work of Hodgkin, Huxley and Katz (Hodgkin & Huxley, 1939; Hodgkin & Katz, 1949; Hodgkin & Huxley, 1952) isolated the ionic currents underlying the action potential: voltage-sensitive Na and K currents that depolarise and hyperpolarize the cell membrane in rapid succession. A fundamental property of the action potential is its fixed voltage threshold. When membrane potential is sufficiently depolarised, typically at around –40 mV, regenerative activation of voltage-sensitive currents will trigger an action potential in an all-or-none manner. Since resting membrane potential usually lies below threshold, depolarisation is therefore necessary to generate neuronal output.

Depolarisation can arise from the activation of excitatory synaptic inputs. Fast excitatory synaptic transmission, which, across the central

nervous system, is mediated primarily via glutamate receptor activation, opens a mixed cation conductance which has a reversal potential of 0 mV (Hille, 1992). The reversal potential is defined as the potential at which the net flow of a particular current is zero; an increase in the conductance underlying a given current will move membrane potential closer to that reversal potential. Therefore, sufficient activation of excitatory synaptic conductances will push membrane potential above threshold, generating output in the form of action potentials. Conversely, inhibitory synaptic transmission opens conductances that reverse at membrane potentials more hyperpolarised than threshold. Thus, activation of inhibitory synapses reduces the likelihood of action potential generation. The process by which excitatory and inhibitory synaptic input shapes action potential firing is termed *synaptic integration.*

1.3.1 Synaptic transmission

Communication between neurons occurs primarily via chemical synaptic transmission. Many of the principles of synaptic transmission were established following the work of Bernard Katz and colleagues on the neuromuscular junction. Stimulation of presynaptic axons was found to evoke depolarising potentials within postsynaptic cells. These potentials, originally referred to as endplate potentials (EPPs) in muscle fibres, occur with a small delay (up to a millisecond) following presynaptic stimulation. EPPs, and in neurons, EPSPs, typically rise and decay more slowly than action potentials.

Although electrical stimulation at the neuromuscular junction produces a very large EPP, Fatt and Katz (Fatt & Katz, 1951) also observed small,

spontaneous depolarising potentials in the absence of stimulation. These spontaneous potentials resemble miniature versions of the EPP in their time course and their response to cholinesterase inhibitors, and were therefore named miniature EPPs (mEPPs). It was found that whereas evoked EPP amplitudes showed a strong dependence on external [Ca^{2+}], mEPP amplitude did not fluctuate under such conditions. Further experiments revealed that with sufficiently low Ca^{2+} levels, the evoked EPP became no larger than the size of a mEPP. Under these conditions, successive stimulation of the motor nerve evoked, in a random fashion, EPPs that varied in a stepwise manner, so that each EPP was an integral multiple of a mEPP (Del Castillo & Katz, 1954). Thus, it was concluded that an evoked EPP is composed of an integral number of miniature units – the all-or-none qualities of these units led them to termed *quanta*.

Around the same time, synaptic vesicles were discovered via electron microscopy (Palay & Palade, 1955), and the two findings were unified to form the vesicle hypothesis of chemical synaptic transmission. Briefly, vesicles containing neurotransmitter sit close to the presynaptic membrane – a 'readily-releasable pool' of quanta. Action potential-mediated depolarisation produces Ca^{2+} influx via voltage-gated channels, causing vesicles to fuse with the presynaptic membrane, releasing neurotransmitter in the synaptic cleft. Following diffusion across the synaptic cleft, neurotransmitter activates conductances on the postsynaptic membrane by binding to ligand-gated postsynaptic channels. Using the vesicle hypothesis, it has been possible to define certain parameters that shape the postsynaptic response following synaptic transmission. The release of quanta is probabilistic, thus the exact

number of quanta released by any given nerve impulse fluctuates in a random fashion that can only be described in statistical terms. del Castillo and Katz (Del Castillo & Katz, 1954) expressed this as follows: presynaptic terminals consist of a certain number of active zones (*N*), each of which will release quanta in response to an action potential with a probability (*p*). These two parameters are defined by properties of the presynaptic terminal. Together with a third parameter, the quantal amplitude, *q*, the postsynaptic response to a presynaptic impulse can be described: $p \times N \times q$.

Recordings from neurons in the central nervous system have shown that the quantal amplitude, *q*, varies considerably in amplitude from one trial to the next (Bekkers & Stevens, 1989). Release probability is highly dependent upon $[Ca^{2+}]_i$ (Katz & Miledi, 1965), and averages about 0.3 for synapses in hippocampal slices (Hessler *et al.*, 1993), although it is worth noting that the method these authors employed to estimate release probability – monitoring the decrement of NMDA currents in the presence of use-dependent blocker, MK-801 – is open to bias as very low *p* synapses will not be sampled. Changes in *p* and *q* both constitute common ways in which synaptic strength is regulated (Regehr & Stevens, 2001).

1.3.1.1 Postsynaptic receptors

Synaptic transmission generates current flow at the postsynaptic membrane. These are termed excitatory postsynaptic currents (EPSCs) and inhibitory postsynaptic currents (IPSCs) respectively. In central neurons, fast excitatory neurotransmission is mediated primarily by glutamate release

activating NMDA- and non-NMDA receptors (AMPA and kainate receptors). The initial component of an EPSC - the first few milliseconds - is dominated by non-NMDA receptor-mediated currents. Several factors contribute to the time course of EPSCs including the time course of the concentration of transmitter in the synaptic cleft and the kinetic properties of the postsynaptic receptors. As a result, EPSCs typically show a rapid exponential rising phase ($\tau \approx 100$ μs), and a slower multi-exponential decay. At the activated synapse, the rising phase of the corresponding EPSP shows a similarly fast rise time, dominated by the time course of the activated synaptic conductance. The EPSP decay is slower, shaped largely by the membrane time constant, τ_m. (Hille, 1992)

NMDA currents have much slower rise and decay times and proportionally contribute most of their charge during the EPSC decay. In addition, NMDA receptors have a number of interesting characteristics. In particular, Mg^{2+} ions plug the receptor in a voltage-dependent manner (Mayer *et al.*, 1984; Johnson & Ascher, 1990). Therefore, in order to activate NMDA receptors, depolarisation of the postsynaptic membrane is required. They are also permeable to Ca^{2+} ions (MacDermott *et al.*, 1986). These properties provide a mechanism by which synapses can detect coincident activation of pre- and postsynaptic neurons, and NMDA receptor-dependent Ca^{2+} influx has been shown to play a key role in many forms of synaptic plasticity (Rauschecker, 1991).

1.3.1.2 Synaptic dynamics

At many synapses, when two action potentials depolarise a presynaptic bouton in rapid succession, the second action potential often generates an EPSC of different amplitude to the first. This change can occur as an enhancement (short-term facilitation), or a reduction (short-term depression). Short-term facilitation results from a transient increase in the probability of transmitter release. It is thought that residual presynaptic Ca^{2+}, left over from the preceding action potential, is responsible for the increase in release probability. As a result, EPSC amplitude increases during a train of presynaptic action potentials (Katz & Miledi, 1965).

At the simplest level, short-term depression is thought to result from the depletion of the readily-releasable pool of synaptic vesicles. Thus, EPSC amplitude decreases with successive stimulations. In addition, postsynaptic receptor desensitisation can also depress the postsynaptic response. These effects may persist for seconds to minutes (Xu-Friedman & Regehr, 2003). Since depression can result from vesicle depletion, synapses with high resting release probabilities are most susceptible to this form of history-dependent plasticity.

1.3.2 Passive synaptic integration

The integration of synaptic inputs within a neuron requires summation of synaptic potentials (PSPs): excitatory postsynaptic potentials (EPSPs) and inhibitory postsynaptic potentials (IPSPs). Activated synaptic inputs across the

dendritic tree will, in the simplest case, passively propagate towards the soma. Wilfred Rall first identified that dendrites behave like electrical cables (Rall, 1962). Therefore, signals are filtered as they pass along the dendrite. Dendritic filtering has the following consequences for PSPs: 1) attenuation of the peak; 2) slowing of the rise time; and 3) delaying of the peak. Thus, dendritically-evoked synaptic PSPs become smoother and flatter as they progress towards the soma.

The manner in which two synaptic potentials interact depends crucially on their location with respect to each other. One factor that contributes to PSP summation is local driving force. The driving force at a particular synapse is defined as the difference between membrane potential and the reversal potential of the activated conductance. Thus, if two synaptic inputs are activated close to each other, the depolarisation produced at each site will be seen by the other, reducing the driving force at each synapse. As a result, PSP amplitude will be smaller than would be predicted from the linear sum of the two inputs. Additionally, activating synaptic conductances lowers local input resistance: this will reduce the membrane time constant, τ and space constant, λ. Consequently, each PSP will decay faster and attenuate over a shorter distance than would a single PSP on its own. Taken together, under passive conditions, neighbouring PSPs will summate sub-linearly.

In contrast, two distantly spaced PSPs will not interact and will therefore summate linearly at the soma. The most efficient way for synaptic potentials to summate is if they occur synchronously. However, since synaptic potentials are not instantaneous, they can also summate asynchronously: a process known as *temporal integration*. The decay of synaptic potentials is

determined by the membrane time constant τ, which is the time taken for a voltage to fall to 1/e of its peak voltage. τ_m is the product of Cm and the specific membrane resistance, R_m, and is typically between 10-50 ms. C_m is considered to be roughly constant (about 1 $\mu F/cm^2$), but the effective R_m can vary, depending upon the conductance state of the neuronal membrane, changing τ_m and thereby the time window for temporal synaptic integration.

1.3.3 Synaptic inhibition

Synaptic inhibition can interfere with the summation of EPSPs in a variety of ways. Across the central nervous system, $GABA_A$ receptor activation is the primary pathway by which 'fast' synaptic inhibition mediates its effects on postsynaptic neurons. $GABA_A$ receptor activation opens a mixed chloride/bicarbonate-mediated conductance (Hille, 1992). The reversal potential of this conductance has been shown to vary considerably across development, and may also be dynamically regulated within different regions of the same neuron (Woodin *et al.*, 2003). Despite this, the somatic reversal potential of the $GABA_A$ receptor-mediated conductance is generally considered to be in the region of –70 to –80 mV, and thus perisomatic IPSPs are hyperpolarizing. Inhibition works in two ways: the first is a simple effect on voltage. Since IPSPs tend to be hyperpolarizing, they can sum together with EPSPs to reduce net depolarisation. Secondly, inhibitory synapses also increase membrane conductance, producing a *shunt* of synaptic charge. This shunting effect is highly sensitive to spatial location, and is only effective whilst the inhibitory conductance is on (typically around 10-20 ms). Shunting

inhibition is spatially and temporally precise, and acts in a manner independent of voltage.

$GABA_A$ receptors not only respond to transient synaptic release of GABA, but can also mediate a persistent tonic conductance. Background levels of GABA in the extracellular space are often sufficient to cause an ongoing activation of high-affinity receptors. Initially characterised in cerebellar granule cells (Kaneda *et al.*, 1995), tonic inhibition has been found across several brain regions (Semyanov *et al.*, 2004). Although such inhibition is not 'visible' at rest, it nevertheless exerts profound effects on the integrative properties of postsynaptic neurons through a shunting mechanism (Brickley *et al.*, 1996; Mitchell & Silver, 2003)

1.3.4 Non-linear synaptic integration

The previously described scenarios assume that the dendritic tree is an electrically passive structure. This is undoubtedly not the case in most neurons: dendrites express a range of active and non-linear conductances that make important contributions to synaptic integration. These conductances influence PSP summation and also underlie the generation and spread of local regenerative events, including dendritic spikes.

1.3.4.1 Backpropagating action potentials

Action potentials initiated in the axon initial segment backpropagate into the soma and dendrites; this phenomenon involves the activation of

dendritic Na^+ channels in many neurons (Stuart & Sakmann, 1994). Backpropagating action potentials provide dendritically located synapses with information about neuronal output. This signal has been shown to play a role in Hebbian mechanisms of learning. Long-term changes in synaptic efficacy have been shown to rely upon coincident activation of the pre- and postsynaptic neurons. Functionally, this scheme is implemented when the peak of an EPSP coincides with the depolarisation produced by a backpropagating action potential on the postsynaptic membrane (Markram *et al.*, 1997).

1.3.4.2 Summation in an active dendritic tree

Dendrites are known to express a wide range of voltage-gated ion channels, distributed in a cell-type specific manner. Active membrane conductances have been shown to compensate for many of the effects of passive filtering of PSPs across the dendritic tree. Distal inputs can be boosted by dendritic voltage-gated channels as they propagate towards the soma. In this manner, it has been proposed that active dendritic currents could act as a normalising mechanism to equalise the amplitude of distal and proximal inputs (De Schutter & Bower, 1994). PSP summation would become effectively linear across the dendrite and soma.

Recent evidence suggests that mechanisms also exist to enable local synaptic potentials to summate supralinearly. NMDA receptors, expressed at excitatory synapses in most neurons, show a highly non-linear voltage-sensitivity, increasing conductivity with membrane depolarisation (Mayer *et*

al., 1984). If two synaptic inputs containing NMDA receptors are activated close to each other, then the depolarisation produced by each will serve to enhance the NMDA conductance at the other. If sufficient depolarization is achieved, an 'NMDA spike' is generated (Schiller *et al.*, 2000; Polsky *et al.*, 2004). The result is a supralinear summation of synaptic potentials.

This mechanism provides a means by which neurons can enhance the effects of spatial and temporal coincidence in their inputs. It has also led to the suggestion that, computationally, single neurons can be considered to consist of multiple non-linear subunits; subunits are represented as small localised regions within the dendritic tree where local conductances set local thresholds for non-linear events such as dendritic spikes (Poirazi *et al.*, 2003b, a).

The ionic basis of dendritic spikes varies across neurons, although Ca^{2+}spikes are commonly observed in many cell types (Augustine *et al.*, 2003). Dendritic spikes may or may not propagate to the soma, depending on factors such as dendritic geometry and distribution of membrane conductances. In cerebellar Purkinje cells, Llinas and Sugimori demonstrated that Na^{+} spikes occur exclusively at the soma, whilst Ca^{2+}spikes are confined to the dendritic tree (Llinas & Sugimori, 1980c, b).

Further to the integration of transmembrane voltage, chemical signalling in neurons also exhibits subtle spatiotemporal dynamics. In particular, transient and long-lasting changes in intracellular [Ca^{2+}] have been shown to play be a significant role in neuronal signalling. Ca^{2+} entry via NMDA receptors has already been highlighted as a critical step in the pathway regulating long-term changes in synaptic efficacy (Rauschecker, 1991).

Increases in $[Ca^{2+}]_i$ are typically local than voltage signals, and can be restricted to small areas of dendrite or individual spines (Sabatini & Svoboda, 2000) by both morphology (e.g. the narrow spine neck) and endogenous buffering proteins such as calretinin and calbindin. $[Ca^{2+}]_i$ increase is often a highly non-linear process, with NMDA receptors, dendritic voltage-gated Ca^{2+} channels (Yasuda *et al.*, 2003) and Ca^{2+} release from intracellular stores (Wang *et al.*, 2000) all favouring supralinear summation of Ca^{2+} transients on short timescales (Waters *et al.*, 2003). The time course of the decay of intracellular Ca^{2+} transients is determined by both active extrusion mechanisms and buffering dynamics.

1.3.4.3 Synaptic integration *in vivo*

Many of the principles of synaptic integration have been investigated in acute brain slices, where spontaneous synaptic input is extremely low. However, within an intact network, it is presumed that at any given time, many synaptic inputs onto a neuron are simultaneously active. The total number of active inputs is likely to strongly depend on the number of synaptic contacts. Neocortical pyramidal cells receive between 5,000 and 60,000 synaptic contacts, and cerebellar Purkinje cells upwards of 175,000. Therefore, even if only a small fraction of these inputs are simultaneously active, these neurons are subject to significant synaptic bombardment. *In vivo* intracellular recordings suggest that this bombardment can alter their integrative properties by reducing input resistance – effectively generating a network-driven shunt (Destexhe *et al.*, 2003). Recent work has highlighted how the

conductance-state of a neuron profoundly affects the manner in which its inputs are integrated. In ketamine-xylazine anaesthetised animals, neocortical pyramidal cells exhibit a slow oscillation (1 Hz) in membrane potential (Petersen *et al.*, 2003), between a depolarised up state and a hyperpolarised down state. This oscillation is abolished in the presence of synaptic blockers, indicating that it results from network activity. It was recently demonstrated that neuronal input resistance is significantly reduced whilst in the up state (Leger *et al.*, 2004). During the up state, subthreshold sensory synaptic responses are smaller, briefer and spatially more confined. Surprisingly, whisker deflections evoke fewer action potentials in barrel cortex neurons despite being closer to threshold (Petersen *et al.*, 2003). These data highlight that the relationship between synaptic input and spike output - the 'input-output relationship' - is not fixed, but can be strongly influenced by levels of background activity.

1.4 THE CEREBELLUM

The structure of the cerebellum has intrigued investigators since Ramon y Cajal first demonstrated its crystal-like organisation (Ramón y Cajal, 1888). Its connectivity is remarkably conserved across the whole of the cortex, and is largely invariant across all vertebrates (Ramón y Cajal, 1904; Palay & Chan-Palay, 1974). Divided amongst three layers, the cerebellar cortex contains relatively few distinct cell types, in contrast to other cortical structures.

Morphologically, the most striking neurons within the cerebellum are the Purkinje cells. These large cells possess near-flat fan-like dendritic arborisations, which extend up to the boundary of the cortex. The arrangement of these neurons is such that the planes of all Purkinje cell dendrites are parallel, thus ensuring they sit in neat rows that overlap with adjacent rows. Orthogonal to the plane of Purkinje dendrites run the parallel fibres: thin unmyelinated axons that run for several millimetres in each direction across the cortex to form the molecular layer. Two classes of interneurons, the stellate and basket cells, lie amongst the parallel fibres and Purkinje dendrites; basket cells sitting closest to Purkinje cell soma.

The granular layer is a densely packed region that lies beneath the cell bodies of the Purkinje cells. It consists mainly of the small but numerous granule cells and larger, sparser Golgi cells. Granule cell axons extend out of this layer and bifurcate to become the parallel fibres of the molecular layer.

1.4.1 Connectivity within the cerebellar circuit

Much of what is known about the connectivity of the cerebellar circuit was first established by Eccles and co-workers in the 1960s (see Eccles *et al.*1967). The cerebellar circuit is generally thought to consist of the cerebellar cortex and its target structure, the deep cerebellar nuclei (Fig 1.1).

1.4.1.1 The granular layer

Two distinct afferent pathways supply the cerebellar cortex: mossy fibres and climbing fibres. Numerically, mossy fibres represent the vast majority of all afferent input to the cerebellum, and make excitatory synaptic contact upon neurons in the granular layer: granule cells and Golgi cells. Granule cells are tiny excitatory interneurons and constitute greater than half the neurons in the entire CNS. They have a simple morphology consisting of a spherical soma and an average of 4 short dendrites (up to 30 μm long) that have claw-like terminations. Upon entering the granular layer, mossy fibres ramify and terminate, making between 20-30 *en passant* synaptic varicosities (Palay & Chan-Palay, 1974). Under the light microscope, these synaptic interactions are seen as thickenings along the mossy fibres, and have been termed rosettes. The ultrastructure of synaptic interactions between mossy fibres and granule cells show several interesting and unique features (Eccles *et al.*, 1967a). Synaptic contacts are found exclusively within a highly specialised structure known as the glomerulus. At the core of each glomerulus

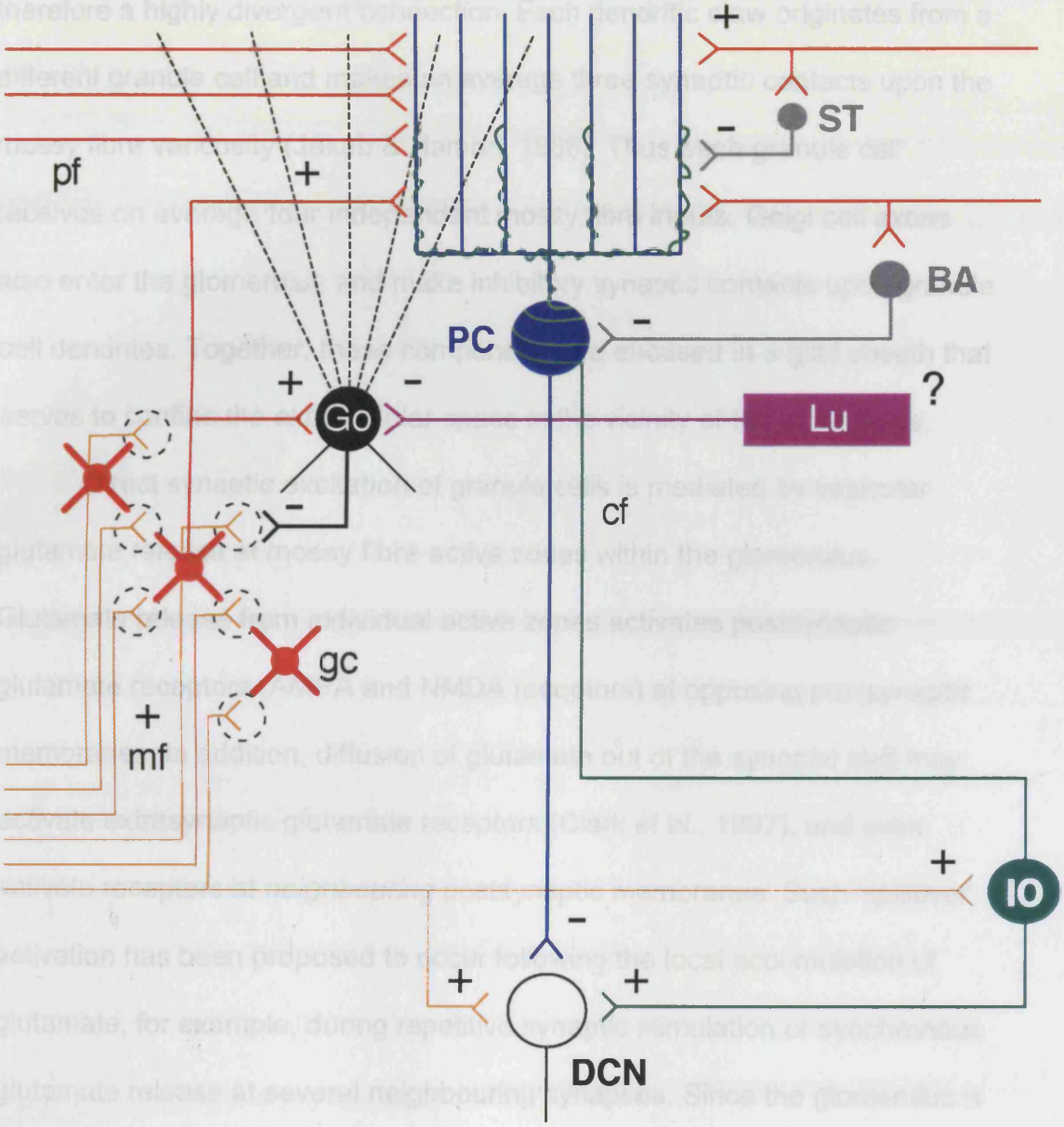

Figure 1.1

Schematic showing network connectivity in the cerebellar hemispheres.
Key: gc, granule cell, mf, mossy fibre; pf, parallel fibre; cf, climbing fibre; Go: Golgi cell; Lu: Lugaro cell; BA, basket cell; ST, stellate cell; IO, inferior olivary nucleus; DCN, deep cerebelar nuclei.

lies a mossy fibre bouton, which is studded with up to 50 granule cell dendritic claws (Hamori & Somogyi, 1983). The mossy fibre-granule cell synapse is therefore a highly divergent connection. Each dendritic claw originates from a different granule cell and makes an average three synaptic contacts upon the mossy fibre varicosity (Jakab & Hamori, 1988). Thus each granule cell receives on average four independent mossy fibre inputs. Golgi cell axons also enter the glomerulus and make inhibitory synaptic contacts upon granule cell dendrites. Together, these components are encased in a glial sheath that serves to confine the extracellular space in the vicinity of the glomerulus.

Direct synaptic excitation of granule cells is mediated by vesicular glutamate release at mossy fibre active zones within the glomerulus. Glutamate release from individual active zones activates postsynaptic glutamate receptors (AMPA and NMDA receptors) at opposing postsynaptic membranes. In addition, diffusion of glutamate out of the synaptic cleft may activate extrasynaptic glutamate receptors (Clark *et al.*, 1997), and even activate receptors at *neighbouring* postsynaptic membranes. Such 'spillover' activation has been proposed to occur following the local accumulation of glutamate, for example, during repetitive synaptic stimulation or synchronous glutamate release at several neighbouring synapses. Since the glomerulus is itself comprises many closely-spaced, independent active zones, it offers a favourable environment in which spillover activation of neighbouring receptors can occur. Recent evidence indicates that neurotransmitter spillover onto neighbouring synapses, and activation of extrasynaptic receptors, produce a broadening of excitatory and inhibitory synaptic currents in granule cells (DiGregorio *et al.*, 2002; Hamann *et al.*, 2002). Furthermore, baseline levels of

neurotransmitter within the glomerulus are sufficient to cause ongoing activation of some neurotransmitter receptors. In particular, ambient glomerular GABA concentrations are sufficient to activate GABA-A receptors containing high-affinity $\alpha_6\delta$ subunits (Stell *et al.*, 2003), which have been shown to underlie a tonic inhibitory GABAergic conductance in granule cells (Brickley *et al.*, 1996).

Mossy fibres also make synaptic contact upon the soma and dendrite of Golgi cells, which are inhibitory, therefore providing a means of feed-forward inhibition upon granule cells. Golgi cell dendrites extend through both the granular and molecular layers, in an approximately cylindrical volume (Eccles *et al.*, 1967a). Therefore, Golgi cell dendrites also receive input from parallel fibres. Eccles and colleagues demonstrated that electrical stimulation of parallel fibres could reduce the evoked electrical potential recorded in the granular layer upon subsequent stimulation of mossy fibres (Eccles *et al.*, 1966). Thus Golgi cells also exert feedback inhibition upon granule cell activity. It is estimated that there are between 1000 and 3000 granule cells per Golgi cell. The extent of overlap of dendritic and axonal arborisations between Golgi cells is disputed, some studies argue against much overlap in the in the axonal spread of Golgi cells (Eccles *et al.*, 1967a), whereas other groups believe them to be subject to significant overlap (Fox *et al.*, 1967). Therefore, it is not known whether single granule cells are inhibited by one or several Golgi cells. However, it remains highly likely that individual Golgi cells exert a powerful modulatory influence over a great many granule cells.

Granule cells are silent in *in vitro* slice preparations, due to the loss of afferent mossy fibre input and their hyperpolarised resting potentials. The

firing patterns of individual granule cells *in vivo* has, until this point, remained unknown. This is due to their small size and high packing density, which has precluded the unambiguous isolation of single units. Golgi cells have previously been reported to exhibit an ongoing spiking at low frequencies (5-25 Hz), both *in vivo* and *in vitro* (Edgley & Lidierth, 1987; Dieudonne, 1998).

Finally, it is worth mentioning two other granular layer neurons that are often overlooked components of the cerebellar circuit. Lugaro cells are fusiform-shaped neurons, located at the top of the granular layer, just below the Purkinje cell bodies. Comparatively little is known about these neurons, both in terms of their synaptic connections and their physiological activity. However, recent *in vitro* and *in vivo* studies report that they discharge rhythmically at low frequencies, 5-20 Hz (Dieudonne & Dumoulin, 2000; Holtzman *et al.*, 2003), and thus provide oscillatory inhibitory input to their downstream targets, in particular Golgi cells. It has been shown in cerebellar slice preparations, that their activity is highly dependent upon serotonergic input (Dieudonne & Dumoulin, 2000).

The unipolar brush cell (UBC) is often ignored due to its asymmetric distribution across different areas of the cerebellar cortex. UBCs each receive a single mossy fibre input to a large brush-like perisomatic synapse. Their axons remain restricted to the granular layer and innervate granule cells in a similar manner to mossy fibres. UBCs are found in particularly high levels in the some areas of the flocculus, whilst being mostly absent in many other areas of the cerebellum. *In vitro* studies indicate that they faithfully relay mossy fibre activity in a spike-to-burst manner (Rossi *et al.*, 1995; Dino *et al.*, 2000), and would therefore be expected to amplify mossy fibre signals within

the granular layer. They have recently been shown to exhibit high discharge rates *in vivo* (8-20 Hz; J Simpson, personal communication).

1.4.1.2 The molecular layer

The second afferent input to the cerebellum, the climbing fibres, arise from the axons of inferior olivary nuclear neurons, and terminate upon the dendritic trees of Purkinje cells. Each Purkinje cell is innervated by a single climbing fibre input, which entwines the main portion of dendritic tree (Llinas & Walton, 1998). Climbing fibre impulses generate powerful excitatory effects within Purkinje cells, and typically generate a rapid burst of action potentials known as a complex spike (Ito, 1984). Purkinje cells also receive excitatory synaptic inputs via parallel fibres and the ascending limb of granule cell axons. The sheer number of parallel fibre/ascending limb synapses received by Purkinje cells is impressive: up to 175,000 per Purkinje cell in rat (Napper & Harvey, 1988). This excitatory convergence is the largest known in the nervous system. Each parallel fibre is estimated to make only one or two synaptic contacts upon every second or third Purkinje cell dendrite that it passes (Palay & Chan-Palay, 1974; Napper & Harvey, 1988). Thus the contribution of individual parallel fibres in shaping the response of Purkinje cells is often assumed to be extremely small (Bower, 2002).

In acute slices, Purkinje cells are typically observed to fire regular action potentials (also referred to as simple spikes) at high tonic rates around 50 Hz. Similar firing rates are also observed *in vivo,* although simple spike rates are considerably more variable, and subject to powerful modulation by

complex spikes (Bell & Grimm, 1969; Armstrong, 1974), which are observed at a rate of 1 per second (Ito, 1984).

The dendritic processes of stellate and basket cells are located exclusively within the molecular layer. Both cell types receive excitatory synaptic inputs via parallel fibres and exert feed-forward inhibitory action upon their targets, Purkinje cells (Mittmann *et al.*, 2004). Basket cells are larger than stellate cells, and innervate Purkinje cell soma and axon rather than dendrites. However, both sets of neurons are generally assumed to constitute variations within one class. Stellate and basket cells outnumber Purkinje cells by 16:1 and 6:1 respectively. Both stellate and basket cells are spontaneously active at low rates, around 10 Hz in slice preparations (Häusser & Clark, 1997), and in the intact cerebellum (Jorntell & Ekerot, 2003b)

1.4.1.3 The cerebellar nuclei

Purkinje cells are GABAergic and represent the sole output of the cerebellar cortex. Their myelinated axons run down through the granular layer, into the white matter and out of the cortex. Deep cerebellar nuclear neurons are the primary target of Purkinje axons and integrate Purkinje cell inputs together with collaterals from the mossy fibre and climbing fibre systems to generate the output of the cerebellar circuit (Bloedel & Courville, 1981). Deep cerebellar nuclear neurons are a heterogeneous population of large and small projection neurons and local circuit neurons, and are spontaneously active in both slice preparations and *in vivo* (Aizenman *et al.*, 2003; Rowland & Jaeger, 2003).

1.4.2 Spatial organisation of the cerebellum

Whilst the basic circuitry is almost invariant across cerebellum, the distribution of afferent and efferent connections shows a distinct spatial organisation. An interesting feature of the cortical hemispheres is their unbroken continuity across the midline. Anatomically, and functionally, the cerebellar cortical hemispheres have often been subdivided along the lines of efferent projections to the three deep cerebellar nuclei. Vermal, intermediate and lateral zones of the hemispheres project to the medial, interposed and dentate nuclei respectively, whilst the flocculonodular lobe projects to the vestibular nuclei (Jansen & Brodal, 1940). However, the positions of the borders between the three hemispheric cortical zones depend on the position of arbitrary borders between cerebellar nuclei themselves, and not on specific landmarks in the cortex. In the rat cerebellum, much information has been gathered on the fine spatial organisation of projections to and from the lateral hemispheres. The following sections focus on the organisation of these projections.

1.4.2.1 Afferent inputs to the lateral cerebellar hemispheres

The pontine nuclei in the rat provide a major projection to the cerebellar hemispheres. It is generally held that the pontocerebellar projection is very precisely organised and characterised both by patterns of convergence and divergence (Flumerfelt & Hrycyshyn, 1985). Individual folia receive mossy

fibres from diverse regions of the pontine nuclei. Additionally, mossy fibre labelling experiments have shown that collateral projections from the same pontine neuron often project to different lobules within the same hemisphere and even to both hemispheres.

The pontine nuclei receive afferent inputs from a number of sources including various regions of the cerebral cortex, the superior and inferior colliculi and the deep cerebellar nuclei. Corticopontine fibres originate from somatosensory and motor areas, and also from visual and auditory areas. However, it is the somatosensory and motor cortex that provides the greatest input, particularly from facial areas in the rat. Many pontine neurons also receive convergent inputs from functionally different cortical areas.

Neurons from the trigeminal sensory nuclei also project directly to the lateral hemispheres of the cerebellum (Voogd & Glickstein, 1998). Comparatively little is known about this projection, although recent labelling experiments indicate that trigeminal mossy fibres send collaterals to both cerebellar hemispheres (Bukowska *et al.*, 1998). The direct nature of this pathway is believed to underlie the very short latencies (less than 10 ms; Morissette & Bower, 1996) of stimulus-evoked activity in the cerebellar hemispheres. It is not known whether mossy fibres from the pontine and trigeminal systems are segregated in the granule cell layer.

1.4.2.2 Micro-organisation of afferent inputs to the lateral cerebellar hemispheres

The fine spatial structure of afferent projections to the cerebellum was first characterised in Wally Welker's laboratory in the 1970s. Using high-density 'micro-mapping' techniques, several surprising findings were made. The predominant sensory input within the lateral cerebellar hemispheres of the rat was discovered to be tactile. Furthermore, the tactile structures represented were found to be perioral, mainly representing the lips and vibrissae (Shambes *et al.*, 1978a; Shambes *et al.*, 1978b). This finding was a surprise, especially when viewed in the context of the cerebellum's traditional role in motor coordination (see section 1.4.3.2). In addition, the topographic pattern of these projections was very different from those found in other somatosensory structures (Shambes *et al.*, 1978b). In contrast to the somatotopic organisation of somatosensory cortex, for example, tactile projections to the cerebellar cortex exhibited 'an usual patch-like mosaic representation of different body parts' (Fig 1.2). Adjacent cortical areas often receive inputs from non-adjacent body parts, and different patches distributed across the cortex often represent the same body part. Within each patch, body surface is somatotopically organised. Thus, this projection pattern is described as 'fractured somatotopy'.

Within folium Crus IIa of lateral cerebellar hemispheres, a comparison of afferent projections in different rats revealed striking similarities in both the fractured patterns and the parts of the body surface represented (Bower & Kassel, 1990). Also, peripheral lesions, e.g. denervation of the upper lip area

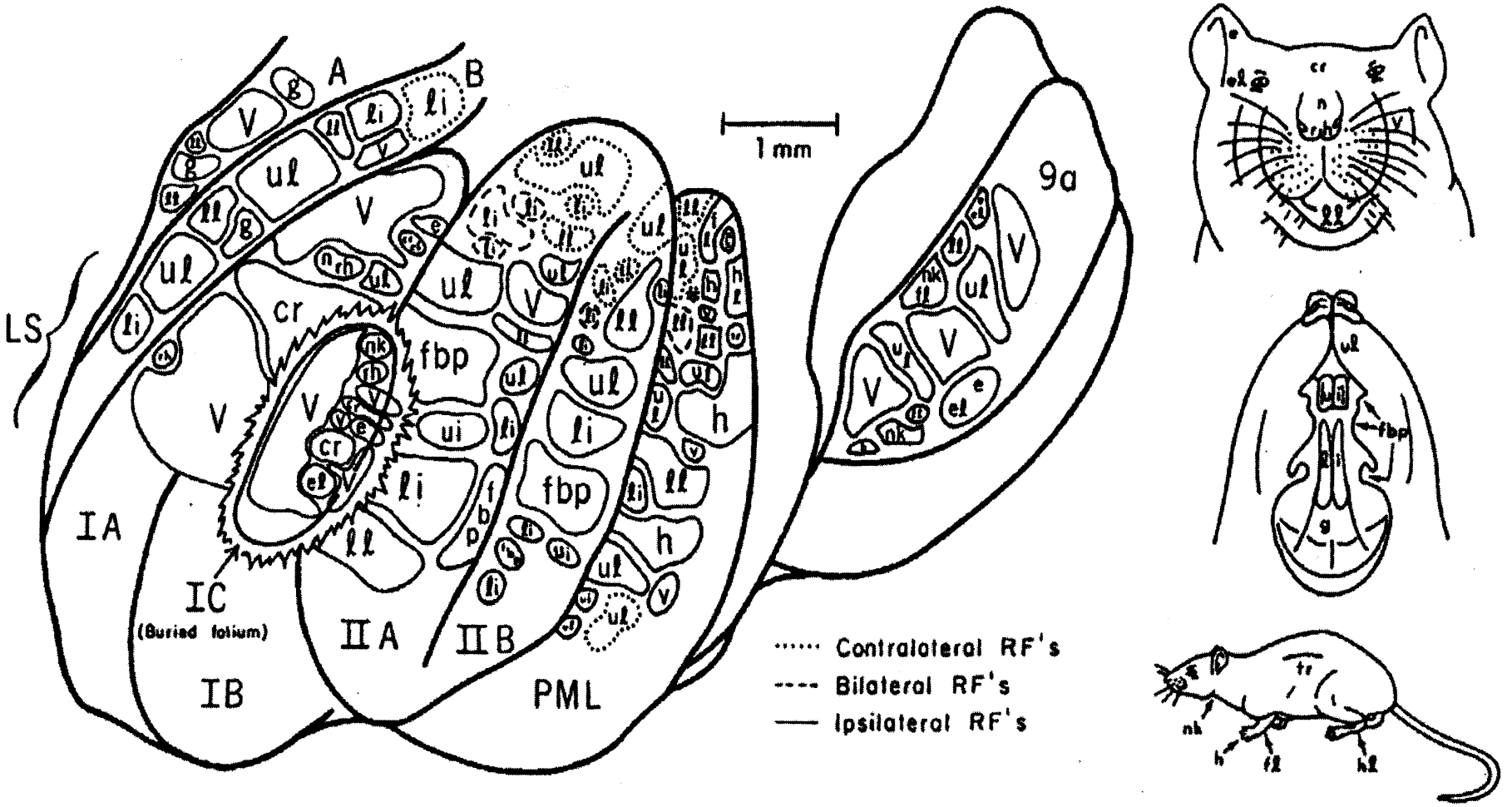

Figure 1.2

Fractured somatotopy in the lateral cerebellar hemispheres. Schematic representation showing the source of tactile inputs in lateral folia of the rat cerebellum. Selected key: RF, receptive field; PML, paramedial lobule; v, vibrissae; fbp, front buccal pad; li, lower incisor; ul, upper lip. Reproduced from Bower and Woolston (1983).

of the face, reveal that these fractured patterns are retained, even if the lesions occur early in development (Ito *et al.*, 1982; Gonzalez *et al.*, 1993). In lesioned animals, the upper lip area representation is instead replaced by representation of the ipsilateral upper incisor, which is normally not strongly represented in Crus IIa. Functionally, the result of this reorganisation is that tactile information about the upper lip is to some extent retained: touching the deafferented lip produces a response in the cerebellum through the indirect contact of the upper lip on the upper incisor.

These afferent projection patterns are mirrored in the patterns of activation of neurons within the cerebellum. Similar clumps of activation were found in the field responses of cerebellar granule cells during tactile stimulation (Bower & Woolston, 1983). Surprisingly, the activation profile of Purkinje cells shows a very high degree of congruence with the granule cells situated directly beneath them in the cortex. The vertical organisation within the cerebellar cortex was unexpected, since the structure of the cerebellum, and in particular the organisation of parallel fibres, had led many to predict the activation of 'beams' of Purkinje cells (Eccles *et al.*, 1967a). Subsequently, it has been proposed that functional basis of this vertical organisation may rely upon powerful synaptic connections onto Purkinje cells from granule cell ascending limb axons (Llinas, 1982), and/or a high proportion of weak or silent synapses between parallel fibres and Purkinje cells (Isope & Barbour, 2002).

1.4.2.3 Efferent projections from the lateral cerebellar hemispheres

Efferents from the lateral cerebellar hemispheres project to the dentate nucleus. In the past, the dentate was thought to contain a single map of the body and project via the thalamus in a somatotopic fashion to the primary motor cortex. However, recent transneuronal tracing experiments have revealed that the dentate also makes projections to nonmotor cortical areas including the prefrontal and posterior parietal cortex (Middleton & Strick, 1994, 2001). Glutamatergic projection neurons convey most of the output from the cerebellum (Czubayko *et al.*, 2001). However, smaller GABAergic projection neurons carry feedback signals to the inferior olive and are not known to project elsewhere (de Zeeuw *et al.*, 1989).

1.4.3 Theories of Cerebellar Function

The structural regularity of cerebellum has led many to infer that the all areas of the cerebellar serve a common function. Unfortunately, it is still the case that investigators know very little about how the cerebellum works, and what it *actually does*.

1.4.3.1 Early discoveries

Our attempts to understand cerebellar function have been heavily influenced by the earliest lesion studies (Rolando, 1809; Flourens, 1824) and subsequently the work of Gordon Holmes (Holmes, 1917). By carefully

examining World War I shrapnel victims, suffering specific cerebellar lesions, he was able to establish the cerebellum's crucial involvement in motor control. It was apparent that the cerebellum does not serve a primary role in either sensory or motor function since its destruction doesn't produce sensory deficits or paralysis. However, sufferers of cerebellar damage do show extreme difficulties in initiating and concluding movements, and over- and undershoot their targets (dysmetria). Collectively, these deficits are known as ataxia, and are the most commonly observed symptoms in animal models of cerebellar dysfunction. Both force and timing of movement are severely affected by cerebellar dysfunction (Hore *et al.*, 2002). With these deficits in mind, working models have been proposed where the primary function of the cerebellum is the modulation and coordination of movement.

1.4.3.2 Theories of motor learning in the cerebellum

David Marr (1969) and James Albus (1971) developed two of the most influential models of cerebellar cortical function. Both believed that complex patterns of motor activity are represented in the activity of parallel fibres and that the cerebellum, and specifically Purkinje cells, act as a pattern recognition device. A key proposal of both theories is that parallel fibre-Purkinje cell synapses are subject to modulation, for example, when a signal indicates an error in motor output. This 'error signal', conveyed to the cerebellum by climbing fibres, can therefore alter the strength of active parallel fibre synapses and hence induce a form of learning. Patterns may therefore be stored in the cerebellum as synaptic weights at parallel fibre-

Purkinje cell synapses. The sign change undergone by parallel fibre synaptic weights during learning was originally proposed to be positive in response to climbing fibre input i.e. potentiating active parallel fibre inputs (Marr, 1969). However, this assumption did not take into account the inhibitory output of the cerebellar cortex, or the high rates of spontaneous spiking activity often observed in Purkinje cells *in vivo*. Therefore, the original theory was modified slightly to propose that the synaptic weights of active parallel fibre synapses would instead be *weakened* by climbing fibre signalling (Blomfield & Marr, 1970; Albus, 1971). Extensive experimental evidence has since been gathered in support of climbing fibre-driven long-term depression (LTD) at parallel fibre synapses (Ito, 2001). Complex spike activity in Purkinje cells of monkeys is strongly correlated with motor errors during limb movements (Gilbert & Thach, 1977). However, it is also important to mention that other long term changes in parallel fibre synaptic efficacy, both potentiation (Lev-Ram *et al.*, 2002) and depression (Hartell, 1996; Rancz & Hausser, 2004), have been reported in the absence of climbing fibre activation. Therefore, it is still far from established that climbing fibre-dependent LTD is the primary mechanism of motor learning in the cerebellum (Hansel *et al.*, 2001).

Both Marr and Albus also made predictions as to the function of the cerebellar granular layer. As indicated earlier, the mossy fibre-granule cell synapse represents a site of enormous divergence. The efficiency of Purkinje cells to discriminate between the largest number of distinct parallel fibre patterns is greatly enhanced if the number of active inputs is kept low (less than 1%). Thus, a key prediction of both theories is that during periods when mossy fibre input is high, those inputs will be sparsely represented as

granular layer outputs. This prediction has remained untested due to problems with recording granule cell unit activity.

1.4.3.3 The vestibulo-ocular reflex

In order to investigate the functional role of the cerebellum, simple behavioural paradigms are necessary. As an example of motor coordination, the vestibulo-ocular reflex (VOR) is a relatively simple neuronal system. Visual fixation of points in space has the potential to be disrupted by head movements. However, the brain copes with such a problem by generating motor output to rotate the eyes in the opposite direction of head movement. In this manner, point fixation is maintained in spite of head movement. The VOR also occurs in the dark, as the eye movements are driven by vestibular information: this affords a convenient means of testing the VOR in the absence of other eye movements. Vestibular nuclei in the brainstem receive signals related to head movement and project to neurons in the oculomotor nuclei; the flocculus and paraflocculus of the cerebellum form an inhibitory side-loop to this circuit. The 'gain' of the VOR can be manipulated experimentally, by increasing or decreasing the expected slip of the visual field on the retina compared to what is expected. A change in the gain of VOR will occur to match the change in gain of retinal slip and this change is interpreted as motor learning. Lesion and recording studies have revealed the necessity of the cerebellum for motor learning in the VOR: disruption abolishes the ability to modify gain (Ito *et al.*, 1982). Furthermore, Purkinje cells exhibit altered responses during performance of the VOR after motor

learning. Masao Ito proposed a simple model (Ito, 1982) to explain this learning based upon Marr-Albus theories, whereby cerebellar mossy fibres supply information from the vestibular organs in response to circular head acceleration. If the oppositely directed eye-movement does not hold the gaze on the fixation point, then retinal slip will occur. In Ito's model, retinal slip is signalled to the cerebellar cortex via climbing fibres, thus providing an 'error' or 'learning' signal. Parallel fibres that are coincidently active with the climbing fibre will be subject to LTD. It is this synaptic plasticity that is postulated to mediate the subsequent gain change. In accordance with this model, evoked climbing fibre responses have been recorded in the flocculus during retinal slip (Simpson & Alley, 1974; Ghelarducci *et al.*, 1975). However, evidence also exists that indicates that the predominant site of motor learning in the VOR may lie outside the cerebellar cortex, in the vestibular nuclei (Miles & Lisberger, 1981). It has been found that responses of vestibular nucleus neurons during VOR cancellation exhibit learning-related changes that cannot be accounted for in the responses of Purkinje cells during VOR cancellation (Lisberger, 1994). More recently, it has been shown that plasticity at both cortical and vestibular nucleus sites is required for the VOR, but that specific timing constraints are only necessary for the former (Ramachandran & Lisberger, 2005).

1.4.3.4 Classical conditioning

Classical, or Pavlovian, conditioning is another simple behaviour that is thought to exhibit a component of cerebellar learning. In this paradigm, a

noxious stimulus (called the 'unconditioned stimulus' - US) to the eyeball, such as an air puff or electric shock, is preceded in a fixed temporal manner by a neutral conditioning stimulus (CS; e.g. a tone); the US causes an eye-blink reflex. After a period of training, however, the eye-blink precedes the US and is instead cued by CS in a temporally precise manner. Indeed, the precise timing relationship between the CS and US can be learnt and relearnt as it is varied by several hundreds of milliseconds. Classical conditioning's dependence upon the cerebellum was first revealed through lesion studies (McCormick *et al.*, 1982), and subsequently the auditory input of the CS has been shown to be conveyed by cerebellar mossy fibres (Hesslow *et al.*, 1999). Thus, classical conditioning is often cited to support of a role for the cerebellum in the precise timing of behaviours (Ohyama *et al.*, 2003b).

Once again, the proposed site of motor learning is disputed. Some groups have reported that some residual learning remains in the absence of a functional cerebellar cortex (Lavond *et al.*, 1987; Lavond & Steinmetz, 1989; Ohyama *et al.*, 2003a). However, a recent study used drug microperfusion to selectively inactivate cerebellar cortex and nuclei during classical conditioning. Inactivation of the cerebellar cortex was sufficient to abolish learning and expression of the eye-blink response (Attwell *et al.*, 2002), suggesting that 'motor memory' *is* stored in this structure. The precise locus of learning during classical conditioning is therefore still rather controversial.

1.4.3.5 Sensory data acquisition

The role of the cerebellum in motor control has been strongly emphasised by many theorists and experimentalists. However, there are several pieces of experimental data that do not sit comfortably with simple feedback control of limb movements. For example, afferent input to the lateral hemispheres is predominantly tactile, rather than proprioceptive. Certain body parts, such as the perioral region in rodents, are highly over-represented in the lateral cerebellar hemispheres, whilst input from other areas of the body is unexpectedly small. Hindlimb representation is almost completely absent from lateral areas of the cerebellum (Shambes *et al.*, 1978a; Kassel *et al.*, 1984; Welker *et al.*, 1988), which is surprising for a structure proposed to mediate general motor coordination.

Instead, Bower has argued that the primary function of the cerebellum is the manipulation of the motor system in order to optimise the acquisition of sensory information (Bower, 1997). As already stated, inputs to the lateral cerebellar hemispheres of rodents arise mainly from the perioral regions; these are the areas employed by rodents during tactile sensory exploration. Cats and primates mainly make use of their forelimbs during exploratory sensory behaviours. Tactile inputs from distal regions of the forelimb constitute the largest representation within the lateral hemispheres of these animals (Kassel *et al.*, 1984; Welker *et al.*, 1988).

Activity within the cerebellum is also more poorly correlated with simple coordinated movement, than tasks requiring fine sensory discrimination. This has been elegantly demonstrated in humans, using fMRI to study activation

levels during a variety of motor and non-motor behaviours (Gao *et al.*, 1996). The contribution of the cerebellar hemispheres to behaviour was assayed as fMRI activity in the dentate nucleus, the sole output of the lateral cerebellar cortex. Cerebellar activation was determined whilst subjects were asked to perform: 1) a simple motor task (finger movements); 2) a sensory discrimination task without movement (identifying the roughness of sand paper); 3) a sensory discrimination task requiring movement (identifying balls from within a bag). The level of dentate activity during these different tasks is revealing. Fine finger movements in the absence of sensory discrimination produced little or no activation within the nucleus. In contrast, maximal levels of activation were found during active sensory discrimination. Interestingly, significant activation was also observed during sensory discrimination *in the absence* of movement. These results strongly support of role for the cerebellum distinct from the pure modulation of movement. Instead, it is argued that the cerebellum uses sensory information to guide the motor system in such a way as to facilitate efficient sensory data collection. Although, the output of the cerebellum may still modulate motor behaviour, the function of this output is markedly different. The cerebellum's role in eye movements can be comfortably explained by this hypothesis, as the efficiency of this system is vital to the successful collection of visual information. Similarly, the lateral hemispheres of the cerebellum receive auditory input (Huang *et al.*, 1991), and stimulation in the lateral nucleus evokes movement of the pinna (Cicirata *et al.*, 1992). Since the pinna influences sensory data received by the auditory system, this also fits with the hypothesis. Finally, it has been suggested that some forms of autism may result from cerebellar

dysfunction (Kern, 2002). Autistic subjects have difficulty in relating to the world around them, and often report that sensory data is overwhelming or confusing (Frith, 1997). A hypothesis where the cerebellum is necessary for the efficient manipulation of sensory data would be consistent with an association of these type of behavioural defects with cerebellar dysfunction.

1.4.3.6 Cerebellar contributions to non-motor behaviour

In accordance with the large cerebellar projection to prefrontal and parietal areas of the cerebrum (Middleton & Strick, 1994, 2001), experimental work with human sufferers of cerebellar dysfunction has begun to reveal the contribution of the cerebellum to cognition. Patients with lateral cerebellar lesions show specific language defects, in particular verb generation and antonym generation (Gebhart *et al.*, 2002). Since cognition represents neural activity without a necessary motor output, this work provides further support for the proposal that cerebellar function extends beyond simple coordination of the motor system. Instead, it appears that the cerebellum is vital for the efficient operation of many elements of the central nervous system.

1.5 THE AIMS OF THIS STUDY

Over the past twenty-five years, much has been determined about synaptic and intrinsic properties of neurons within the cerebellar cortex. This work has mainly been performed in acute cerebellar slices, where afferent input is absent. It is now necessary to determine how these properties interact in cerebellar neurons *in vivo*, to shape sensory processing within the cerebellum.

1.5.1 Outline of thesis

In this study, *in vivo* patch clamp techniques have been used to isolate single neurons within the cerebellar cortex, enabling both synaptic and spiking activity to be monitored. Recordings have been made from folia in the lateral cerebellar hemispheres in anaesthetised, freely-breathing rats. These areas are known to receive somatosensory inputs (Shambes *et al.*, 1978a). As such, it has been possible to observe sensory-evoked activity within cerebellar granule cells and Purkinje cells. This thesis is divided into three experimental chapters.

Following a methods chapter, the first two experimental chapters deal with observations made in cerebellar granule cells. In chapter three, I report that granule cells show low ongoing firing rates *in vivo*. The intrinsic and synaptic conductances that contribute to these low firing rates are described. In particular, it will be seen that a tonic GABAergic conductance is extremely important in regulating the activity of granule cells *in vivo*.

In chapter four, I discuss the integration of sensory signals within granule cells. The relationship between sensory-evoked synaptic input and spike output is determined. High frequency spiking is observed to convey sensory information to and from the cerebellar granule cell layer. Within individual granule cells, temporal summation is found to be necessary in order to generate the observed patterns in granule cell output.

In the final results chapter, I describe the activity of granule cell target neurons, interneurons and Purkinje cells. Both classes of neuron are spontaneously active. However, the patterns of Purkinje cell output reflect an intrinsic membrane bistability. The factors contributing to membrane bistability in Purkinje cells are discussed.

The thesis concludes with a general discussion.

Chapter 2: MATERIALS AND METHODS

2.1 INTRODUCTION

The data presented in this thesis were obtained from neurons within the cerebella of freely breathing anaesthetised rats. Electrophysiological recordings were carried out using the patch clamp technique (Neher & Sakmann, 1975) in the cell-attached and whole-cell configurations, using both voltage-recording and voltage-clamp modes.

2.2 SURGICAL PROCEDURES

18-27 day old (P18-27) Sprague-Dawley rats were anaesthetised with urethane (1.2 g kg^{-1}) or a ketamine (50 mg kg^{-1}) / xylazine (5 mg kg^{-1}) mixture via intraperitoneal injection. Following the cessation of spontaneous whisker movements, the depth of anaesthesia was assessed using a pinch to the hindlimb. When animals were areflexive, they were secured in stereotaxic apparatus by use of ear- and bite-bars (Fig 2.1). A sagittal cut was made through the skin of the head and haemostatic forceps were used to secure the skin and expose the cranium. Connective tissue was removed over one side of the cerebellum using a bone-scraper (Fine Science Tools, Germany). A dental drill (Osada, Japan) was used to make a small craniotomy (1.5 mm x 1.5 mm) above the vermis (3 mm posterior, 0.5 mm lateral of lambda), or folia Crus I and II (3 mm posterior, 5 mm lateral of lambda). In order to expose the cerebellar cortex, the dura was removed by use of a fine needle (30 G, Harvard Apparatus, UK), and fine forceps (Inox forceps: tip size = 0.05 x 0.01

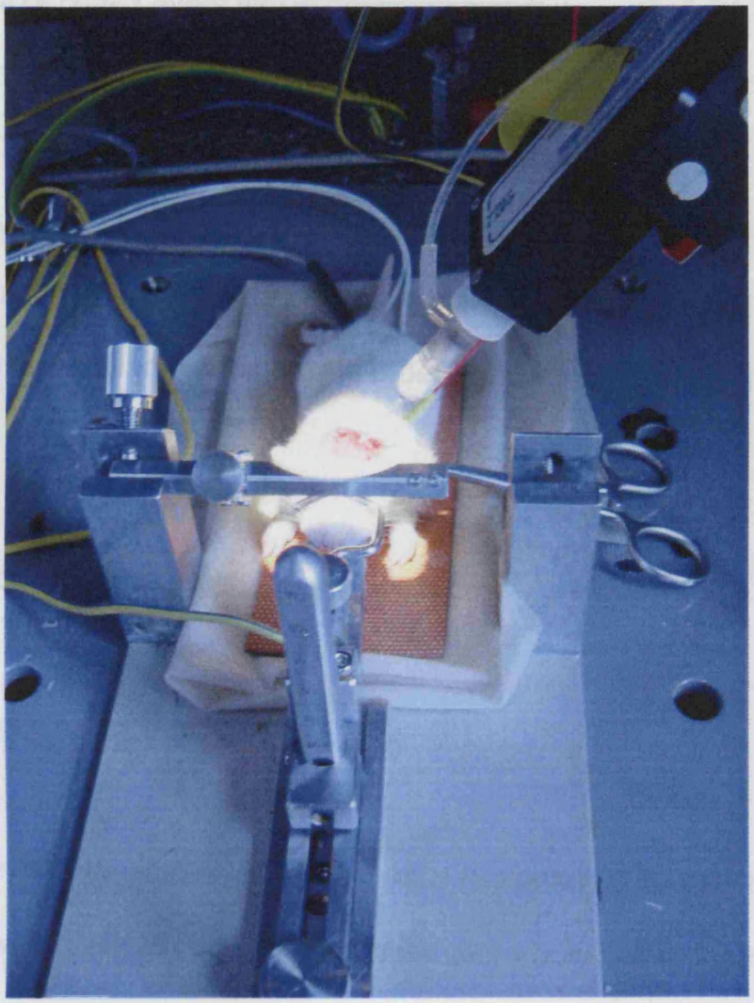

Figure 2.1

P18-27 rats were anaesthetised and secured using ear- and bite-bars. A homeothermic blanket was used to maintain a stable body temperature.

mm; Fine Science Tools, Germany). Subsequently, artificial cerebrospinal fluid (aCSF), continuously bubbled with 5% CO_2/ 95% O_2, was applied to the exposed area of cortex every few minutes in order to keep the area moist. Throughout all experiments rectal temperature was monitored and maintained at 37 ± 0.5°C by a homothermic blanket (FHC, Bowdoinham, USA). The depth of anaesthesia was tested every 10 minutes using a pinch to the hindlimb. When a ketamine/xylazine mixture was used, animals were injected with 1/3 of the original dose every 45 minutes in order to maintain a sufficient depth of anaesthesia.

2.3 ELECTROPHYSIOLOGY

2.3.1 *In vivo* patch clamp recordings

Low-resistance patch pipettes (4-7 MΩ) (Sakmann & Neher, 1983; Pei *et al.*, 1991) were used to obtain cell-attached and whole-cell recordings *in vivo*. Pipettes were fabricated from filamentous borosilicate glass capillaries (outer diameter: 1.5 mm, inner diameter: 0.86 mm; Harvard Apparatus, UK), using a Narishige PC10 vertical puller (Narishige, Japan). Typically, the tip size was 1-2 μm (Fig 2.2).

Using a Multiclamp 700A amplifier (Axon Instruments, USA), controlled via Multiclamp Commander software, voltage-clamp mode was used to search for cells *in vivo* (Margrie *et al.*, 2002). The evoked current in response to a square voltage step (+10 mV, 10 ms steps at 100 Hz) was monitored and used as an indicator of pipette resistance, which increases when the pipette

A

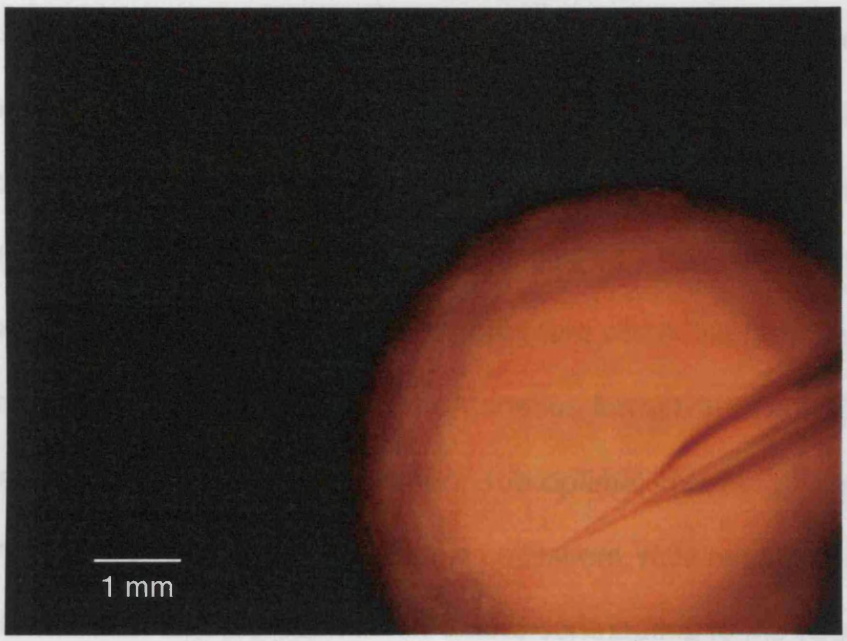

B

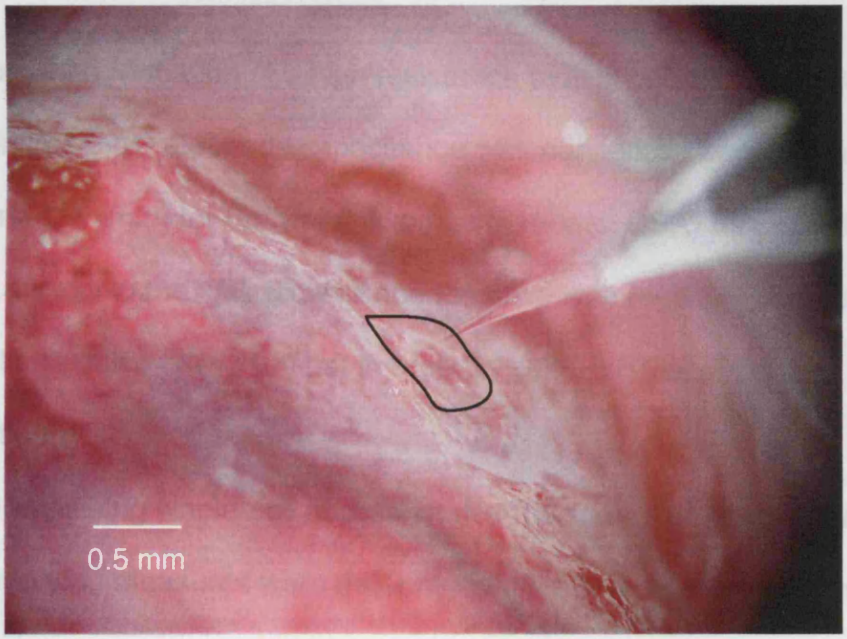

Figure 2.2

Patch clamping in the cerebellum *in vivo*. **A** Patch pipette viewed under dissecting scope to illustrate shank geometry. **B** Patch pipettes were carefully advanced onto the exposed surface of the cerebellum. Outline indicates approximate area of craniotomy, made above folium Crus IIa.

contacts cell membranes. Pipettes were rapidly advanced into the area of interest under high positive pressure (100-200 mbar) in order to minimise the likelihood of blockage. When reaching the area of interest, positive pressure was reduced to 25-35 mbar and the pipette advanced in 2 μm steps. Three consecutive steps associated with increased pipette resistance indicated the proximity of a cell membrane, and pressure was rapidly released. Under optimal conditions, the removal of positive pressure within the granule cell layer was usually associated with the spontaneous formation of a 1-10 GΩ seal (greater than 66% of attempts). Under sub-optimal conditions, and more generally within the molecular and Purkinje cell layers, mild negative pressure was applied to facilitate seal formation. Factors contributing to the success rate of patch clamp recordings *in vivo* are well described in Margrie *et al.* (2002).

Following formation of a high resistance seal in cell-attached voltage-clamp configuration, electrode capacitance was cancelled semi-automatically (Multiclamp Commander Software; Axon Instruments, USA) before obtaining electrical access to the cell. Slow ramped suction was regularly combined with a brief voltage pulse (+1V, 100 μs) in order to establish the whole-cell configuration.

Upon gaining whole-cell access, series resistance and membrane capacitance (C_m) measures were determined directly from the amplifier settings. Granule cell series resistances were in the range of 20-80 MΩ (mean: 39 ± 3 MΩ, n = 15), and were automatically compensated using Multiclamp Commander.

In whole-cell voltage recordings, electrode capacitance compensation (≈ 2.5 pF) was applied via Multiclamp Commander. Bridge-balancing was performed in Purkinje cells and interneurons, but was not routinely used in granule cell recordings, due to a much smaller R_s: R_{input} (D'Angelo *et al.*, 1995, 1998).

2.3.2 Drug Application

During whole-cell patch clamp recordings, drugs were dissolved in aCSF and applied directly to the exposed surface of the cerebellum using a custom-made micropipette.

Gabazine (SR95531; 0.5 – 1 mM) was used to selectively antagonise $GABA_A$ receptors. This compound avoids the non-selective antagonistic actions of the classical $GABA_A$ receptor antagonist, bicuculline, upon K^+ channels (Seutin *et al.*, 1997; Debarbieux *et al.*, 1998). The action of gabazine was assessed in voltage-clamp mode at holding potentials between –30 and 0 mV in order to visualise spontaneous IPSCs. 30-240 sec following gabazine application, the disappearance of spontaneous IPSCs indicated $GABA_A$ receptor blockade had occurred.

NBQX (0.5 mM) was used to selectively antagonise non-NMDA glutamate receptors. The action of NBQX was assessed in voltage-clamp mode at –70 mV in order to visualise spontaneous EPSCs. 30-240 sec following NBQX application, the disappearance of spontaneous EPSCs indicated that non-NMDA glutamate receptor blockade had occurred.

TTX was used to block voltage-gated Na^+ channels within the

cerebellar cortex, thus preventing action potential-mediated synaptic transmission in the local region of the cerebellar cortex. The action of TTX was assessed using strong depolarizing current commands to confirm the blockade of action potential generation in the cell being recorded from.

2.3.3 Sensory stimulation

Sensory responses were evoked using an air puff (30-300 ms, 60 p.s.i.) timed by a Picospritzer II (General Valve, USA). Rigid plastic tubing (inner diameter: 0.8 mm) was used to convey the stimulus from the main unit directly to a glass pipette (inner diameter: 0.86 mm) near the animal's face (Fig 2.3). The onset and duration of the stimulus was acquired directly from the Picospritzer. The delay from stimulus onset to the air puff reaching the face was measured by placing the end of stimulating pipette adjacent to a recording pipette (in bath configuration), and measuring the onset of the electrical signal in Axograph. An 11 ms delay was measured between stimulus onset and the air puff reaching the face. This value was subsequently subtracted from the onset latencies of all sensory-evoked responses. Typically, the tip of the pipette was placed 5 mm from the animal's face: each air puff stimulated 3-4 whiskers and/or a small circular area of skin (approx. diameter: 4 mm). During whole-cell recordings in voltage-clamp or voltage-recording modes, by slowly moving the tip of the pipette around perioral regions, it was possible to detect regions where air puff stimulation was correlated with the incidence of action potentials or synaptic events. Once a reliable sensory response was located, the stimulator was fixed, and

the intensity reduced to the lowest level at which sensory-evoked events could still be evoked (typically 20 - 40 p.s.i). Precise spatial-mapping of sensory responses was not performed in this study.

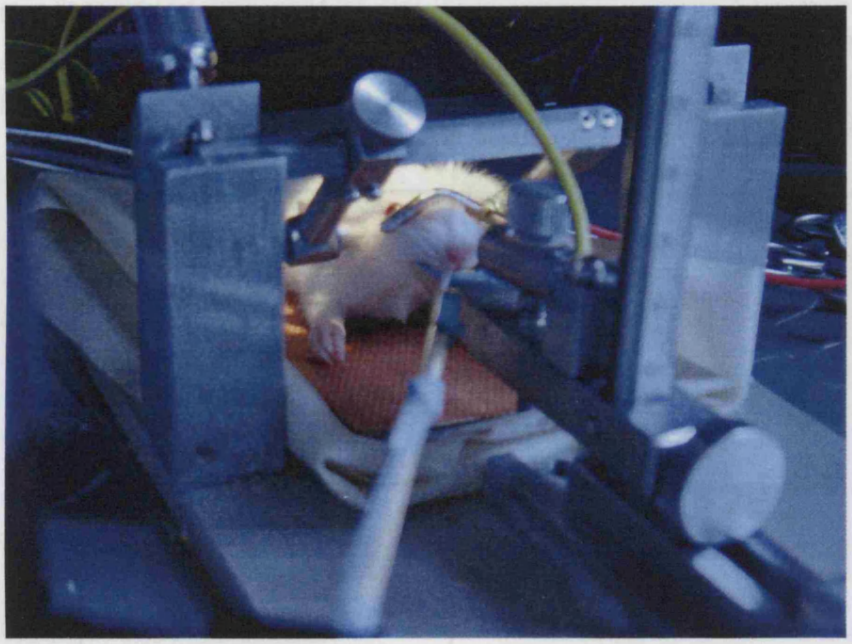

Figure 2.3

A glass capillary connected to a Picospritzer was placed close to the rat's face. Brief air puffs were used to stimulate whisker and lip areas.

2.4 DRUGS AND SOLUTIONS

2.4.1 Internal solution

COMPOUND	CONCENTRATION (mM)
K-Methanesulphonate	133
KCl	7
HEPES	10
Mg-ATP	2
Na_2-ATP	2
Na_2-GTP	0.5
EGTA	0.05

Internal solution was calibrated to pH 7.2 with KOH, and had an osmolarity in the range 280-290 mOsm. The internal Cl^- concentration was set to produce an IPSP reversal potential of –69 mV. This is close to the physiological value in granule cells measured using the gramicidin perforated-patch technique (-63 ± 5 mV at P18-21) (Brickley *et al.*, 1996).

2.4.2 Artificial cerebrospinal fluid (aCSF)

COMPOUND	CONCENTRATION (mM)
NaCl	125
$NaHCO_3$	5
NaH_2PO_4	10
KCl	1
$CaCl_2$	2
$MgCl_2$	2
Glucose	25

Extracellular solutions were continuously bubbled with 95% O_2 / 5% CO_2 prior to application to the brain surface.

2.4.3 Abbreviations and purveyors

Abbreviation	Full name	Source
EGTA	Ethylene glycol-bis(2-aminoethylether)-N,N,N',N'-tetraacetic acid	Sigma
Glucose	D-glucose	Sigma
Gabazine	2-(3-Carboxypropyl)-3-amino-6-(4 methoxyphenyl)pyridazinium bromide	Sigma
HEPES	4-(2-Hydroxyethyl)piperazine-1-ethanesulphonic acid	Sigma
KCl	Potassium chloride	Sigma
K-Methanesulphonate	Potassium methanesulphonate	Fluka
Mg-ATP	Magnesium adenosine triphosphate	Sigma
$MgCl_2$	Magnesium chloride	Sigma
NaCl	Sodium chloride	Sigma
$NaHCO_3$	Sodium bicarbonate	Sigma
NaH_2PO_4	Sodium dihydrogen phosphate	Sigma
Na_2-GTP	Disodium guanosine triphosphate	Sigma
NBQX	1,2,3,4-Tetrahydro-6-nitro-2,3-dioxo-benzo[f]quinoxaline-7-sulfonamide	Tocris
TTX	Tetrodotoxin	Tocris

2.5 DATA ACQUISITION AND ANALYSIS

Data were low-pass filtered at 3 - 10 kHz and acquired at 50 kHz via an ITC-18 interface (Instrutech, USA) using Axograph 4.8 software (Axon Instruments, USA). Data were analysed offline using Axograph 4.8 and Igor Pro (Wavemetrics, USA).

Resting membrane potential (V_m) was measured immediately after formation of the whole-cell configuration ('break-in'). The junction potential difference between the internal and extracellular solutions was measured (+10 mV) and corrected for (Neher, 1992), in order to accurately determine V_m.

Granule cell input resistance was calculated from steady-state voltage/current deflections during 400 ms step current (+5 pA) or voltage (-10 mV) injections. Input resistance of interneurons and Purkinje cells was measured using 400 ms step current injections (typically around –20 pA for interneurons, and –200 pA for Purkinje cells).

Accommodation index was calculated for individual granule cells as (mean final ISI) / (mean first ISI) during 400 ms step current injection of sufficient amplitude to induce saturating firing rates.

Spontaneous and evoked synaptic currents were detected using a template-matching algorithm in Axograph 4.8, with evoked EPSCs defined as events within a 50 ms window after the onset of the response. A representative

synaptic event was selected to serve as a template in each cell. Typically, only the rising phase of the EPSC was used as a template, as this improved the detection of closely-spaced events. Events were initially accepted if they exceeded a noise threshold (at least 3 times the standard deviation of the current noise). Subsequently, all events were visually inspected. EPSCs were initially distinguished as 'fast-rising', rather than 'spillover', events if their 10-90% rise times were below 0.25 ms. Thereafter, the rise time gradient of all events was visually inspected.

EPSC waveforms were generated by a double exponential current injection with mean kinetics of all spontaneous EPSCs recorded from a granule cell voltage clamped at –70 mV (τ_{rise} = 0.34 ms, τ_{decay} = 2.1 ms).

Analysis of Purkinje cell membrane potential bistability was performed as follows. Histograms of membrane potential distribution were constructed for each Purkinje cell and Gaussian fits (using Igor Pro) were applied to individual peaks. The modal value of each Gaussian fit was taken as the mean membrane potential for the up state and the down state. To measure the duration of each individual state, transitions between the up and down states were detected using the following thresholding procedure. Two thresholds were set at one quarter and three quarters of the distance between the peaks of the membrane potential distribution. When membrane potential rose above the lower threshold, a down-to-up transition was registered and when membrane potential fell below the upper threshold, an up-to-down transition was registered. To avoid defining noise or single complex spikes as short

states, pairs of lower and upper thresholds that generated a time difference of less than 50 ms were removed.

The deviation from unimodality of the membrane potential of Purkinje cells, as well as that granule cells and interneurons, was tested using a 'dip test' (Hartigan, 1985), on R (version 1.9.1). For each cell, the test was performed on 1000 randomly chosen values of membrane potential.

Statistical comparisons were made using Student's paired *t*-test unless otherwise indicated. In order to determine whether the amplitude distributions of evoked, spontaneous and miniature EPSCs were significantly different, a Kolmogorov-Smirnoff test was used. In cells where sensory-evoked currents were recorded, the Kolmogorov-Smirnoff test was calculated from the entire population of spontaneous and evoked EPSC amplitudes pooled from these cells. In a different group of cells (n = 4), a Kolmogorov-Smirnoff test was performed on the populations of spontaneous and miniature EPSC amplitudes pooled from these cells. Datasets were deemed to be significantly different if $p < 0.05$. Results are presented as mean ± SEM.

Chapter 3: INTRINSIC PROPERTIES OF CEREBELLAR GRANULE CELLS *IN VIVO*

3.1 INTRODUCTION

The activity of granule cells in the intact cerebellum is unknown. Granule cells receive the vast majority of the input to the cerebellum, via the mossy fibres. Each granule cell has only 1-7 short dendrites, with each dendrite receiving a single excitatory mossy fibre (Palay & Chan-Palay, 1974; Hamori & Somogyi, 1983; Jakab & Hamori, 1988). Granule cells also form the majority of excitatory synaptic contacts onto the sole cerebellar cortical output neurons, Purkinje cells, via the parallel fibres. Knowledge of granule cell activity patterns is therefore vital to our understanding of the computations performed within the cerebellum.

The use of traditional electrophysiological techniques to study the activity of individual granule cells within an intact neural network has been unsuccessful. Due to the very small size of their somata ($\approx$ 5 µm diameter), conventional sharp microelectrodes cannot be used to penetrate granule cells. Additionally, the high packing density of the granule cell layer - 3.2×10^6 granule cells per mm^3 (Palay & Chan-Palay, 1974) compared with 1.2×10^5 neurons per mm^3 in V1 of macaque cortex (O'Kusky & Colonnier, 1982) - has meant that extracellular recording techniques have been of limited utility, (Eccles *et al.*, 1971) due to the difficulty in isolating single units with certainty. As such, almost nothing is known about the physiological patterns of activity both received and produced by cerebellar granule cells *in vivo*.

However, use of whole-cell patch clamp techniques has yielded extensive electrophysiological data on the properties of cerebellar granule

cells in acute and cultured brain slices. In particular, it has been shown that *in vitro* granule cells have a very high input resistance - 2.3 ± 1.1 GΩ (D'Angelo *et al.*, 1995) - meaning that their membrane potential undergoes rather large fluctuations in response to small changes in conductance (D'Angelo *et al.*, 1995; Cathala *et al.*, 2003). They also have a fast membrane time constant (τ_m = 6.7 ± 3.3 ms; D'Angelo *et al.*, 1995), resulting in rapid voltage fluctuations (Silver *et al.*, 1992; Traynelis *et al.*, 1993). Modelling and experimental data confirm that granule cells are electrotonically compact, approximating to single electrical compartments (Gabbiani *et al.*, 1994; Cathala *et al.*, 2003). As a result, dendritic synaptic inputs are largely unfiltered when they reach the soma (Silver *et al.*, 1992; Cathala *et al.*, 2003).

Granule cells possess several voltage-sensitive conductances, including a persistent Na^+ conductance (D'Angelo *et al.*, 1998). They express AMPA and NMDA receptors at their excitatory postsynaptic densities (Silver *et al.*, 1992; Farrant *et al.*, 1994; DiGregorio *et al.*, 2002). NMDA receptors are also found at extrasynaptic locations on granule cell dendrites (Clark *et al.*, 1997).

In addition to direct postsynaptic receptor activation, neurotransmitter release has been shown to activate both extrasynaptic receptors (Farrant *et al.*, 1994; Clark *et al.*, 1997) and receptors at neighbouring granule cell synapses – 'spillover' activation - lengthening the decay time of both granule cell EPSC and IPSC waveforms (DiGregorio *et al.*, 2002; Hamann *et al.*, 2002). Additionally, in acute slices, granule cells are subject to a resting tonic inhibitory conductance due to an ongoing activation of their $GABA_A$-receptors by ambient levels of glomerular GABA (Brickley *et al.*, 1996; Wall & Usowicz,

1997; Brickley *et al.*, 2001; Rossi *et al.*, 2003a). This tonic GABAergic conductance exerts very powerful effects on the membrane properties of granule cells, profoundly altering their input-output relationships (Brickley et al 1996; Silver and Mitchell 2003).

Many of the membrane properties intrinsic to granule cells show considerable variation during development. Whilst cell migration is considered to be complete by P14 (Altman, 1972), the glomerulus continues to mature until P60 (Hamori & Somogyi, 1983). The tonic GABAergic conductance increases in magnitude until at least P28 (Brickley *et al.*, 1996). Similarly, synaptic and intrinsic conductance changes have been observed between P8 and P39 (Cathala *et al*, 2003). AMPA EPSCs become faster during development, and input resistance and input capacitance decrease. One result from many of these developmental changes is to speed up the EPSP waveform, suggesting that the time window for temporal summation decreases during development.

In combination with anatomical considerations, these *in vitro* data have been used to make inferences about the nature of information transfer through the granule cell layer (Gabbiani *et al.*, 1994; De Schutter, 2002; Hamann *et al.*, 2002), and will discussed in detail later. However, a key question of how realistically the properties of granule cells *in vitro* mimic those in the intact network has yet to be answered. Procedures used to produce acute brain slices are suspected to damage to dendritic and axonal structures, cause a skewed death of particular cell-types (commonly smaller interneurons) and 'wash-out' of neuromodulators and other extracellular signalling molecules. Most crucially, afferent input to the cortex is obliterated.

To address these issues, I have used blind cell-attached and whole-cell patch clamp techniques, targeted to the granule cell layer of the cerebella of anaesthetised, freely-breathing rats. This approach allows the unequivocal isolation of single neurons, and additionally, the study of sub- and supra-threshold electrical activity (Pei *et al.*, 1991; Ferster & Jagadeesh, 1992; Margrie *et al.*, 2002).

In this chapter I will explain how granule cells can be identified within the intact cerebellar cortex from their characteristic electrophysiological properties, and how synaptic and intrinsic conductances interact to set low granule cell activity rates in the lateral hemispheres of the anaesthetised rat cerebellum.

3.2 RESULTS

3.2.1 Characterisation of cerebellar granule cells

Blind cell-attached and whole-cell patch clamp recordings were made from the cerebella of freely breathing anaesthetised rats. Granule cells were identified by their depth within the cerebellar cortex (> 400 µm from the pial surface) and subsequently by their characteristic electrophysiological properties. Upon gigaseal formation, 'break-in' to whole-cell configuration was normally achieved rapidly (within 10 s) by combining mild negative pressure with a brief voltage pulse (+1V, 100 µs; Fig 3.1 A-C) – see chapter 2 for more details. The appearance of a capacitative transient (Fig 3.1D) indicated that whole-cell configuration had been established. Total membrane capacitance (C_m) was normally determined directly from the amplifier following automatic series resistance and capacitance compensation in voltage-clamp mode. An extremely small total membrane capacitance of granule cells *in vivo* was found to be characteristic (C_m = 3.8 ± 0.3 pF, n = 15), and consistent with patch-clamp recordings made from granule cells *in vitro* (D'Angelo *et al.*, 1995; Cathala *et al.*, 2003).

Immediately following break-in, step-current injections were made in voltage-recording mode to investigate granule cell membrane properties. Small current injections caused large, rapid deflections in membrane potential as a result of an extremely high input resistance (R_{input}= 1.1 ± 0.1 GΩ at resting potential, n = 62 cells) and a fast membrane time constant (τ= 6.9 ± 0.7 ms, n = 49). 10-40 pA injections from resting V_m were sufficient to

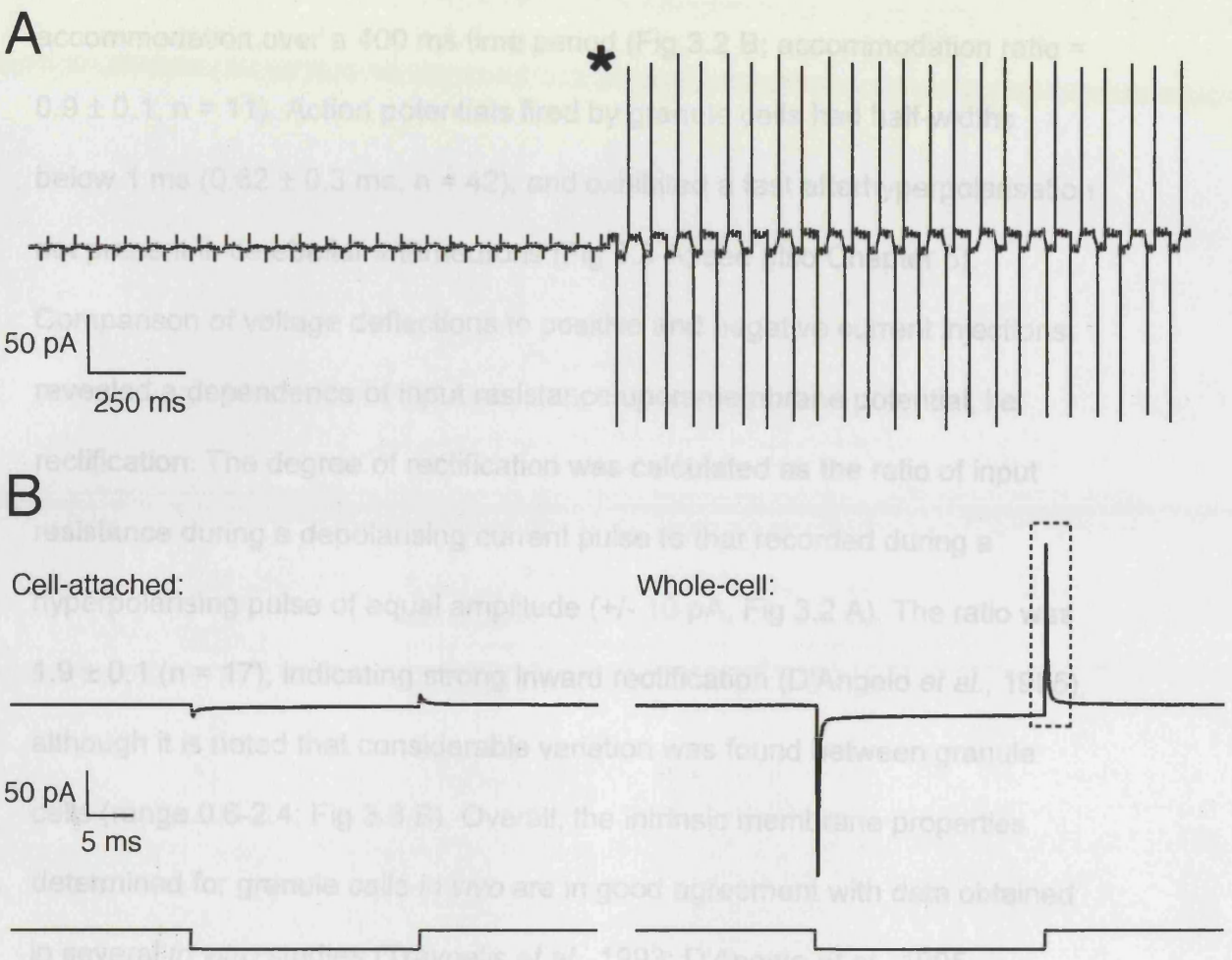

Figure 3.1

Membrane properties of a cerebellar granule cell *in vivo*. **A** Recording of pipette current in response to 10 mV test pulses following gigaohm seal formation and pipette capacitance compensation. At the marker (•), light suction was combined with a brief voltage pulse (+1 V, 100 µs) in order to gain whole-cell access to the cell. **B** Pipette current in response to a 10 mV test pulse in cell-attached (left) and whole-cell recordings (right) from the same granule cell (averages of 78 and 80 consecutive sweeps respectively). Series resistance = 54 MΩ.**C** Time constants were determined from exponential fits of current decay following the termination of a 10 mV test pulse in whole-cell configuration (in this example, trace corresponds to the hatched box in **B**, right). τ_{fast} was used to calculate total membrane capacitance, C_m. For this cell, C_m = 2.9 pF.

generate action potential firing (Fig 3.2 A) and strong depolarising current injections induced saturating firing rates of up to 250 Hz with little or no accommodation over a 400 ms time period (Fig 3.2 B; accommodation ratio = 0.9 ± 0.1, n = 11). Action potentials fired by granule cells had half-widths below 1 ms (0.62 ± 0.3 ms, n = 42), and exhibited a fast afterhyperpolarisation not present in cerebellar interneurons (Fig 3.3 A; see also Chapter 5). Comparison of voltage deflections to positive and negative current injections revealed a dependence of input resistance upon membrane potential, i.e. rectification. The degree of rectification was calculated as the ratio of input resistance during a depolarising current pulse to that recorded during a hyperpolarising pulse of equal amplitude (+/- 10 pA, Fig 3.2 A). The ratio was 1.9 ± 0.1 (n = 17), indicating strong inward rectification (D'Angelo *et al.*, 1995), although it is noted that considerable variation was found between granule cells (range 0.6-2.4; Fig 3.3 B). Overall, the intrinsic membrane properties determined for granule cells *in vivo* are in good agreement with data obtained in several *in vitro* studies (Traynelis *et al.*, 1993; D'Angelo *et al.*, 1995; Brickley *et al.*, 2001; Cathala *et al.*, 2003), allowing their unequivocal identification.

3.2.2 Spontaneous spiking activity of cerebellar granule cells

In order to determine the activity of granule cells at rest, voltage-recordings were made in the absence of DC current injection. Soon after break-in (within 2 minutes), resting membrane potential (V_m) and spontaneous firing rates were monitored for a 30-60 s period. Mean resting membrane

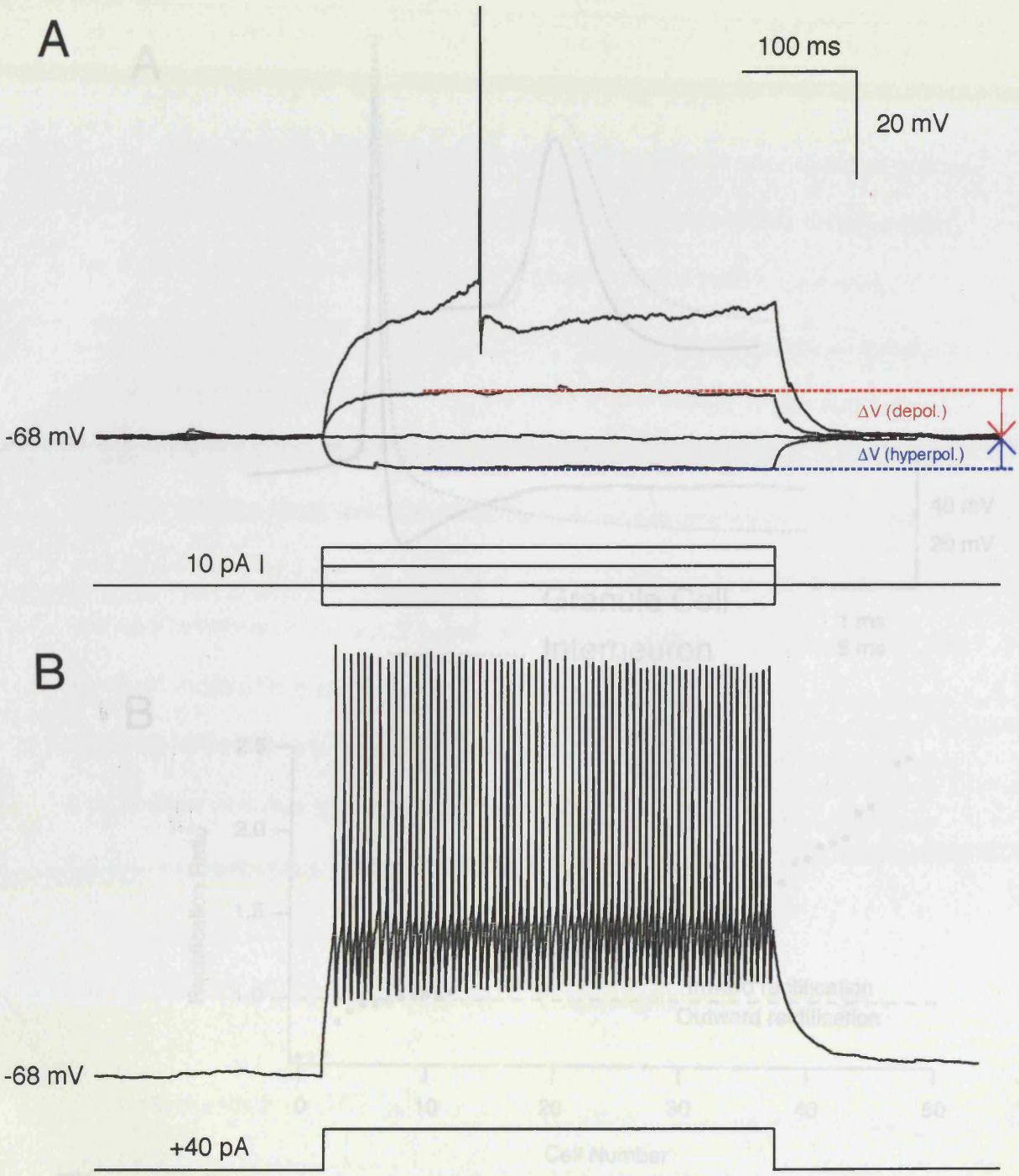

Figure 3.2

Current-voltage relationship for a single cerebellar granule cell. **A** Small current injections can trigger action potential firing. Granule cells show a characteristic inward rectification, calculated from ΔV (depol.)/ΔV (hyperpol.) following 10 pA step current injections. **B** Granule cells can fire action potentials at rates of up to 250 Hz with little or no accommodation.

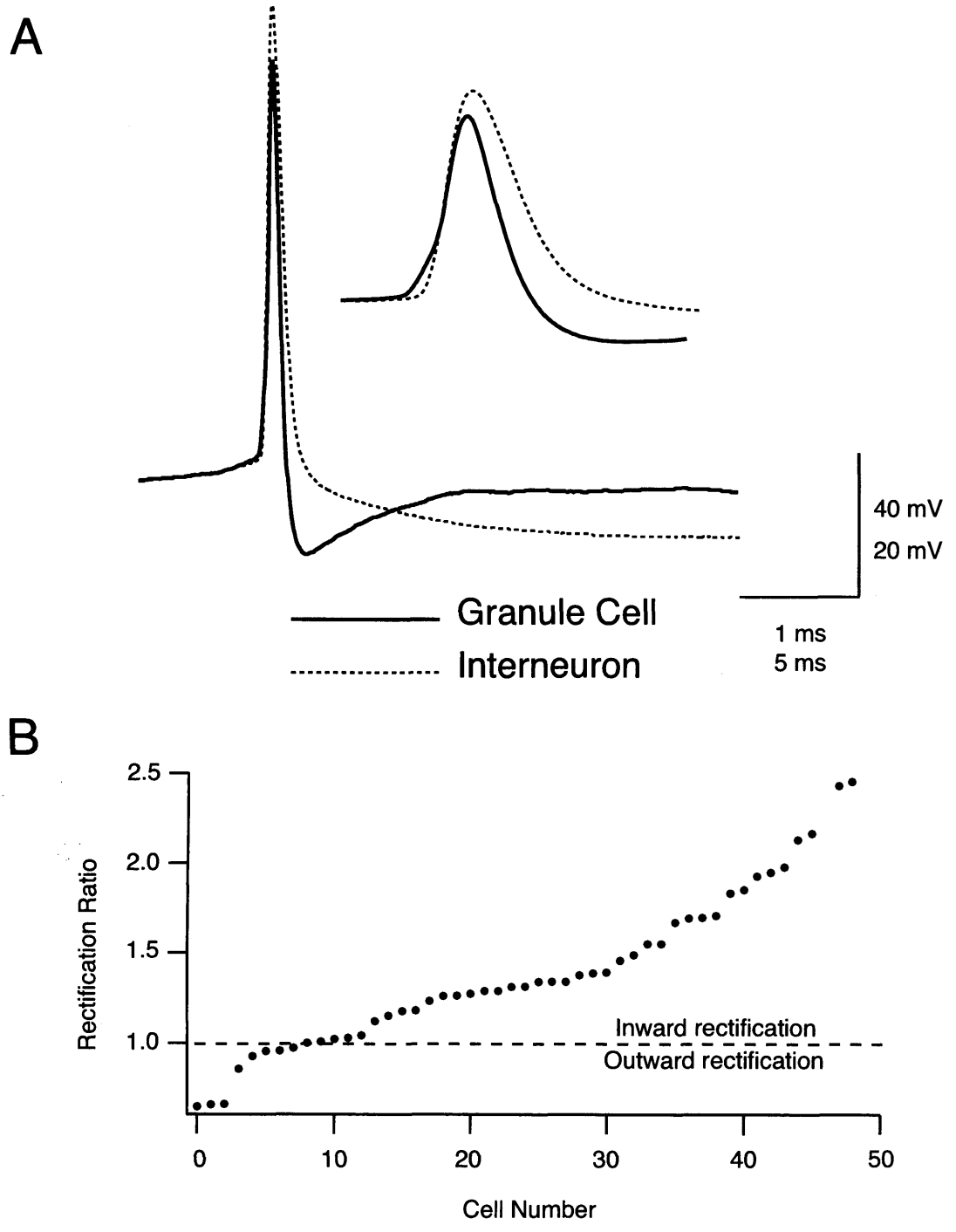

Figure 3.3

Intrinsic membrane properties of cerebellar granule cells *in vivo*. **A** Action potential waveform of cerebellar granule cell and granular-layer interneuron. Granule cell action potentials are brief and display a characteristic fast AHP. **B** The rectification ratio in cerebellar granule cells. Most granule cells show inward rectification.

potential was found to be –64 ± 1 mV, which was 24 ± 1 mV hyperpolarized to threshold (n = 75; Fig 3.4 A). The spontaneous firing rate of cerebellar granule cells *in vivo* was found to be low (0.5 ± 0.2 Hz, n = 46), and in many cases (70%), cells remained silent for the duration of recording.

Cell-attached recordings were not used to assess spontaneous granule cell firing rates because it was rarely possible to remain in this configuration for a sufficient period of time and then break-in successfully. Generally, in order to gain whole-cell access to granule cells, it was necessary to break-in as soon as possible after gigaohm seal formation, usually within seconds.

The low ongoing firing rates observed in whole-cell configuration are in keeping with the large average distance between resting membrane potential and threshold (Fig 3.4 B, C). A variety of factors are likely to contribute to the low spontaneous firing rate of cerebellar granule cells *in vivo*. In particular, low levels of mossy fibre excitatory input and/or strong inhibitory input from Golgi cells might be expected to decrease the likelihood of spike generation. The contribution of these two distinct synaptic inputs on granule cell output was therefore investigated.

3.2.3 Excitatory spontaneous synaptic activity to cerebellar granule cells

Mossy fibre synaptic events were observed in both voltage-recording (Fig 3.4 B) and voltage-clamp modes. Voltage-clamp recordings were made at –70 mV (the reversal potential of $GABA_A$ receptor-mediated conductance), affording good resolution of mossy fibre EPSCs (Silver *et al.*, 1992) in the absence of IPSCs (Fig 3.5 A). Spontaneous EPSCs with amplitude of -8.7 ±

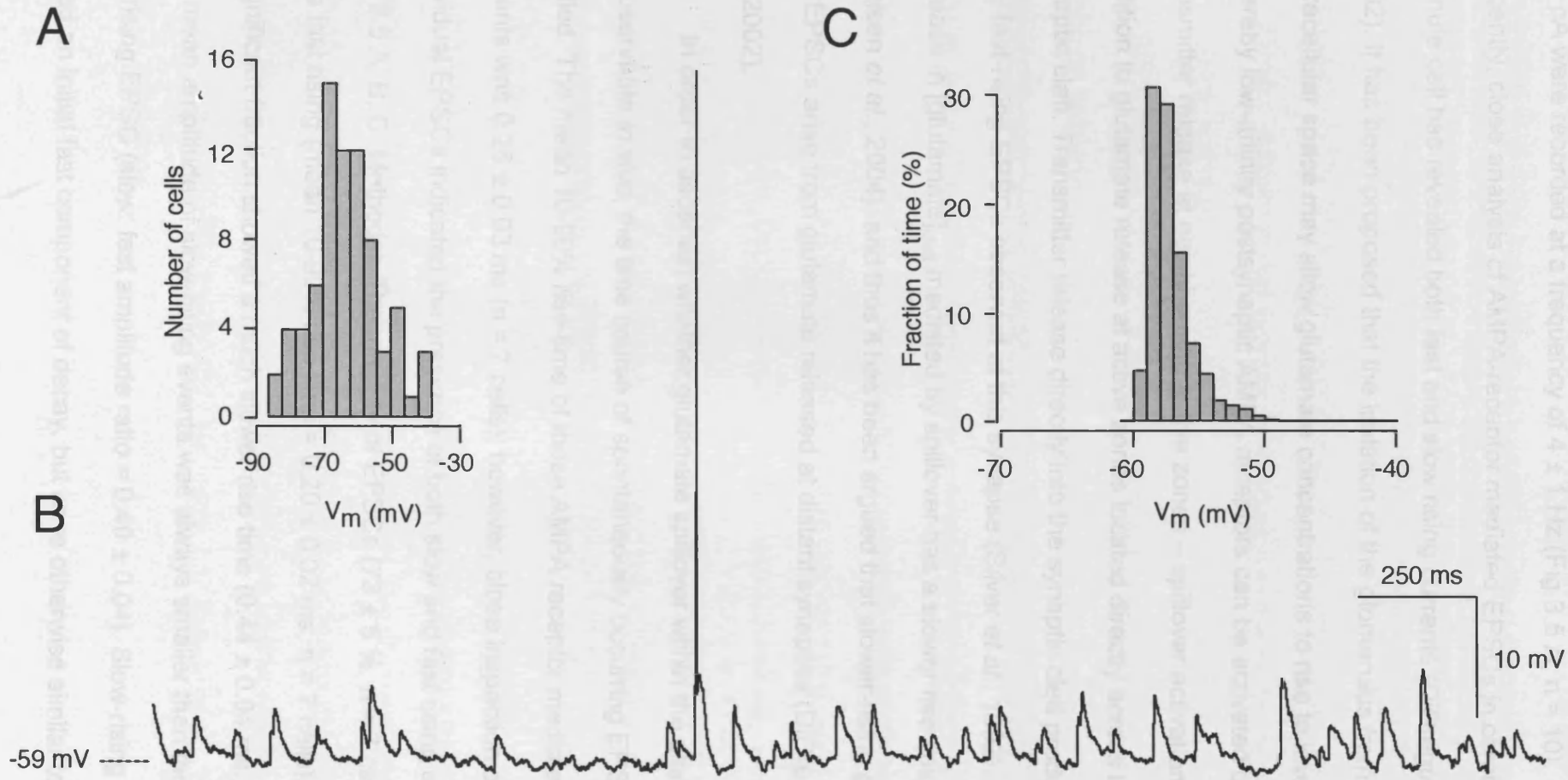

Figure 3.4

Spontaneous activity of cerebellar granule cells *in vivo*. **A** Histogram of granule cell resting membrane potential (V_m; bin size = 4 mV), immediately following 'break-in'.**B** Voltage recording from a single granule cell in the absence of injected current. Ongoing excitatory synaptic activity at around 10 Hz is rarely sufficent to drive action potential firing. **C** Histogram of membrane potential (V_m; bin size = 1 mV) from the same cell.

1.1 pA were recorded at a frequency of 4 ± 1 Hz (Fig 3.5 A; n = 10). Recently, close analysis of AMPA-receptor mediated EPSCs in cerebellar granule cell has revealed both fast and slow rising currents (DiGregorio *et al.*, 2002). It has been proposed that the isolation of the glomerulus from the extracellular space may allow glutamate concentrations to rise to levels whereby low-affinity postsynaptic AMPA receptors can be activated by transmitter release at neighbouring active zones – spillover activation – in addition to glutamate release at active zones located directly across the synaptic cleft. Transmitter release directly into the synaptic cleft produces the very fast-rising EPSCs observed at this synapse (Silver *et al.*, 1992). The increase in $[glutamate]_{cleft}$ mediated by spillover has a slower rise time (Nielsen *et al.*, 2004), and thus it has been argued that slower-rising granule cell EPSCs arise from glutamate released at distant synapses (DiGregorio *et al.*, 2002).

In order to ascertain whether glutamate spillover within the glomerulus is observable *in vivo*, the time course of spontaneously occurring EPSCs was studied. The mean 10-90% rise-time of these AMPA receptor mediated currents was 0.26 ± 0.03 ms (n = 7 cells); however, close inspection of individual EPSCs indicated the presence of both slow and fast rising events (Fig 3.5 A, B, C; Methods). The majority of EPSCs (73 ± 5 %, n = 7 cells) were fast rising (mean 10-90% rise time = 0.20 ± 0.02 ms, n = 7 cells), whilst a significant fraction showed a much slower rise time (0.44 ± 0.04 ms, n = 6). The mean amplitude of slow-rising events was always smaller than the mean fast-rising EPSC (slow: fast amplitude ratio = 0.49 ± 0.04). Slow-rising EPSCs lacked an initial fast component of decay, but were otherwise similar to both

the overall and fast-rising means at late times (> 2 ms; 50-10 % decay time = 7.7 ± 2.0 ms and 8.9 ± 1.4 ms for fast- and slow-rising current respectively, n = 7, P > 0.5, unpaired *t*-test; Fig 3.5 D). These data are quantitatively similar to those described in granule cells in cerebellar cortical slices at physiological temperature in P24-26 rats (DiGregorio *et al.*, 2002), and thus support a role for glutamate spillover in fast synaptic transmission at the mossy fibre-granule cell connection *in vivo*.

Since granule cell input resistance commonly increased with membrane potential depolarisation, and granule cells are known to express both synaptic and intrinsic voltage-sensitive conductances, it seemed likely that summation of excitatory postsynaptic potentials (EPSPs) would be a non-linear process. In order to assess the role of membrane voltage to the shaping of synaptic potentials, spontaneous EPSPs were recorded at a range of membrane potentials. Depolarisation from –70 mV to –55 mV was associated with an increase in both the peak (2.4 ± 0.4 mV at –65 mV to 2.9 ± 0.4 mV at –50 mV, p = 0.11, n = 8 cells, Fig 3.6 A, B, C) and the half-width of spontaneous EPSPs (12.9 ± 2.0 ms at –70 mV to 20.5 ms at –50 mV, $p < 0.01$, n = 8 cells; Fig 3.6 D). The increase in input resistance with depolarisation of membrane potential (Fig 3.2 A) will necessarily account for some of the boosting of EPSP amplitudes. However, the dramatic broadening of the EPSP waveform can only be accounted for by activation of voltage-sensitive synaptic and intrinsic conductances, of which NMDA receptors (D'Angelo *et al.*, 1995) and a persistent Na^+ current (D'Angelo *et al.*, 1998) are probable candidates.

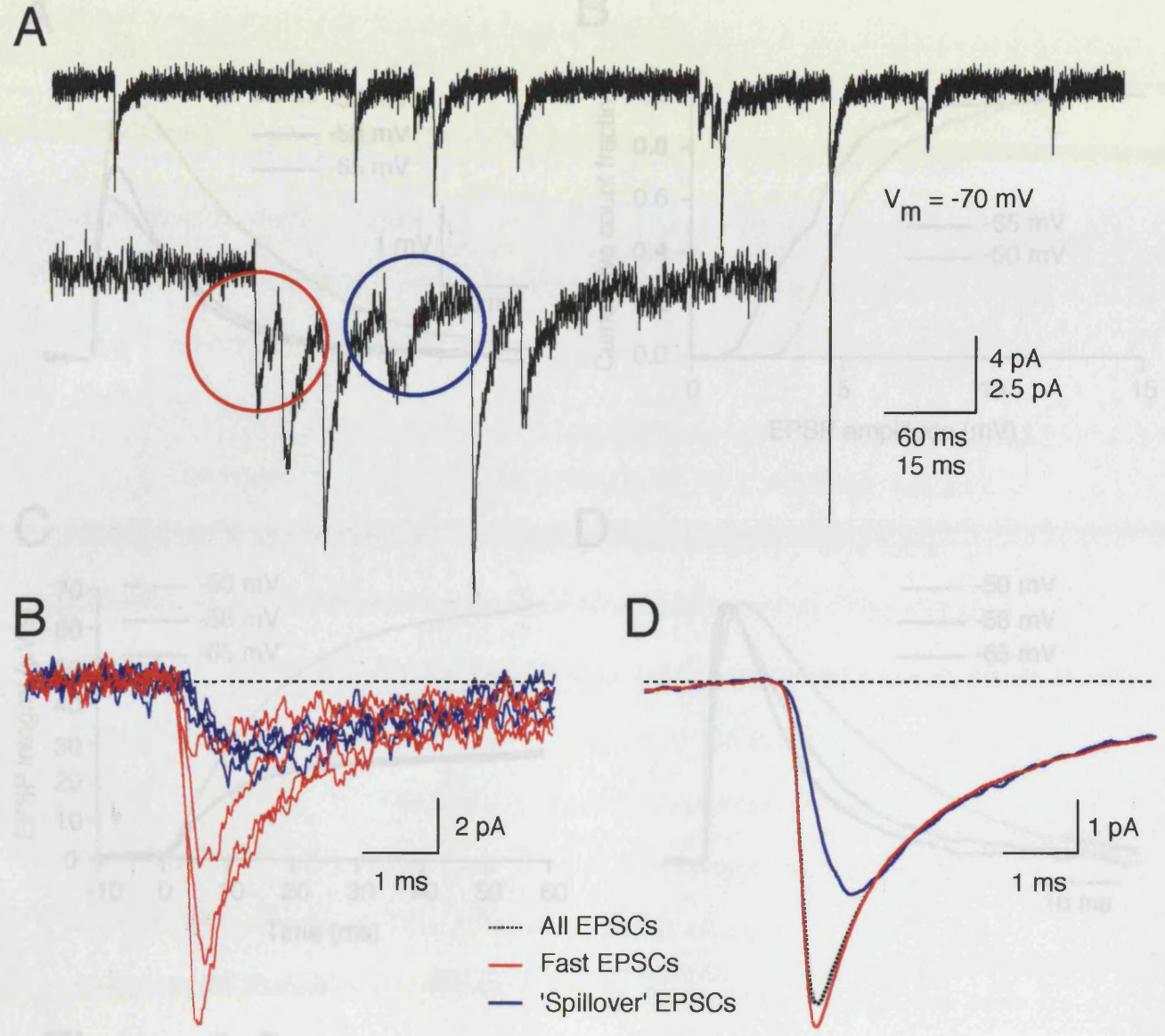

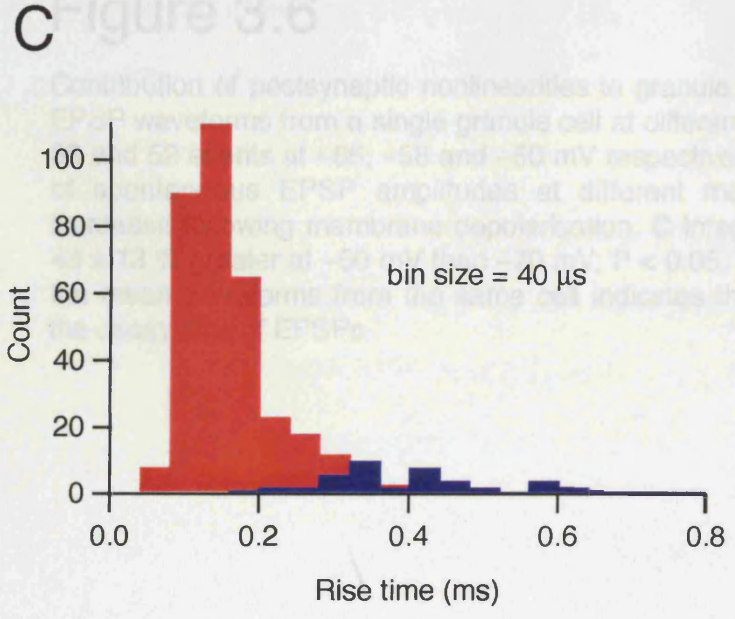

Figure 3.5

Evidence for spillover of glutamate within the glomeruli of cerebellar granule cells *in vivo*. **A** Top trace: Spontaneous mossy fibre EPSCs recorded at -70 mV. Bottom trace: Both fast (red circle) and slow (blue circle) rising currents were identified. **B** Captured EPSC waveforms from a single granule cell, both fast (red) and slow ('spillover': blue). Waveforms were selected using a template matching algorithm, and visual sorting of fast and slow rise currents. **C** Histogram of EPSC rise-times from a single granule cell. **D** Mean EPSC waveforms for fast (red), spillover (blue) and all (dotted) waveforms. The timecourse of decay is identical for both fast and spillover currents.

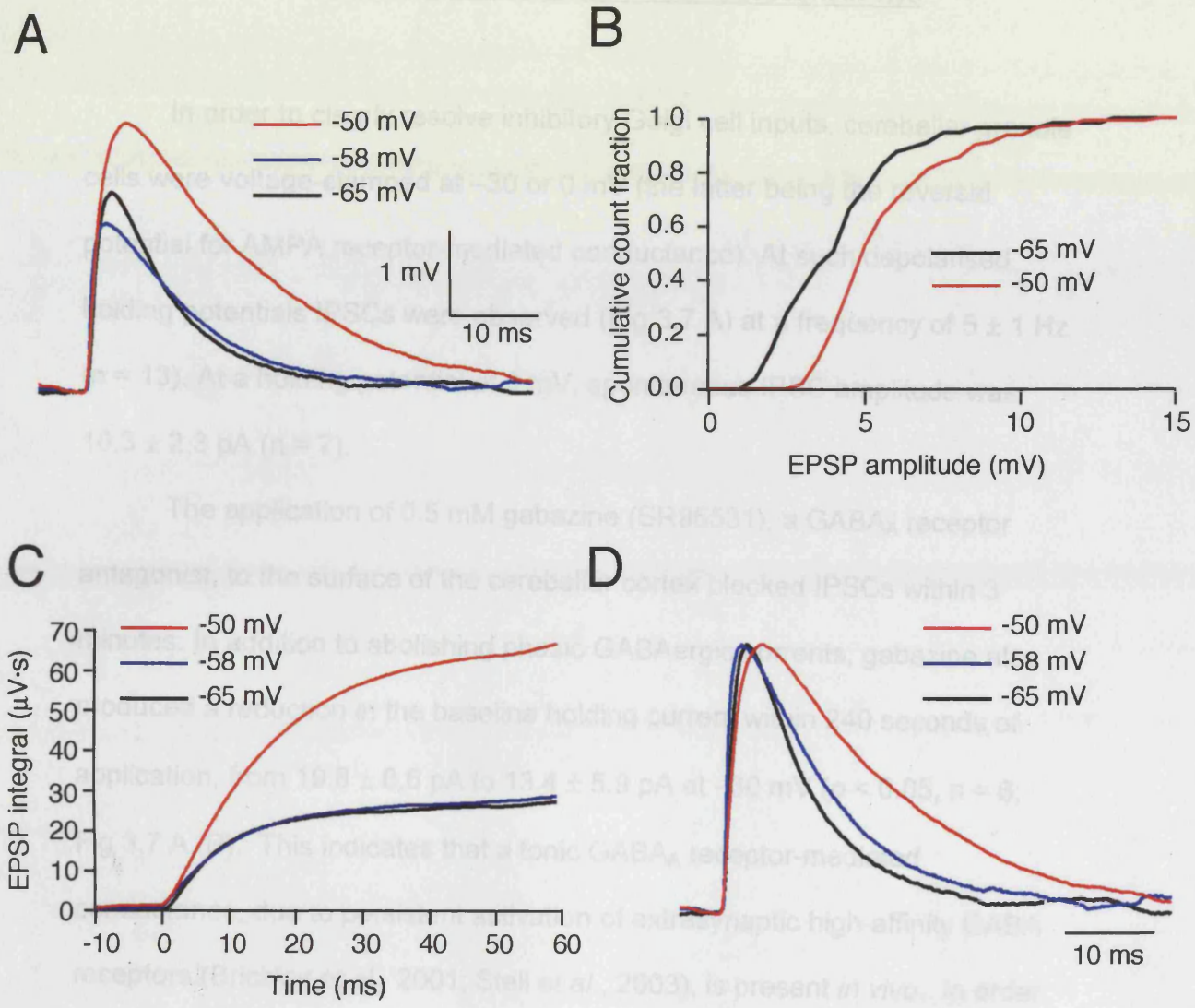

Figure 3.6

Contribution of postsynaptic nonlinearities to granule cell integration *in vivo*. **A** Spontaneous EPSP waveforms from a single granule cell at different membrane potentials (averages of 41, 33 and 52 events at –65, –58 and –50 mV respectively). **B** Normalised cumulative histogram of spontaneous EPSP amplitudes at different membrane potentials. EPSP amplitude increased following membrane depolarisation. **C** Integral of the EPSPs shown in **A** (integral 43 ± 13 % greater at –50 mV than –70 mV; $P < 0.05$, $n = 5$ cells). **D** Normalisation to peak of the mean waveforms from the same cell indicates that membrane depolarisation lengthens the decay time of EPSPs.

3.2.4 Tonic GABAergic inhibition to granule cells is present *in vivo*

In order to clearly resolve inhibitory Golgi cell inputs, cerebellar granule cells were voltage-clamped at –30 or 0 mV (the latter being the reversal potential for AMPA receptor-mediated conductance). At such depolarised holding potentials IPSCs were observed (Fig 3.7 A) at a frequency of 5 ± 1 Hz (n = 13). At a holding potential of 0 mV, spontaneous IPSC amplitude was 10.3 ± 2.3 pA (n = 7).

The application of 0.5 mM gabazine (SR95531), a $GABA_A$ receptor antagonist, to the surface of the cerebellar cortex blocked IPSCs within 3 minutes. In addition to abolishing phasic GABAergic currents, gabazine also produced a reduction in the baseline holding current within 240 seconds of application, from 19.8 ± 6.6 pA to 13.4 ± 5.9 pA at –30 mV ($p < 0.05$, n = 6; Fig 3.7 A, B). This indicates that a tonic $GABA_A$ receptor-mediated conductance, due to persistent activation of extrasynaptic high-affinity GABA receptors (Brickley *et al.*, 2001; Stell *et al.*, 2003), is present *in vivo*. In order to investigate the role that Golgi cell firing has in the maintenance of this tonic current, correlations between IPSC rates (presumed to represent Golgi cell spiking) and the amplitude of the tonic conductance were examined for individual granule cells. Granule cells with higher IPSC rates did generally show larger tonic conductances, although this relationship was not statistically significant ($p > 0.5$, n = 7, Spearman Rank Order correlation; STATISTICA 5.1; StatSoft, Tulsa, USA; see Appendix B, Fig B1 C).

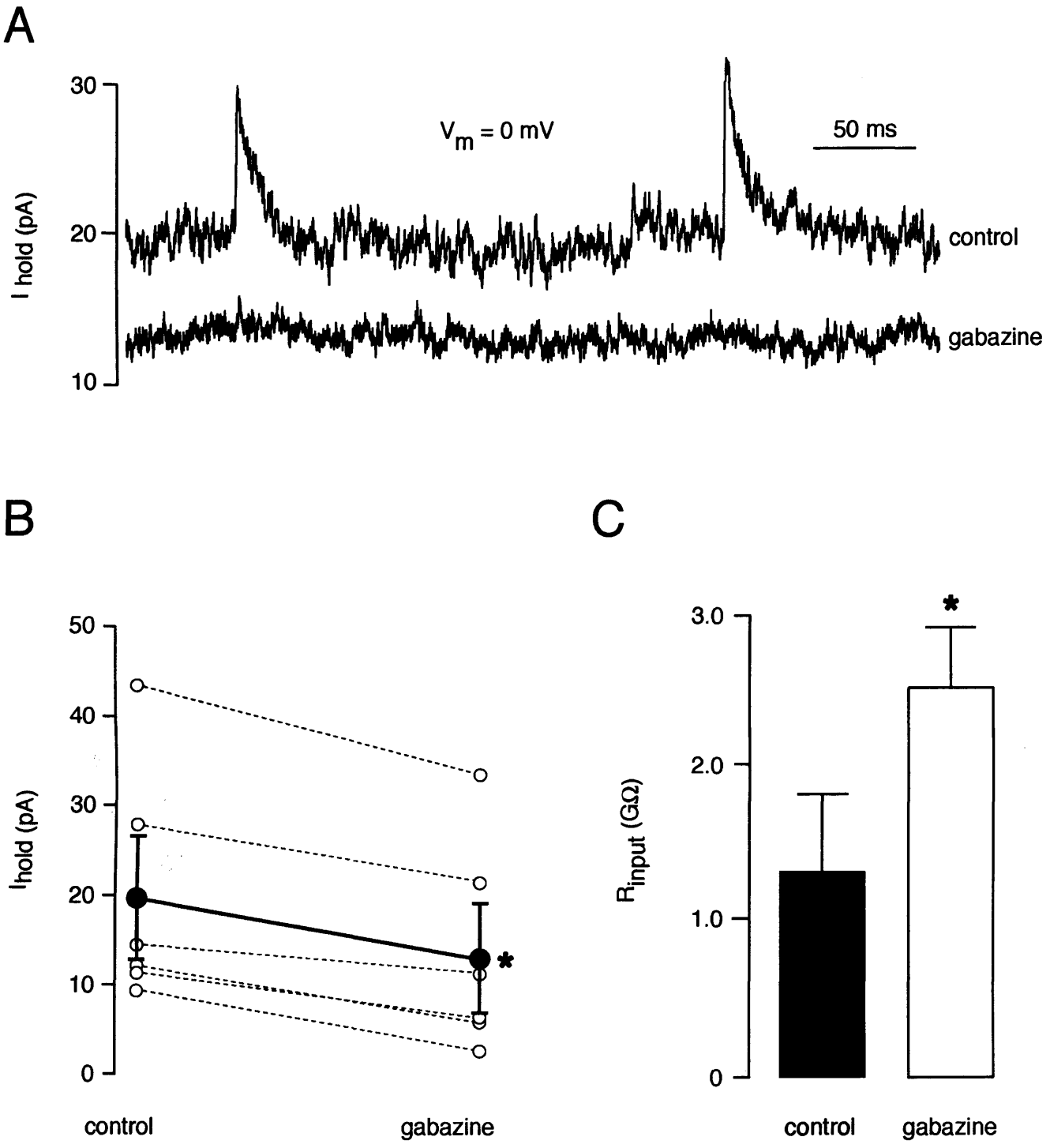

Figure 3.7

Phasic and tonic components of GABAergic inhibition to cerebellar granule cells. **A** Voltage-clamp recording at 0 mV. Gabazine (0.5 mM) abolished outward currents and reduced the tonic holding current (gabazine trace: 30 s after drug application). **B** $GABA_A$-receptor blockade produced a drop in the mean holding current required to clamp granule cells at -30 mV (6.3 ± 1.0 pA, *$p < 0.05$, $n = 6$). **C** Input resistance, measured at -60 mV, increased following gabazine application (*$p < 0.05$, $n = 6$).

3.2.5 Tonic inhibition causes a rightward shift in granule cell current- spike frequency relationship

It was considered likely that a tonically-active inhibitory conductance would exert effects on the current-voltage (I-V) relationship of granule cells, and hence on the likelihood of crossing action potential threshold (Brickley *et al.*, 1996). Active conductances reduce neuronal input resistance, increasing the 'leak' of current across the cell membrane. Therefore, I investigated what effect block of tonic inhibition would have on the relationship between injected current and action potential generation (the f/I relationship). In voltage-recording mode, DC current was used to maintain membrane potential at –60 ± 2 mV, and small incremental (+2.5 pA) current injections were used to establish the relationship between current amplitude and the number of evoked action potentials. Under control conditions, there was an approximately linear relationship between the amplitude of the 400 ms step current injection and the number of evoked action potentials (see Fig 3.8 A, B). Blockade of $GABA_A$ receptors produced an approximate doubling of the input resistance measured at –60 mV (1.3 ± 0.5 to 2.5 ± 0.4 GΩ, $p < 0.01$, n = 6; Fig 3.7 C) and caused a profound increase in the granule cell excitability: the number of action potentials generated by given current steps increased ($p > 0.01$, n = 3; Fig 3.8 A) and the mean 'current threshold' necessary to evoke action potentials fell from 8.3 ± 4.4 to 2.5 ± 1.8 pA. The observed increase in granule cell excitability was reflected in a leftward shift in the f/I relationship (Fig 3.8 B), with no detectable change in the slope. These results highlight the

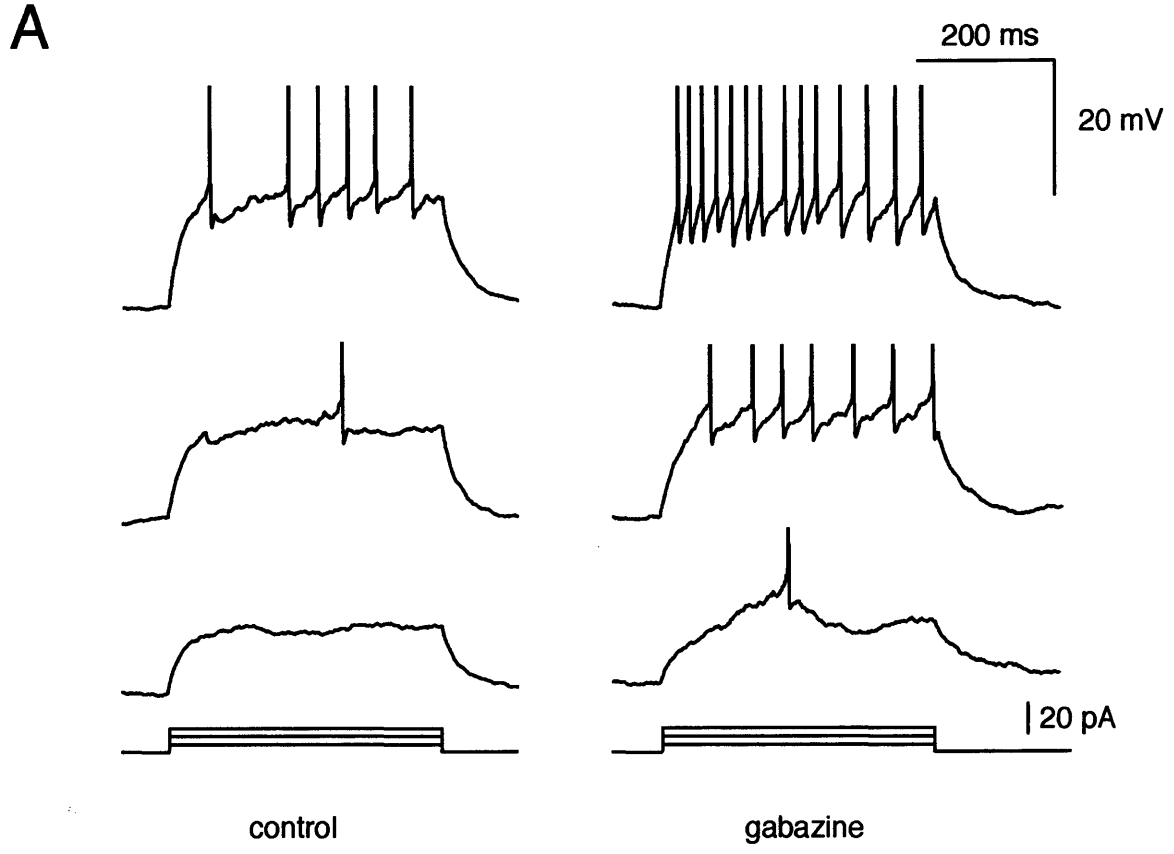

Figure 3.8

Tonic inhibition dampens excitability of cerebellar granule cells *in vivo*.
A Response of a single granule cell to current injection (5, 10, 15 pA) before and after $GABA_A$-receptor blockade (action potentials are truncated). **B** Increased excitability in gabazine is reflected in a leftward shift in the *f-I* curve.

potential importance of the tonic inhibitory conductance in regulating granule cell excitability.

3.2.6 Effect of tonic inhibition on mossy fibre EPSPs

Having shown that tonic inhibition alters the f/I relationship of granule cells *in vivo*, I wished to assess the contribution that the inhibitory conductance makes to the shaping of mossy fibre synaptic potentials. Changes in the peak amplitude and the decay time of granule cell EPSPs are likely to alter synaptic integration and consequently influence spontaneous action potential firing. Voltage recordings were therefore made of spontaneous EPSPs, in the absence of injected current, before and after gabazine application. Block of inhibition produced a small but significant depolarisation of resting membrane potential (3.8 ± 1.4 mV, $p < 0.05$, n = 7), and the amplitude and duration of spontaneously occurring EPSPs were greatly enhanced (Fig 3.9 A): mean EPSP amplitude rose from 1.9 ± 0.4 to 3.7± 0.5 mV ($p < 0.05$, n = 4) and EPSP half-width increased from 19.7 ± 5.4 to 36.8 ± 8.2 ms ($p < 0.01$, n = 4). Furthermore, in the absence of tonic inhibition, single EPSPs were on occasion sufficient to trigger action potential firing (Fig 3.9 A), a phenomenon not observed control conditions.

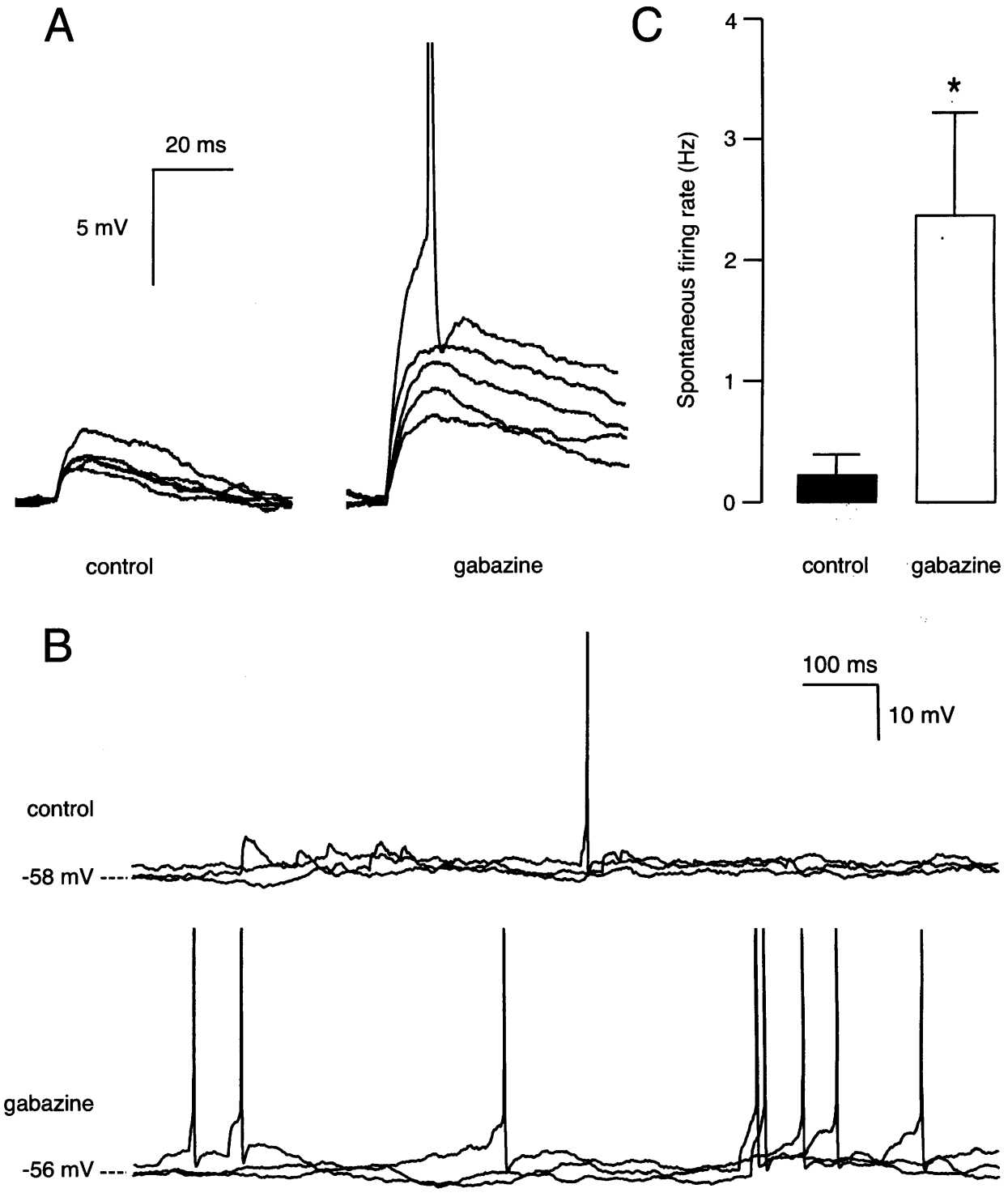

Figure 3.9

Low spontaneous firing rates are enforced by tonic inhibition *in vivo*. **A** Representative spontaneous EPSPs before and after $GABA_A$ receptor blockade (action potential is truncated). **B** Voltage recording (three overlaid traces) from a granule cell at rest (top) and after $GABA_A$ receptor blockade (bottom). **C** Spontaneous firing rates increased in the presence of gabazine (*$p < 0.05$, $n = 5$).

3.2.7 Spontaneous firing rates are reduced by tonic inhibition

The spontaneous firing rates of granule cells were monitored under control conditions, and following $GABA_A$ receptor blockade. Firing rates were assessed 30-120 seconds after gabazine application, over a period of at least 30 seconds. The block of inhibition caused the firing rate to rise from 0.2 ± 0.2 to 2.4 ± 0.9 Hz ($p < 0.05$, $n = 5$; Fig 3.9 B, C). This large increase - an order of magnitude - demonstrates that tonic inhibition is an extremely important regulator of granule cell excitability *in vivo*.

3.3 DISCUSSION

3.3.1 Intrinsic properties of cerebellar granule cells

The extremely small size of granule cell somata, and the limited branching pattern of a small number of dendrites, endow granule cells with a high degree of electrical compactness. This is reflected in a very small membrane capacitance (>5 pF; Cathala *et al.*, 2003, Fig 3.1), and an extremely high input resistance, measured both in the slice (τ = 6.9 ± 3.3 ms, R_{input} = 2.3 ± 1.1 GΩ; D'Angelo *et al.*, 1995) and *in vivo* (τ = 6.9 ± 0.7 ms, R_{input} = 1.1 ± 0.1 GΩ). As a consequence, very small currents are sufficient to cause significant depolarisation of membrane potential and trigger action potential firing. This suggests that only a small number of synaptic inputs might be sufficient to drive granule cell membrane potential above threshold, and generate spiking. When sufficiently depolarised, granule cells can be driven to fire at high frequencies (up to 250 Hz). High frequency firing is known to generate supralinear effects downstream of the granule cell at the parallel fibre-Purkinje cell synapse. For example, paired pulse facilitation of transmitter release (Konnerth *et al.*, 1990; Perkel *et al.*, 1990; Dittman *et al.*, 2000), activation of postsynaptic metabotropic glutamate receptors (Takechi *et al.*, 1998; Wang *et al.*, 2000), endocannabinoid release (Brown *et al.*, 2003) and long-term changes in synaptic efficacy (Casado *et al.*, 2002) all show strong dependence upon the frequency of parallel fibre firing. The work presented in chapter 4 of this thesis will investigate whether high frequency firing is seen in response to physiological stimuli.

Throughout this study, a low level of Ca^{2+} buffering was employed (0.05 mM EGTA), and it is therefore possible that the endogenous Ca^{2+} buffering capacity of granule cells is reduced in whole-cell recordings. Previous studies have shown that granule cells express the buffering protein calretinin (Rogers & Resibois, 1992; Gall *et al.*, 2003), and several Ca^{2+}-dependent conductances (Gabbiani *et al.*, 1994; D'Angelo *et al.*, 1997, 1998; D'Angelo *et al.*, 2001) which are expected to be susceptible to altered Ca^{2+} dynamics. However, the active and passive properties of granule cells in this study are qualitatively and quantitatively similar to previous *in vitro* studies, suggesting that granule cell intrinsic properties are not dramatically altered.

The wide range of granule cell resting membrane potentials (Fig 3.4 A) is likely to result from several factors. Both excitatory and inhibitory synaptic inputs contribute to the value of V_m, as will be discussed below. Additionally, a 'standing-outward' K^+ current has been reported in cerebellar granule cells, mediated by two-pore domain potassium channels such as TASK-1 and TASK 3 (Millar *et al.*, 2000; Kang *et al.*, 2003). TASK-1 channels are subject to cholinergic modulation by M_3 receptors (Millar *et al.*, 2000), and it thus seems likely that variability in this modulation *in vivo* will accordingly result in a variability of granule cell V_m. Such modulation may also account for the observed variation in granule cell inward rectification (Fig 3.3 B).

An additional source of variability within the dataset is likely to result from the maturation of synaptic and intrinsic conductances that has been observed to occur until at least P39. These factors contribute to a negative change in granule cell input resistance and resting membrane potential during development (Brickley *et al.*, 1996; Cathala *et al.*, 2003).

3.3.2 Granule cells have low spontaneous firing rates *in vivo*

Using whole-cell patch clamp recordings it has been possible to unambiguously record the activity of single cerebellar granule cells for the first time. Previous studies that have investigated the activity of cerebellar granule cells in the intact brain have mostly relied upon LFP recordings (Bower & Woolston, 1983). A handful of studies have used extracellular recordings to monitor granule cell spiking. Eccles and colleagues (1971) used such techniques to distinguish between the activity of mossy fibres and granule cells in the cerebella of decerebrate cats, and reported firing rates of between 4 and 70 Hz for putative granule cells (described as 'Type II units'). In results presented here, ongoing granule cell firing was found to occur at far lower frequencies (0.5 ± 0.2 Hz).

The whole-cell patch-clamp technique affords two major advantages in the study of neuronal spiking activity. Firstly, it permits the unambiguous isolation of single units, unlike extracellular recording techniques. Secondly, extracellular recording requires spiking activity in order to 'see' neurons. Cells that are silent, or that are firing at low rates, are detected with far greater difficulty than highly active neurons. Thus, patch-clamp avoids a major bias in the recording of neuronal spiking, and perhaps explains the order-of-magnitude difference in granule cell spike rates observed between this study and the earlier work of Eccles.

The theoretical works of Marr and Albus (Marr, 1969; Albus, 1971) argue that the activity of granule cells and thus the parallel fibres must be kept

low in order to allow the discrimination of the largest number of distinct patterns by Purkinje cells. Specifically, pattern discrimination within the cerebellum is optimised when the total fraction of concomitantly active parallel fibre inputs to Purkinje cells is kept below 1% (Albus, 1971; Tyrrell & Willshaw, 1992). The low rates of granule cell activity at rest observed here provide the first experimental evidence in support of these hypotheses. Furthermore, granule cell quiescence establishes the cerebellar network as a 'low-noise' environment in which to represent sensory information.

3.3.3 Excitatory synaptic inputs to cerebellar granule cells

In order to understand the factors contributing to the low spontaneous firing rates of cerebellar granule cells *in vivo*, incoming synaptic activity to these neurons was studied. The compact morphology of cerebellar granule cells provides a major technical advantage in this pursuit, allowing exceptional temporal resolution of synaptic currents (Silver *et al.*, 1992). Granule cells typically receive ongoing mossy fibre inputs at low rates (4 ± 1 Hz). I have recorded excitatory synaptic currents at –70 mV, indicating that they are mediated by AMPA receptors at this potential. AMPA receptors are known to have a low-affinity for glutamate (EC50 ≈ 0.5 mM) (Jonas & Sakmann, 1992; Hausser & Roth, 1997), and thus it might be expected that only glutamate release directly onto postsynaptic receptors would activate them. However, the unique morphology of the cerebellar glomerulus, where many release sites lie within a restricted diffusional space, offers an environment where

glutamate release at active zones can potentially activate AMPA receptors at neighbouring postsynaptic densities. The finding that both fast- and slow-rising EPSCs can be observed in granule cells provides support for the hypothesis that spillover of glutamate within the glomerulus plays a functional role in synaptic transmission at this synapse. DiGregorio and colleagues conducted a careful study in granule cells *in vitro*, showing that slow-rising mossy fibre EPSCs result from activation of AMPA receptors, not from dendritic filtering (DiGregorio *et al.*, 2002), implicating spillover from neighbouring synapses within the glomerulus as the source of glutamate. Importantly, in both my results and DiGregorio *et al.*'s data, fast- and slow-EPSCs showed very similar decay kinetics, save for a very fast component (≤ 2 ms) absent in slow-rising currents (Fig 3.5 D). This suggests that the slow-rising component is a major determinant of the AMPA EPSC waveform *in vivo.*

Spillover AMPA currents within the cerebellar glomerulus will have two major functional consequences for synaptic transmission at the mossy fibre–granule cell connection. Firstly, since release probability is considerably less than 1 at this synapse (Sargent *et al.*, 2003; Sola *et al.*, 2004), spillover EPSCs are likely to compensate for failures in transmitter release at the primary release site, thus boosting the reliability of information transfer. Secondly, glutamate spillover contributes significantly to the time course of mossy fibre EPSCs (Fig 3.5.D; DiGregorio *et al.*, 2002), lengthening the decay time. It has been shown that slowly decaying synaptic currents can significantly affect integration in neurons (D'Angelo *et al.*, 1995; Harsch & Robinson, 2000), by broadening the time window over which synaptic inputs

can summate to trigger action potential firing. Taken together, it seems that glutamate spillover within the glomerulus may serve an ingenious role in the facilitation of information transfer at the mossy fibre-granule cell connection.

Factors affecting synaptic integration in granule cells were examined directly in voltage recordings of spontaneous synaptic activity. Granule cell input resistance varies with membrane voltage (Fig 3.2 A; D'Angelo *et al.*, 1995), increasing with depolarisation. As such, it is expected that summation of mossy fibre EPSPs will be a supralinear process. This expectation was supported by the finding that spontaneous EPSP amplitudes increased with membrane potential depolarisation (Fig 3.6 A, B).

A large cell-to-cell variability in the rectification ratio was observed in this study (Fig 3.3 B). There is recent evidence that the inward rectification observed in granule cells is regulated by $GABA_B$ receptors (Rossi *et al.*, 2003b), thus there exists the possibility that the degree of inward rectification may be subject to dynamic modulation. Rossi's data suggest a possible role for $GABA_B$ receptors in regulating the input-output relationship for cerebellar granule cells.

In addition to the dependence of EPSP amplitude upon membrane voltage, EPSP half width was also lengthened at potentials positive to –55mV. Previous studies have highlighted the importance of both persistent Na^+ currents (D'Angelo *et al.*, 1998) and NMDA receptor currents (D'Angelo *et al.*, 1995) in favouring prolonged depolarisations at these membrane potentials. It is likely that one or both of these conductances are responsible for the membrane potential-dependent broadening of EPSPs, seen *in vivo*. The use of ketamine as an anaesthetic may have been problematic, due to its known

antagonistic action upon NMDA receptors (Anis *et al.*, 1983; Thomson *et al.*, 1985). To address this problem, comparison was made between EPSPs recorded from granule cells under ketamine/xylazine and urethane anaesthesia. No significant differences were found in spontaneous EPSP waveforms recorded at – 50 mV between the two anaesthetics. The voltage-dependent broadening of EPSPs was observed under both anaesthetics (Appendix A, Fig A1), indicating that NMDA receptor function is not noticeably diminished at cerebellar granule cell synapses. Alternatively, the observed voltage-dependent broadening of EPSPs is mediated solely by the action of a persistent Na^+ current, but this is not supported by the work of D'Angelo and colleagues (1995). The described non-linearities are likely to have several effects upon granule cell integration and summation. The number of synaptic events required to cross threshold will be reduced as EPSP amplitude increases with depolarisation. Furthermore, the activation of slowly-inactivating conductances via NMDA receptors and Na^+ channels will serve to extend the time window over which synaptic potentials can summate and trigger action potentials. Put another way, these conductances serve to lessen the requirement for precise coincidence of synaptic inputs in order to generate output, increasing the time window over which inputs can summate from a few to tens of milliseconds.

3.3.4 Inhibitory synaptic inputs to cerebellar granule cells

Granule cells *in vivo* are subject to ongoing inhibitory inputs (5 ± 1 Hz), known to arise from Golgi cells (Eccles *et al.*, 1966; Farrant & Brickley, 2003).

Ongoing inhibitory synaptic inputs in granule cells indicate that interneurons are spontaneously active in the cerebella of anaesthetised animals. The activity of cerebellar interneurons is also discussed in chapter 5 of this thesis.

In addition to phasic inputs, I have shown that a powerful form of inhibitory control is mediated by a tonic $GABA_A$-receptor mediated current. Blockade of this current results in increased granule cell excitability to step current injection, as shown by a leftward shift in the *f-I* curve (Fig 3.8). Changes in neuronal gain are reflected by a change in the slope of the *f-I* curve, which was not observed in this study. However, it has been recently demonstrated that pure changes in neuronal gain can only be observed in response to fluctuating synaptic input, rather than step current injection in both neocortical pyramidal cells (Chance *et al.*, 2002) and cerebellar granule cells *in vitro* (Mitchell & Silver, 2003). These studies thus support the notion that tonic inhibition modulates the gain of cerebellar granule cell *in vivo*. Similar effects on granule cell excitability have been reported upon block of tonic inhibition *in vitro*, either by complete $GABA_A$ receptor antagonism (Brickley *et al.*, 1996), or via antagonism of the tonic current with furosemide (Hamann *et al.*, 2002). The work presented here provides the first evidence for the existence of tonic inhibition *in vivo*. Importantly, it has been possible to observe the functional consequences of tonic inhibitory activity on information transfer though the granule cell layer. Spontaneous firing rates of granule cells rose by an order of magnitude following block of tonic inhibition, meaning that information transfer through the granule cell layer (i.e. the conversion of mossy fibre action potentials into parallel fibre action potentials) is considerably dampened at rest. This conductance exerts its influence over

granule cell integration in two ways: firstly, the ongoing conductance lowers neuronal input resistance (Fig 3.6 C), causing a shunt of mossy fibre EPSPs (Fig 3.9 A). Secondly, the resting conductance also generates a hyperpolarisation of membrane potential, decreasing the likelihood of positive voltage deflections crossing threshold or activating voltage-sensitive conductances. Together, these effects combine to cause a significant reduction in the probability of action potential firing.

It is important to highlight that the effect of tonic inhibition upon granule cell resting potential under normal conditions may not always be hyperpolarising. In particular, the choice of reversal potential, -69 mV in this study, crucially determines the contribution of the Cl^-/HCO_3^- conductance to resting potential.

Tonic inhibition of granule cells is known to result from the persistent activation of extrasynaptic high-affinity $GABA_A$ receptors containing the $\alpha_{\square}$and δ subunits (Brickley *et al.*, 2001; Stell *et al.*, 2003). Several groups have shown that Golgi cell activity can modulate the amplitude of the tonic current (Farrant & Brickley, 2003; Carta *et al.*, 2004), and it thus seems likely that mossy fibre- and parallel fibre-driven activation of Golgi cells (Eccles *et al.*, 1966; Dieudonne, 1998) will serve to boost tonic inhibition and dampen granule cell excitability. I found a small, but statistically insignificant, correlation between phasic IPSC rate, representing Golgi cell firing (Farrant & Brickley, 2003), and the amplitude of the tonic current. However, it has already been noted that the amplitude of the tonic GABAergic conductance continues to increase over the age range of the animals used in this study (Brickley *et al.*, 1996). It is possible that age-dependent variability in the

amplitude of the tonic conductance may, in this case, have obscured a relationship between Golgi cell activity and conductance amplitude. This leaves open the question as to precise role that Golgi spiking plays in modulation of the tonic current. Neurosteroids (Stell *et al.*, 2003), nitric oxide release (Wall, 2003), acetylcholine (Rossi *et al.*, 2003a) and alcohol (Wallner *et al.*, 2003; Carta *et al.*, 2004) are all known to exert modulatory effects on tonic inhibition at the level of the glomerulus, suggesting additional mechanisms by which information transfer through the granule cell layer could be regulated in a $GABA_A$ receptor-dependent manner.

Following blockade of tonic inhibition, unitary EPSPs were often capable of triggering action potential firing, a phenomenon not observed at rest. This finding is extremely interesting when viewed in the context of Marr's hugely influential theory of cerebellar cortical function (Marr, 1969). Marr states that a key function of the cerebellum is to effectively discriminate different patterns of activity. A key requirement of his theory is that in order to maximise the number of distinct patterns that can be distinguished by Purkinje cells, the activity of the parallel fibres must be kept low. Under conditions of increasing afferent input to the cerebellum, levels of parallel fibre activity are maintained by increasing the threshold for granule cell activation, in effect, lowering the gain of information transfer. Golgi cell modulation of tonic inhibition to granule cells is one mechanism by which such a process could occur. However, one of the less well-known predictions of Marr's theory is that at very low levels of mossy fibre activity, activity from single inputs may be transferred through the granule cell layer. Information arriving via a single mossy fibre action potential can be transferred into parallel fibre activity, thus

ensuring that the cerebellar cortex remains sensitive to low levels of activity. The finding that single EPSPs can trigger spikes in granule cells when tonic inhibition is blocked, suggests the cerebellum is capable of performing such a transformation. However, it remains to be seen whether this sensitivity is ever usefully exploited within the cerebella of behaving organisms.

Chapter 4: SENSORY INTEGRATION IN CEREBELLAR GRANULE CELLS

4.1 INTRODUCTION

Knowledge of how sensory signals are represented within the cerebellar cortex is vital to our understanding of how information is processed within this structure. By mediating the conversion of mossy fibre activity into parallel fibre input to Purkinje cells, granule cells represent the first information-processing step within the cerebellum. A long-held goal of cerebellar researchers has been to understand how sensory-driven activity in the granule cell layer drives downstream activity in the molecular and Purkinje cell layers (Eccles *et al.*, 1967b; Bower & Woolston, 1983). Previously, sensory-evoked electrical activity within the granule cell layer has been studied using local field potential and multiunit activity. These signals are believed to represent predominantly synaptic and spiking activity respectively, but in both cases the observed signal derives from a large, indeterminate number of neurons. As such, the contribution of single granule cells to sensory-evoked responses in Purkinje cells and interneurons is unknown. Additionally, the role of individual mossy fibres in the generation of sensory-driven granule cell output has never been investigated. A key unresolved question remains as to whether sensory signals conveyed by activity in a single mossy fibre could ever be sufficient to affect granule cell action potential firing (Marr, 1969; Gabbiani *et al.*, 1994; D'Angelo *et al.*, 1995).

Historically, the cerebellum has been viewed as a motor structure (Holmes, 1939) and, as such, it had been expected that the majority of afferent projections to the lateral hemispheres of the cerebellum would be

proprioceptive. Welker and colleagues were the first group to explore the nature of projections to the lateral cerebellum of the rat using 'micro-mapping' techniques. Surprisingly, the only sensory input found in the lateral hemispheres, and specifically folia Crus I and II, was found to be tactile input from perioral regions (Shambes *et al.*, 1978a; Shambes *et al.*, 1978b) – see also section 1.4.3.5. Afferent input via mossy fibres can be divided into two groups, as determined by the response latency to sensory stimulation. Stimulation of the lip or whisker produces a short latency response in the granule cell layer field potential (less than 10 ms) and a longer latency response (≈ 40 ms), shown to derive from primary somatosensory regions of the neocortex (Morissette & Bower, 1996). Thus far, the contributions of these two classes of input to sensory processing within single granule cells have remained unexplored.

In addition to mossy fibre inputs, granule cells also receive inhibitory synaptic input from Golgi cells. Golgi cells receive excitatory synaptic inputs from both feed-back (via parallel fibres) and feed-forward (via mossy fibres) pathways (Eccles *et al.*, 1967a; Palay & Chan-Palay, 1974) and exert their influence through both tonic and phasic activation of granule cell GABA receptors. The activity of Golgi cells during sensory stimulation has been studied (Vos *et al.*, 2000; Volny-Luraghi *et al.*, 2002), although the implications of Golgi cell activity for sensory processing in granule cells has not been investigated directly. The precise role of granule cell inhibition during sensory processing in the cerebellum is not known, although a variety of roles have been suggested. The most popular is that of automatic gain control: Golgi cells modulate the input-output relationship of granule cells in order to

maintain net parallel fibre activity constant across the broadest possible range of mossy fibre activities (Eccles *et al.*, 1966; Marr, 1969; Albus, 1971). Additionally, it has been suggested that Golgi cells may regulate the precise timing of granule cell spikes, thus contributing to oscillatory activity (Maex & Schutter, 1998).

To investigate these issues, I have combined whole-cell patch clamp recordings from the granule cell layers of Crus I and II with tactile stimulation of the whisker and perioral areas of the rat. In granule cells, this approach has allowed me to study both incoming sensory-evoked mossy fibre and Golgi cell synaptic activity, and resultant action potential firing. This has enabled me to directly investigate the input-output relationship of single neurons during sensory processing.

In the course of obtaining whole-cell patch clamp recordings from granule cell layer, it has occasionally been possible to record from structures with strikingly different electrophysiological properties. One subgroup of recordings made from the cerebellar granule cell layer display characteristics that are inconsistent with a somatic recording location. Both mossy fibres and Golgi cell axons ramify and terminate throughout the granule cell layer. In particular, mossy fibres form large unmyelinated structures (up to 5 μm diameter) at their branch points and terminals (Ramón y Cajal, 1904; Palay & Chan-Palay, 1974). In this chapter, I present data obtained from whole-cell recordings of putative presynaptic terminals, and subsequently describe the activity of these structures in response to sensory stimulation.

4.2 RESULTS

4.2.1 Sensory-evoked firing in cerebellar granule cells

In order to study the activity of individual granule cells in response to physiologically-relevant stimuli, air-puff stimulation of the whisker and perioral regions of the face was combined with whole-cell recordings from granule cells within folia Crus I & II of ketamine / xylazine or urethane-anaesthetised rats (Fig 2.2, 2.3). The granule cell layers of these folia have previously been shown to produce strong field and multiunit responses during somatosensory stimulation in both awake and anaesthetised animals (Shambes *et al.*, 1978a; Shambes *et al.*, 1978b; Bower & Woolston, 1983). I therefore looked for sensory-evoked responses during cell-attached and whole-cell patch clamp recordings of cerebellar granule cells.

In 62 out of 74 granule cells tested (84%), sensory stimulation failed to produce any observable excitatory response. However, in 8 out of 12 whole-cell recordings where excitatory evoked responses were observed, sensory stimulation produced action potential firing. In the remaining granule cells (4 out of 12), stimulation resulted in a subthreshold EPSP. Although the somatosensory receptive fields of individual granule cells were not precisely characterised, typically, responses were produced in an all-or-none manner following an air puff (70 ms, 40 psi) to a small area of the rat's face (less than 5 mm diameter). The deflection of a small number of whiskers (less than 4) proved the most effective stimulus (10 out of 12 responses).

When suprathreshold responses were evoked in granule cells, the most common discharge pattern consisted of a burst of several action potentials (3.2 ± 0.2 action potentials, range: 2.7 - 4.1, burst duration = 42 ± 11 ms; n = 5, Fig 4.1). The mean frequency of action potentials within evoked bursts was 77 ± 16 Hz, with maximal instantaneous frequencies being as high as 250 Hz (mean = 168 ± 31 Hz, n = 5). Rarely, sensory-evoked action potentials could be recorded in cell-attached mode prior to break-in (n = 2, Fig 4.2). In both cases, a burst of action potentials was observed (3.5 ± 0.2 action potentials at 79 ± 18 Hz), strongly supporting the notion that responses recorded in whole-cell configuration represent physiological patterns of output.

The intrinsic properties of granule cells exhibiting bursting responses to sensory stimulation were not noticeably different from other granule cells. Input resistance, rectification and the spontaneous IPSC rate were not significantly different in bursting cells when compared with the population as a whole, or with non-bursting, sensory-responsive granule cells only. The membrane potential was slightly more depolarised in bursting granule cells (V_m for bursting granule cells = -55 ± 5 mV, n = 5), although, this was also not significantly different from the population as a whole (V_m for population = -64 ± 1 mV, $p > 0.1$, unpaired *t*-test).

Most commonly, a 70 ms air puff was used to effect stimulation of the skin and whisker. In order to investigate whether stimulus duration shapes the sensory response in cerebellar granule cells, air puff duration was varied from 30 to 300 ms. No distinguishable differences were observed in the output pattern of action potential following altered stimulus duration (Fig 4.3 A). Changing the stimulus duration did not significantly affect the number of

Figure 4.1

Evoked sensory responses in cerebellar granule cells. **A** Action potentials evoked by whisker stimulation (three consecutive trials). **B** Representative peristimulus time histogram of sensory-evoked action potentials (16 trials). **C** Raster plot of evoked action potentials (three trials from three different granule cells; each colour corresponds to a different cell).

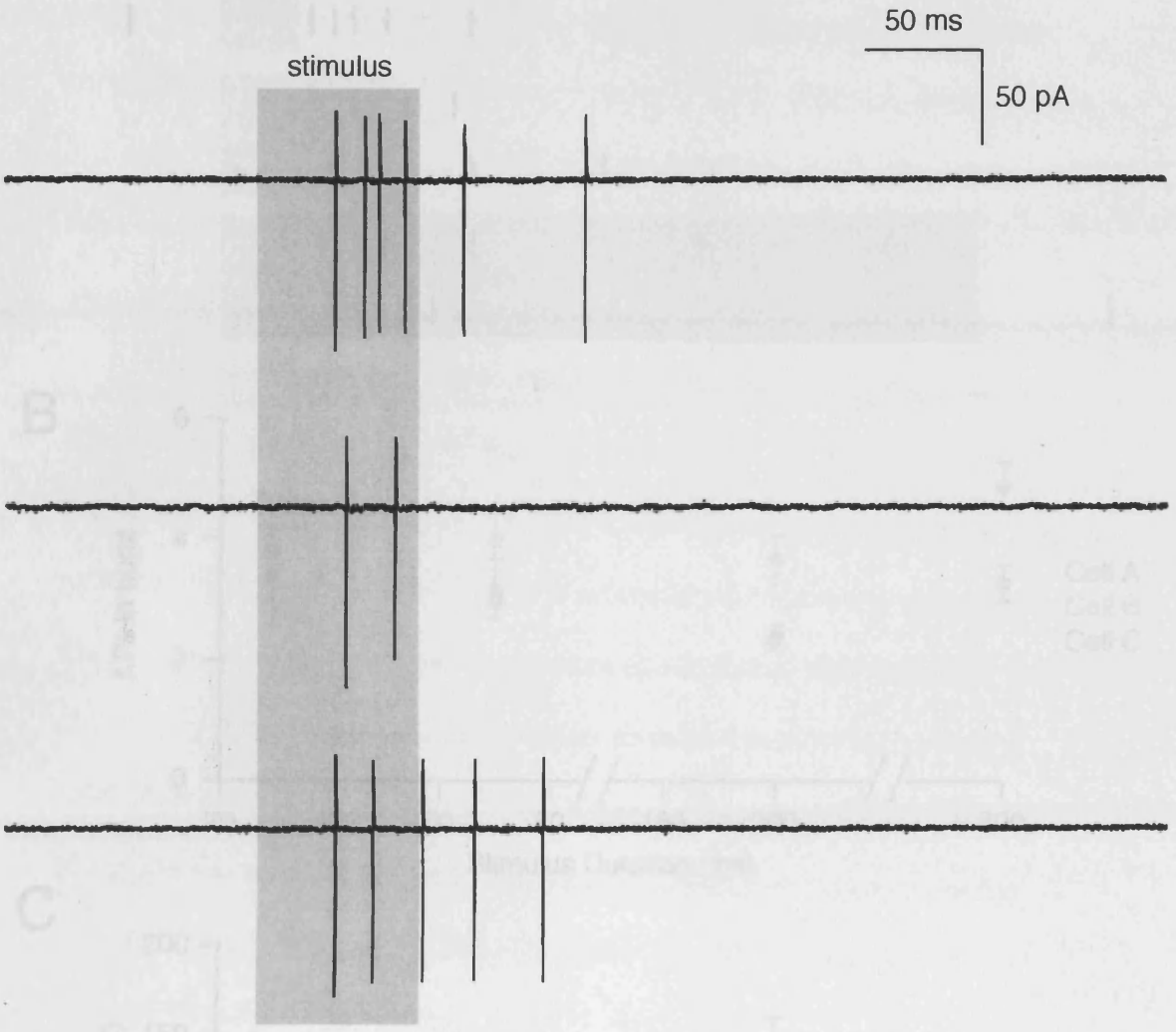

Figure 4.2

Sensory-evoked granule cell spiking recorded in cell-attached mode (three consecutive trials following whisker stimulation).

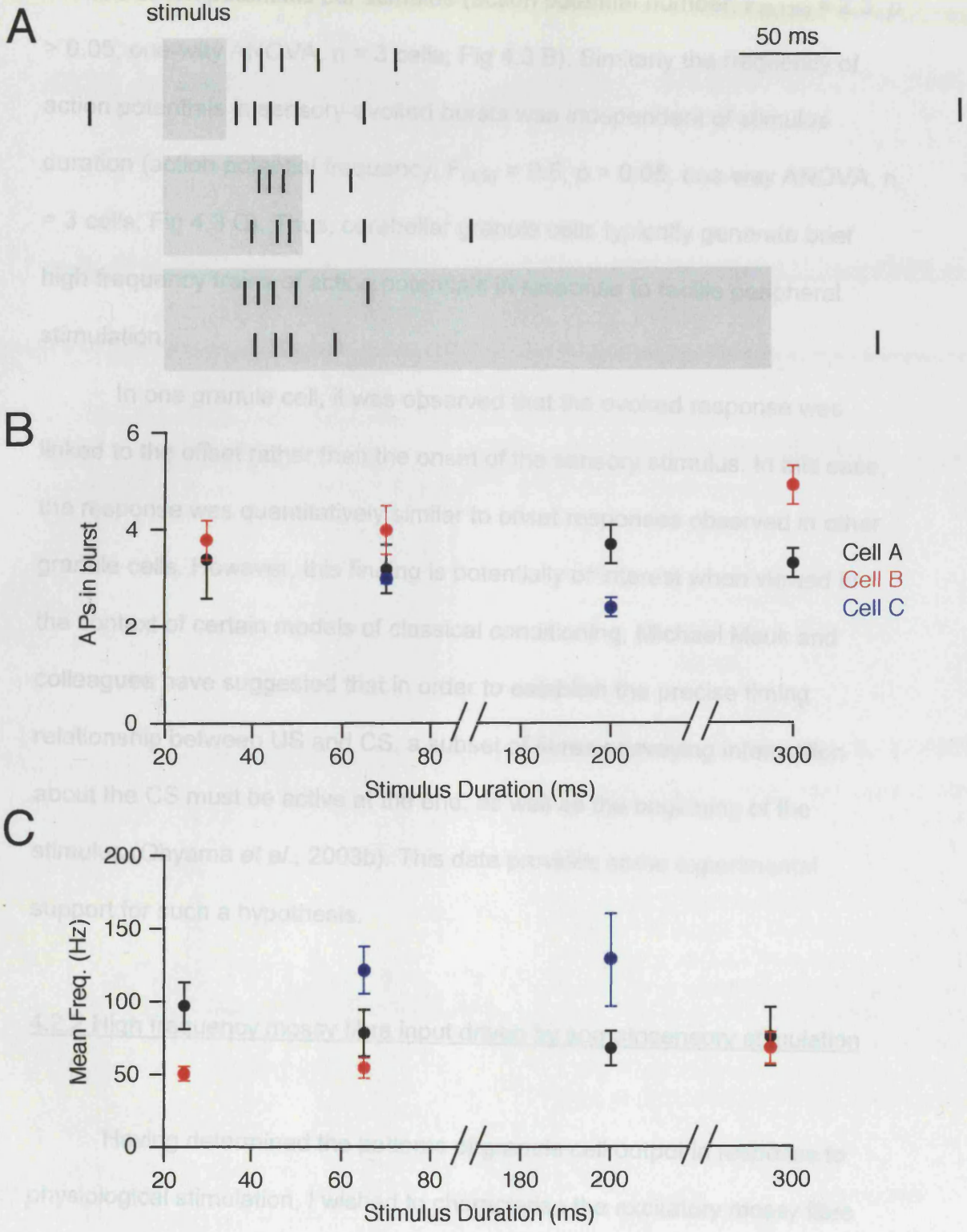

Figure 4.3

Stimulus duration does not shape the sensory response in cerebellar granule cells. **A** Representative raster plot of sensory-evoked action potentials following whisker stimulation of varying duration (top: 30 ms; middle: 70 ms; bottom: 300 ms). **B** Number of action potentials evoked by a single whisker stimulus is independent of stimulus duration (each colour represents a different cell). **C** Frequency of action potentials evoked by a single whisker stimulus is independent of stimulus duration (each colour represents a different cell, with colours corresponding to the same cells as in **B**).

evoked action potentials per stimulus (action potential number, $F_{(3,136)} = 2.3$, $p > 0.05$; one-way ANOVA, n = 3 cells; Fig 4.3 B). Similarly the frequency of action potentials in sensory-evoked bursts was independent of stimulus duration (action potential frequency, $F_{(3,97} = 0.6$, $p > 0.05$; one-way ANOVA, n = 3 cells; Fig 4.3 C). Thus, cerebellar granule cells typically generate brief high frequency trains of action potentials in response to tactile peripheral stimulation.

In one granule cell, it was observed that the evoked response was linked to the offset rather than the onset of the sensory stimulus. In this case, the response was quantitatively similar to onset responses observed in other granule cells. However, this finding is potentially of interest when viewed in the context of certain models of classical conditioning. Michael Mauk and colleagues have suggested that in order to establish the precise timing relationship between US and CS, a subset of fibres conveying information about the CS must be active at the end, as well as the beginning of the stimulus (Ohyama *et al.*, 2003b). This data provides some experimental support for such a hypothesis.

4.2.2 High frequency mossy fibre input driven by somatosensory stimulation

Having determined the patterns of granule cell output in response to physiological stimulation, I wished to characterise the excitatory mossy fibre activity underlying action potential generation. Due to the powerful shunting effect that action potential firing exerts upon synaptic conductances (Häusser *et al.*, 2001), measurement of sensory-evoked mossy fibre activity was made

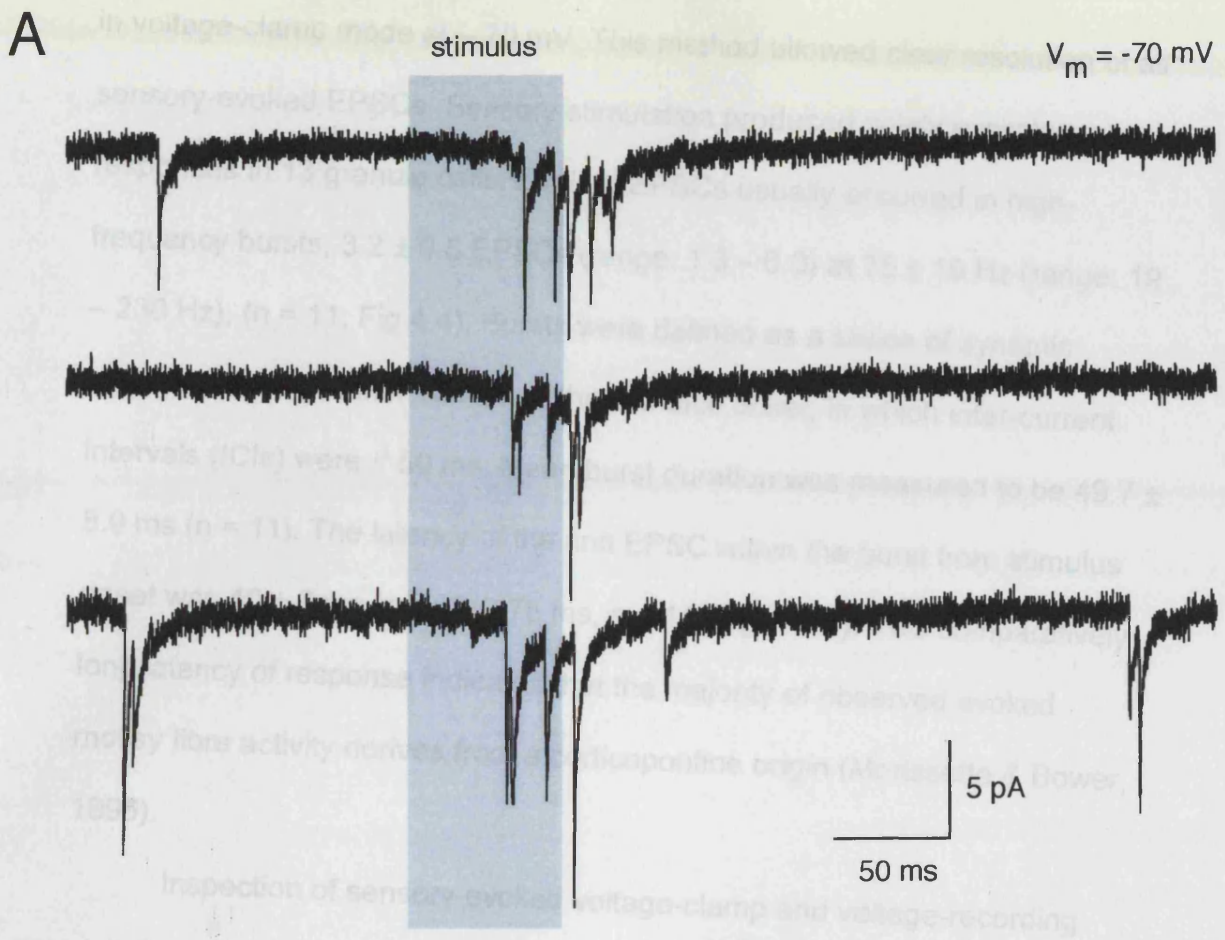

Figure 4.4

Sensory-evoked mossy fibre input to cerebellar granule cells. **A** EPSCs evoked by whisker stimulation recorded in voltage clamp at -70 mV (three consecutive trials). **B** Representative peristimulus time histogram of sensory-evoked EPSCs (16 trials). **C** Raster plot of evoked EPSCs (three trials from three different granule cells; Colour corresponds the same cells shown in Fig 4.1 **A**). **D** Histogram of excitatory response onset for all granule cells (bin size = 5 ms). Dashed line indicates max. latency of trigeminal inputs (Morissette and Bower, 1996).

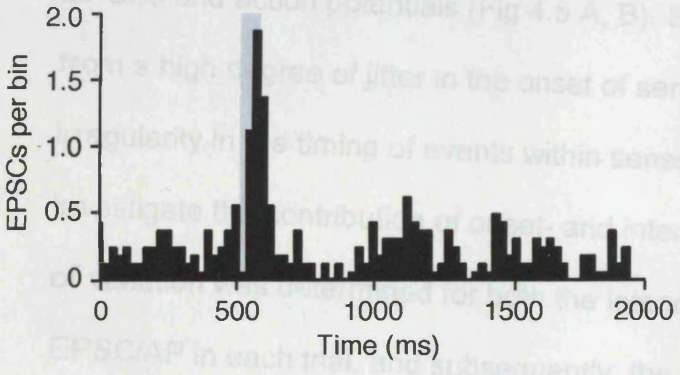

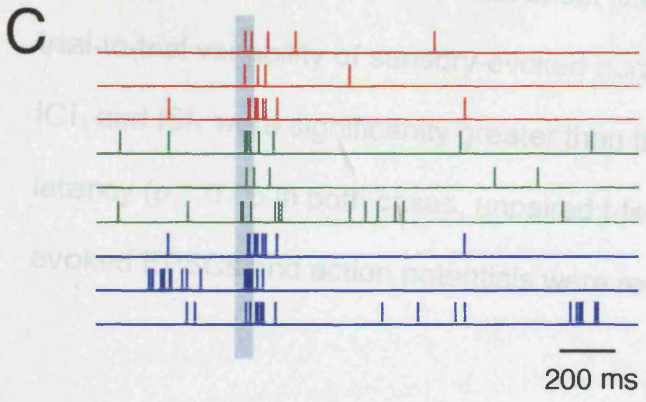

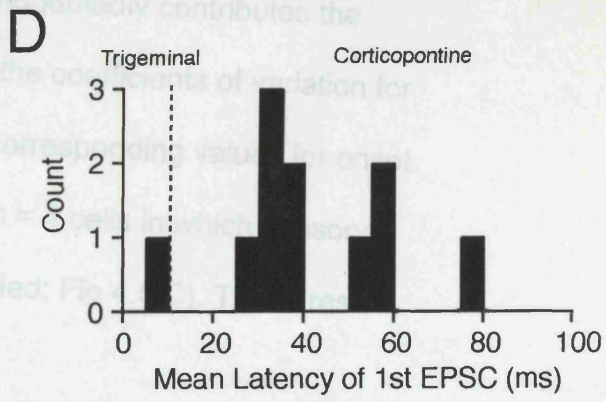

in voltage-clamp mode at – 70 mV. This method allowed clear resolution of all sensory-evoked EPSCs. Sensory stimulation produced solely excitatory responses in 13 granule cells. Evoked EPSCs usually occurred in high-frequency bursts, 3.2 ± 0.5 EPSCs (range: 1.3 – 6.0) at 75 ± 19 Hz (range: 19 – 230 Hz), (n = 11; Fig 4.4). Bursts were defined as a series of synaptic events occurring within 100 ms of the stimulus onset, in which inter-current intervals (ICIs) were < 50 ms. Mean burst duration was measured to be 49.7 ± 8.9 ms (n = 11). The latency of the first EPSC within the burst from stimulus onset was 40 ± 6 ms (range: 9-75 ms, n = 11, Fig 4.4 D). This comparatively long latency of response indicates that the majority of observed evoked mossy fibre activity derives from a corticopontine origin (Morissette & Bower, 1996).

Inspection of sensory-evoked voltage-clamp and voltage-recording trials indicated a high trial-to-trial variability in the timing of sensory evoked EPSCs and action potentials (Fig 4.5 A, B). Such variability may have resulted from a high degree of jitter in the onset of sensory response, and/or irregularity in the timing of events within sensory-evoked bursts. In order to investigate the contribution of onset- and inter-burst irregularity, the coefficient of variation was determined for both the latency of the first sensory-evoked EPSC/AP in each trial, and subsequently, the first inter-current/spike interval (ICI_1/ISI_1) within each burst. Whilst onset jitter undoubtedly contributes the trial-to-trial variability of sensory-evoked bursts, the coefficients of variation for ICI_1 and ISI_1 were significantly greater than the corresponding values for onset latency ($p < 0.05$ in both cases, unpaired t-test, n = 4 cells in which sensory-evoked EPSCs and action potentials were recorded; Fig 4.5 C). These results

indicate that trial-to-trial variability in the timing of evoked EPSCs within individual bursts is likely to be a major determinant in the irregular timing of sensory-evoked action potentials.

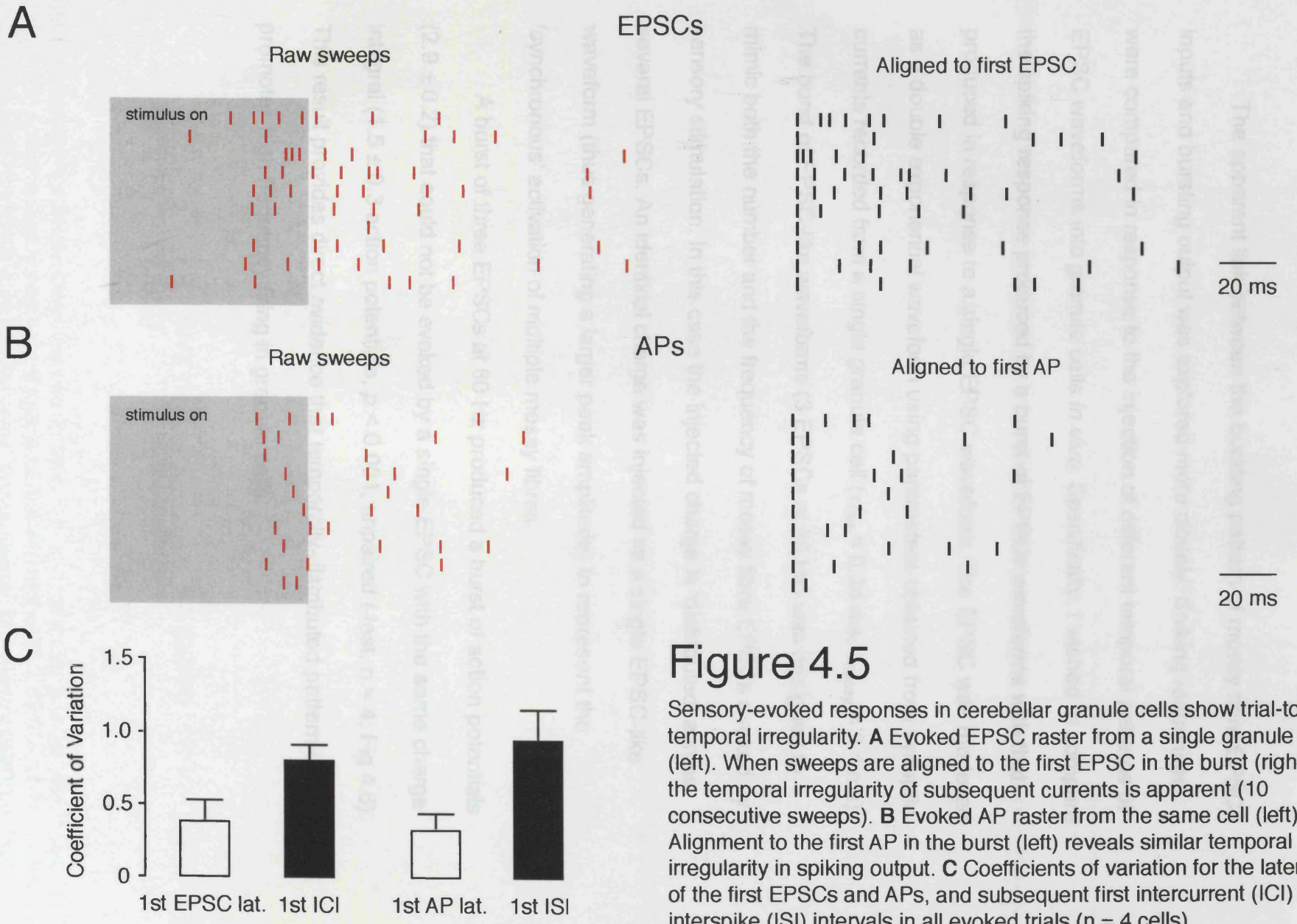

Figure 4.5

Sensory-evoked responses in cerebellar granule cells show trial-to-trial temporal irregularity. **A** Evoked EPSC raster from a single granule cell (left). When sweeps are aligned to the first EPSC in the burst (right), the temporal irregularity of subsequent currents is apparent (10 consecutive sweeps). **B** Evoked AP raster from the same cell (left). Alignment to the first AP in the burst (left) reveals similar temporal irregularity in spiking output. **C** Coefficients of variation for the latencies of the first EPSCs and APs, and subsequent first intercurrent (ICI) and interspike (ISI) intervals in all evoked trials (n = 4 cells)

4.2.3 High frequency output is dependent upon high frequency input

The apparent link between the bursting pattern of mossy fibre EPSC inputs and bursting output was explored more closely. Spiking responses were compared in response to the injection of different temporal patterns of EPSC waveforms into granule cells *in vivo*. Specifically, I wished to compare the spiking response produced by a burst of EPSCs waveforms with that produced in response to a single EPSC waveform. The EPSC was modelled as a double exponential waveform using parameters obtained from synaptic currents recorded from a single granule cell (τ_{rise} = 0.34 ms, τ_{decay} = 2.1 ms). The burst of EPSC-like waveforms (3 EPSCs at 80 Hz) was designed to mimic both the number and the frequency of mossy fibre EPSCs evoked by sensory stimulation. In this case the injected charge is 'distributed' across several EPSCs. An identical charge was injected as a single EPSC-like waveform (thus generating a larger peak amplitude) to represent the 'synchronous' activation of multiple mossy fibres.

A burst of three EPSCs at 80 Hz produced a burst of action potentials (2.9 ± 0.2) that could not be evoked by a single EPSC with the same charge integral (1.5 ± 0.3 action potentials, $p < 0.001$, unpaired *t*-test, n = 4; Fig 4.6). This result provides direct evidence that temporally-distributed pattern of input promotes high frequency firing in granule cells.

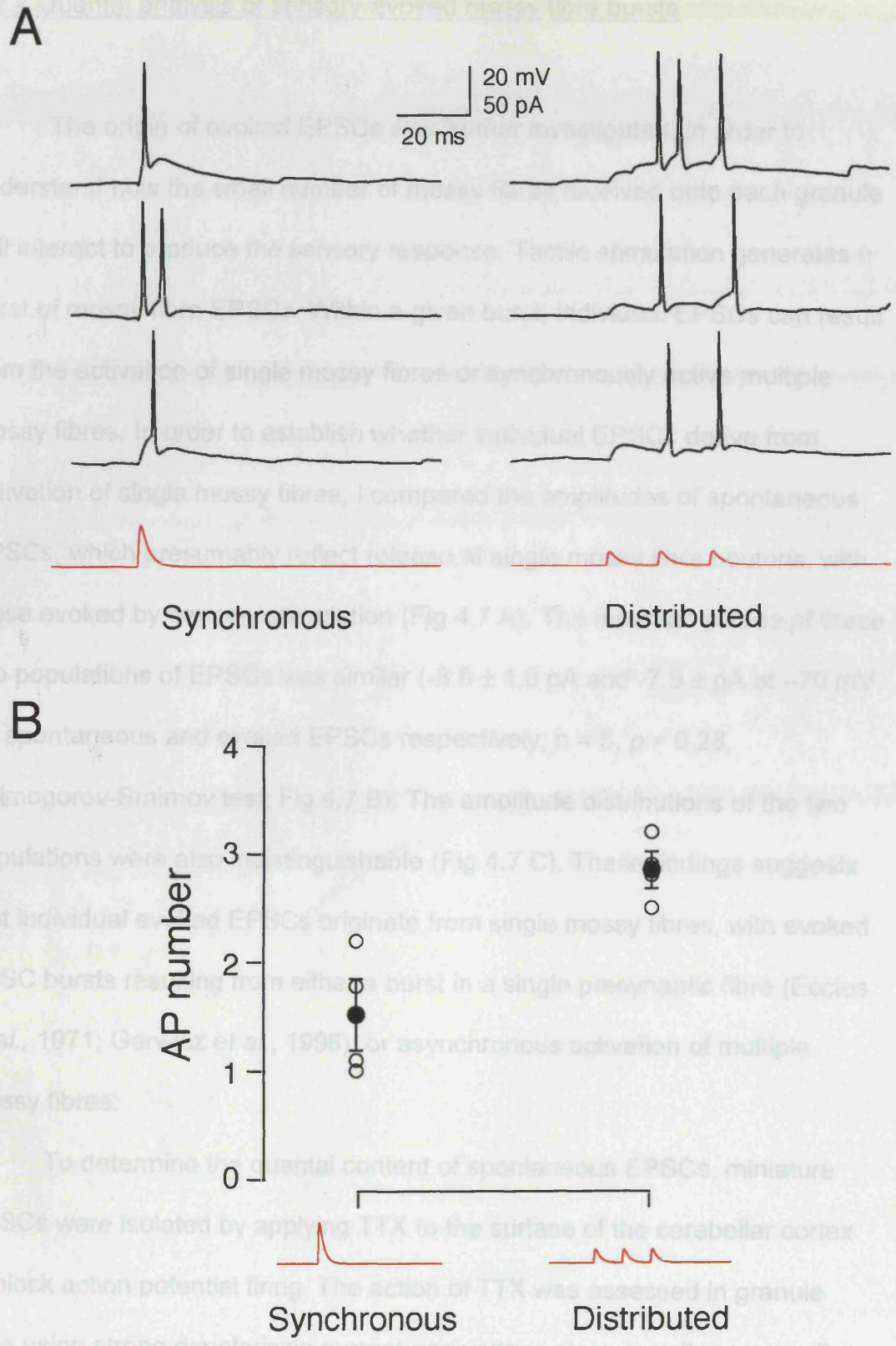

Figure 4.6

The relationship between bursting input and bursting output in cerebellar granule cells *in vivo*. **A** More APs are generated from a train of injected EPSCs (Distributed: 3 EPSCs at 80 Hz) than a single large EPSC (Synchronous) with the same charge integral. **B** Summary data from four granule cells ($p < 0.02$, Student's unpaired *t*-test).

4.2.4 Quantal analysis of sensory-evoked mossy fibre bursts

The origin of evoked EPSCs was further investigated, in order to understand how the small number of mossy fibres received onto each granule cell interact to produce the sensory response. Tactile stimulation generates a burst of mossy fibre EPSCs. Within a given burst, individual EPSCs can result from the activation of single mossy fibres or synchronously active multiple mossy fibres. In order to establish whether individual EPSCs derive from activation of single mossy fibres, I compared the amplitudes of spontaneous EPSCs, which presumably reflect release at single mossy fibre boutons, with those evoked by sensory stimulation (Fig 4.7 A). The mean amplitude of these two populations of EPSCs was similar (-8.9 ± 1.0 pA and -7.9 ± pA at –70 mV for spontaneous and evoked EPSCs respectively; n = 5, p = 0.28, Kolmogorov-Smirnov test; Fig 4.7 B). The amplitude distributions of the two populations were also indistinguishable (Fig 4.7 C). These findings suggests that individual evoked EPSCs originate from single mossy fibres, with evoked EPSC bursts resulting from either a burst in a single presynaptic fibre (Eccles *et al.*, 1971; Garwicz *et al.*, 1998), or asynchronous activation of multiple mossy fibres.

To determine the quantal content of spontaneous EPSCs, miniature EPSCs were isolated by applying TTX to the surface of the cerebellar cortex to block action potential firing. The action of TTX was assessed in granule cells using strong depolarising current and voltage steps in voltage-recording and voltage-clamp modes respectively. The blockade of depolarisation-driven spiking confirmed TTX action (Fig 4.8 A), and was associated with a decrease

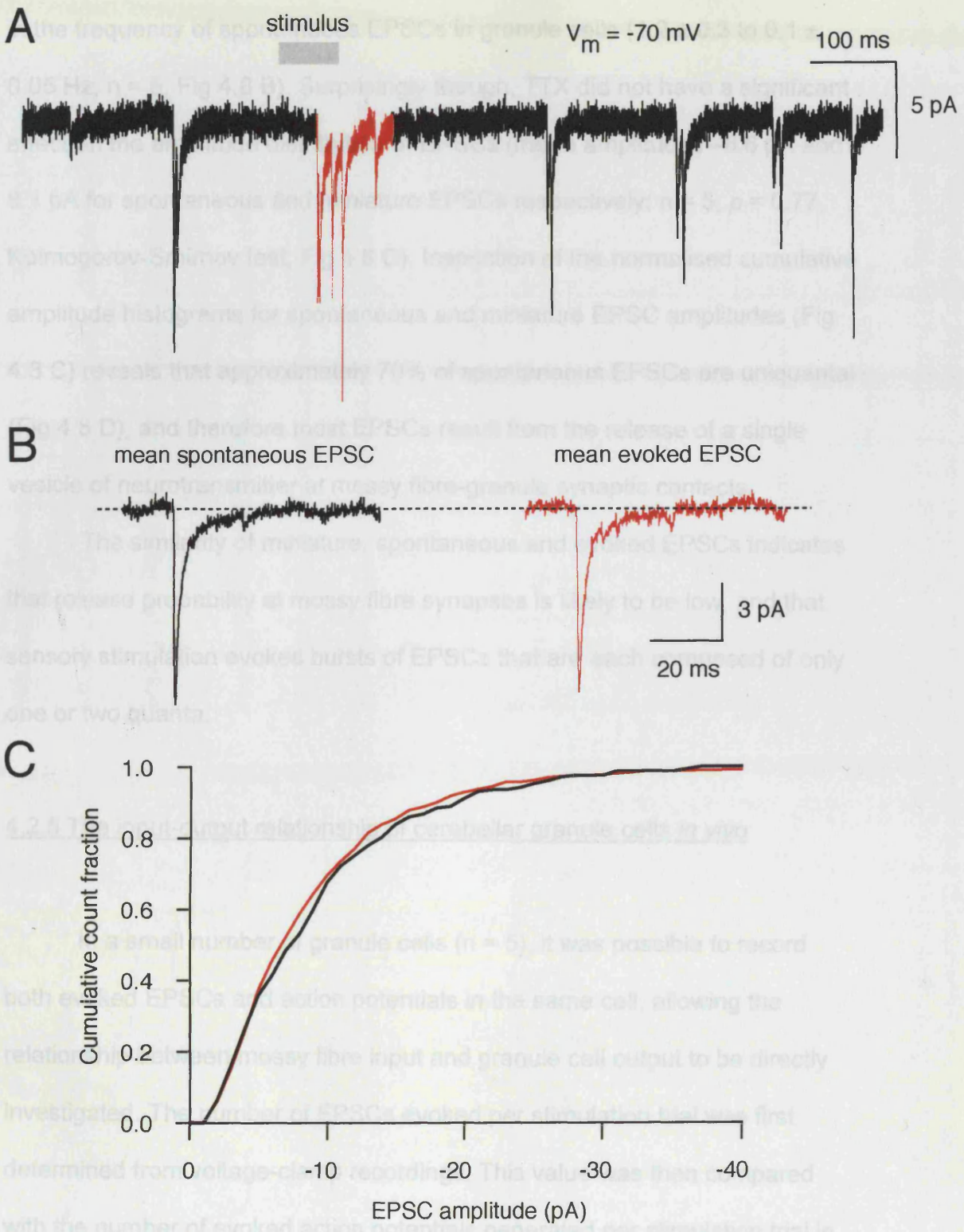

Figure 4.7

Individual sensory-evoked EPSCs derive from activation of single mossy fibres. **A** Sensory-evoked EPSCs (red) were compared with spontaneous events (black) in granule cells voltage-clamped at -70 mV. **B** Average waveforms for sensory-evoked (red, 25 events) and spontaneous EPSCs (black, 25 events) for a single granule cell. **C** Normalised cumulative amplitude histogram for spontaneous and evoked EPSCs (n = 4 cells; 1 pA bins).

in the frequency of spontaneous EPSCs in granule cells (1.2 ± 0.3 to 0.1 ± 0.05 Hz, n = 5, Fig 4.8 B). Surprisingly though, TTX did not have a significant effect on the amplitude distribution of EPSCs (mean amplitudes –8.6 pA and –8.1 pA for spontaneous and miniature EPSCs respectively; n = 5, $p = 0.77$, Kolmogorov-Smirnov test; Fig 4.8 C). Inspection of the normalised cumulative amplitude histograms for spontaneous and miniature EPSC amplitudes (Fig 4.8 C) reveals that approximately 70% of spontaneous EPSCs are uniquantal (Fig 4.8 D), and therefore most EPSCs result from the release of a single vesicle of neurotransmitter at mossy fibre-granule synaptic contacts.

The similarity of miniature, spontaneous and evoked EPSCs indicates that release probability at mossy fibre synapses is likely to be low, and that sensory stimulation evokes bursts of EPSCs that are each composed of only one or two quanta.

4.2.5 The input-output relationship of cerebellar granule cells *in vivo*

In a small number of granule cells (n = 5), it was possible to record both evoked EPSCs and action potentials in the same cell, allowing the relationship between mossy fibre input and granule cell output to be directly investigated. The number of EPSCs evoked per stimulation trial was first determined from voltage-clamp recordings. This value was then compared with the number of evoked action potentials generated per stimulation trial in voltage-recording mode in the absence of injected current (i.e. granule cells were studied at their resting membrane potential). The mean number of evoked EPSCs was plotted against the mean number of evoked action

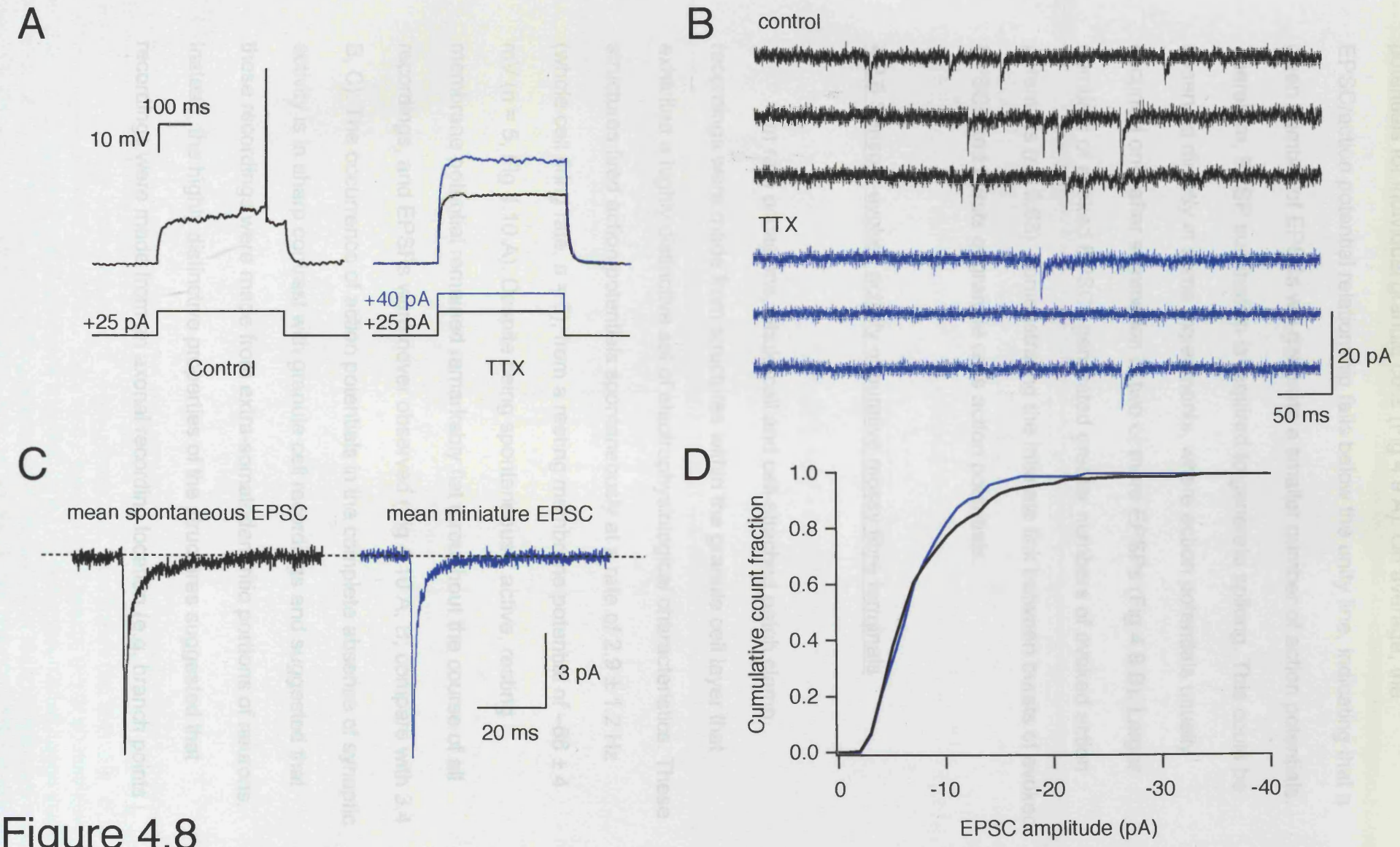

Figure 4.8

Quantal analysis of mossy fibre EPSCs in cerebellar granule cell *in vivo*. **A** TTX application blocked current-driven action potential firing. **B** Spontaneous (black) and miniature (blue) EPSCs following TTX application. **C** Average waveforms for spontaneous (black, 42 events) and miniature (blue, 42 events) EPSCs for a single granule cell. **D** Normalised cumulative amplitude histogram for spontaneous and miniature EPSCs (n = 5 cells; 1 pA bins).

potentials for individual granule cells (Fig 4.9 A). On average, the EPSC/action potential relationship falls below the unity line, indicating that a given number of EPSCs will generate a smaller number of action potentials. Therefore, EPSP summation is required to generate spiking. This could be observed directly in some experiments, where action potentials usually occurred only after summation of two or more EPSPs (Fig 4.9 B). Larger numbers of evoked EPSCs generated greater numbers of evoked action potentials ($r = 0.63$), demonstrating the intimate link between bursts of evoked EPSCs and bursts of granule cells action potentials.

4.2.6 Sensory-evoked activity of putative mossy fibre terminals

On rare occasions, whole-cell and cell-attached patch clamp recordings were made from structures within the granule cell layer that exhibited a highly distinctive set of electrophysiological characteristics. These structures fired action potentials spontaneously at a rate of 2.9 ± 1.2 Hz (whole cell firing rate, $n = 5$), from a resting membrane potential of -66 ± 4 mV ($n = 5$, Fig 4.10 A). Despite being spontaneously active, resting membrane potential remained remarkably flat throughout the course of all recordings, and EPSPs were never observed (Fig 4.10 A, B; compare with 3.4 B, C). The occurrence of action potentials in the complete absence of synaptic activity is in sharp contrast with granule cell recordings and suggested that these recordings were made from extra-somatodendritic portions of neurons. Instead, the highly distinctive properties of the structures suggested that recordings were made from an axonal recording location (e.g. branch points

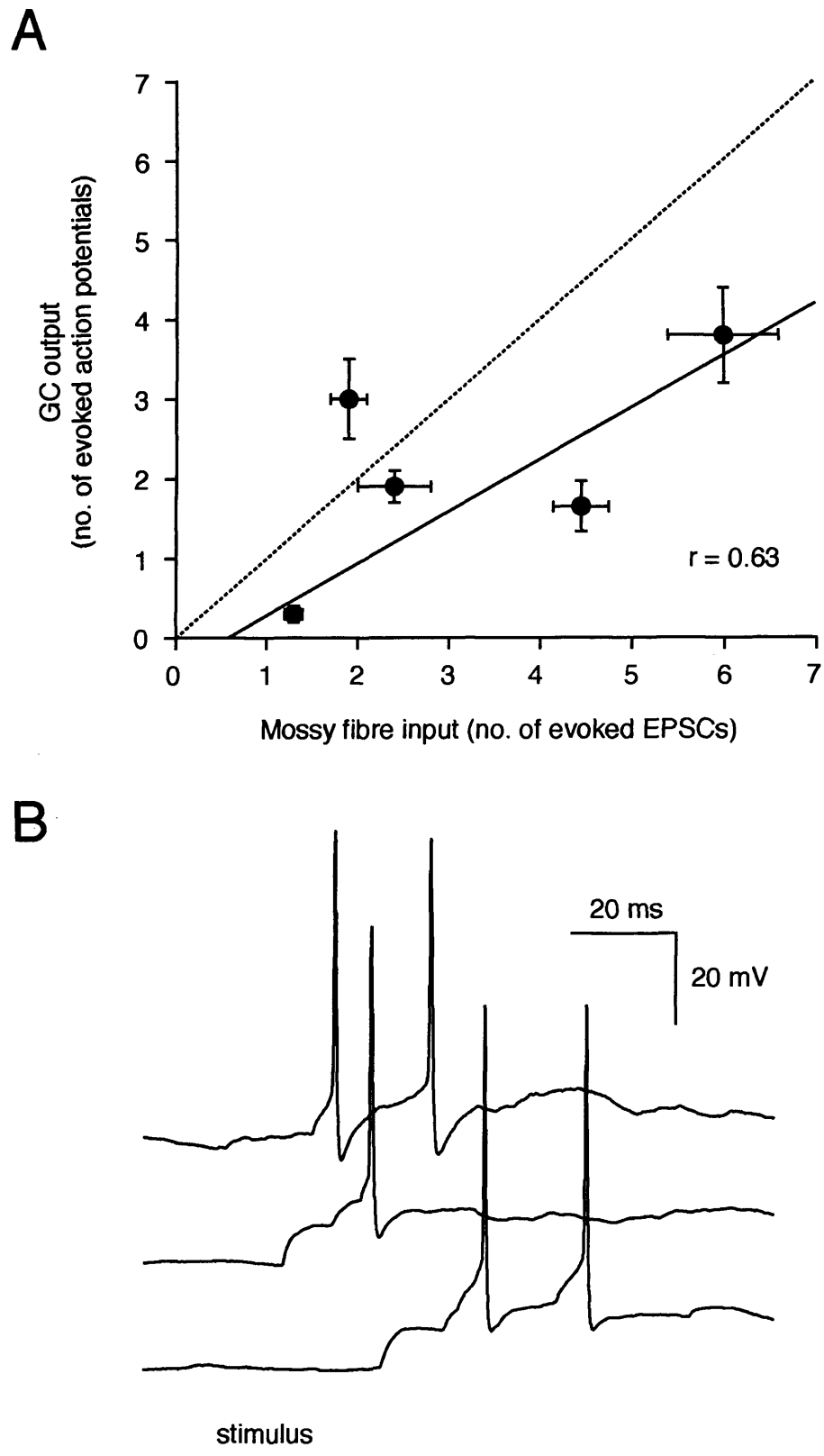

Figure 4.9

The relationship between mossy fibre input and granule cell output. **A** Relationship between the number of evoked mossy fibre EPSCs and granule cell action potentials at resting membrane potential (-55 mV ± 5 mV). Each point represents a single granule cell. The dashed line indicates when EPSC/action potential ratio equals one. Cells below this line (4/5) require EPSP summation in order to generate output. The solid line is a linear fit weighted by s.e.m. **B** Representative traces showing summation of evoked EPSPs and resulting action potentials. In 86% of trials, at least two sensory-evoked EPSPs were required to summate to produce the first action potential in the response.

and boutons) and led me to classify these structures are putative nerve terminals.

The electrical properties of putative nerve terminals were investigated in detail. Voltage-clamping at hyperpolarising potentials was unable to prevent spontaneous firing (-90 mV, n = 5; data not shown), suggesting that action potential initiation is distal to the site of recording. Current-voltage relationships were found to be highly non-linear ($R_{input\ (+ve)}$ = 200 ± 40 MΩ, $R_{input\ (-ve)}$ = 490 ± 180 MΩ, n = 5, Fig 4.10 C). Putative nerve terminals showed strong outward rectification (rectification ratio: 0.5 ± 0.1, n = 5), and hyperpolarising current injection induced membrane potential 'sag', indicative of the presence of an I_h current.

Current injection was used to manipulate membrane potential at the site of recording. Spontaneous action potential firing was ongoing, and independent of membrane potential (Fig 4.10 C). However, action potential amplitude did show a marked dependence upon membrane potential. At depolarised membrane potentials, action potential amplitude was decreased (Fig 4.11 A), in a sigmoidal manner with respect to depolarisation (r = 0.91, Fig 4.11 B). At hyperpolarised membrane potentials (below –70 mV), spike amplitude was unaffected. Together these data suggest local Na^+ channel inactivation is occurring at depolarised membrane potentials. In previous studies in which extracellular recordings have been made from putative single mossy fibre units *in vivo*, firing rates of up to 1 kHz have been reported (Eccles *et al.*, 1971; Garwicz *et al.*, 1998). Therefore, to investigate whether these putative nerve terminals could sustain such high firing rates, brief pulsed current injections were used to generate action potentials. In response

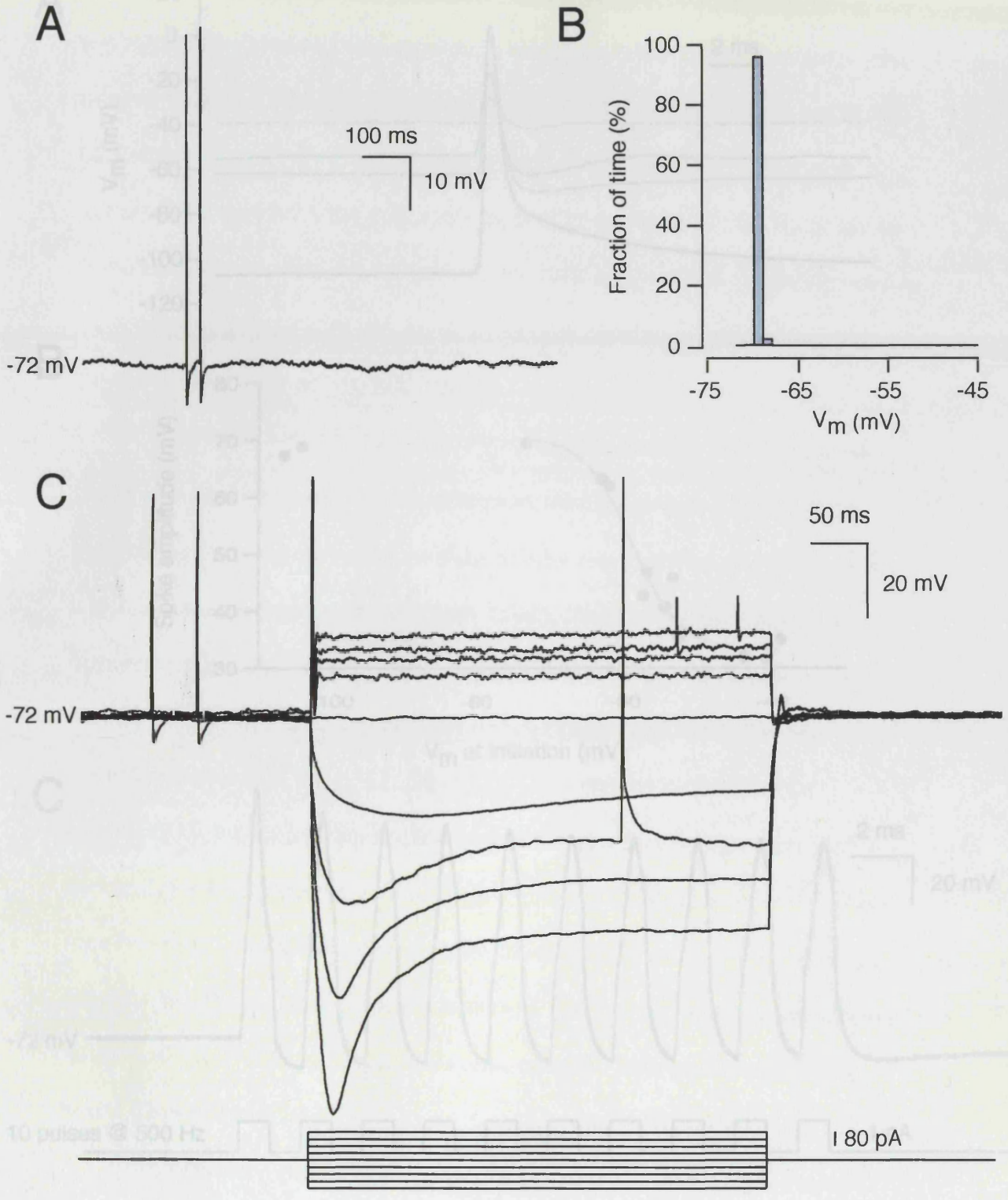

Figure 4.10

Characteristic features of putative mossy fibre terminals *in vivo*. **A** Voltage recording from a single putative mossy fibre in the absence of injected current. Synaptic potentials were never observed (n = 7 structures). **B** Histogram of membrane potential (V_m; 20 sec of activity; bin size = 1 mV) from the same structure. **C** Current-voltage relationship is highly non-linear. Hyperpolarising current injection causes membrane potential 'sag', indicating the presence of I_h. Action potential firing is independent of membrane potential.

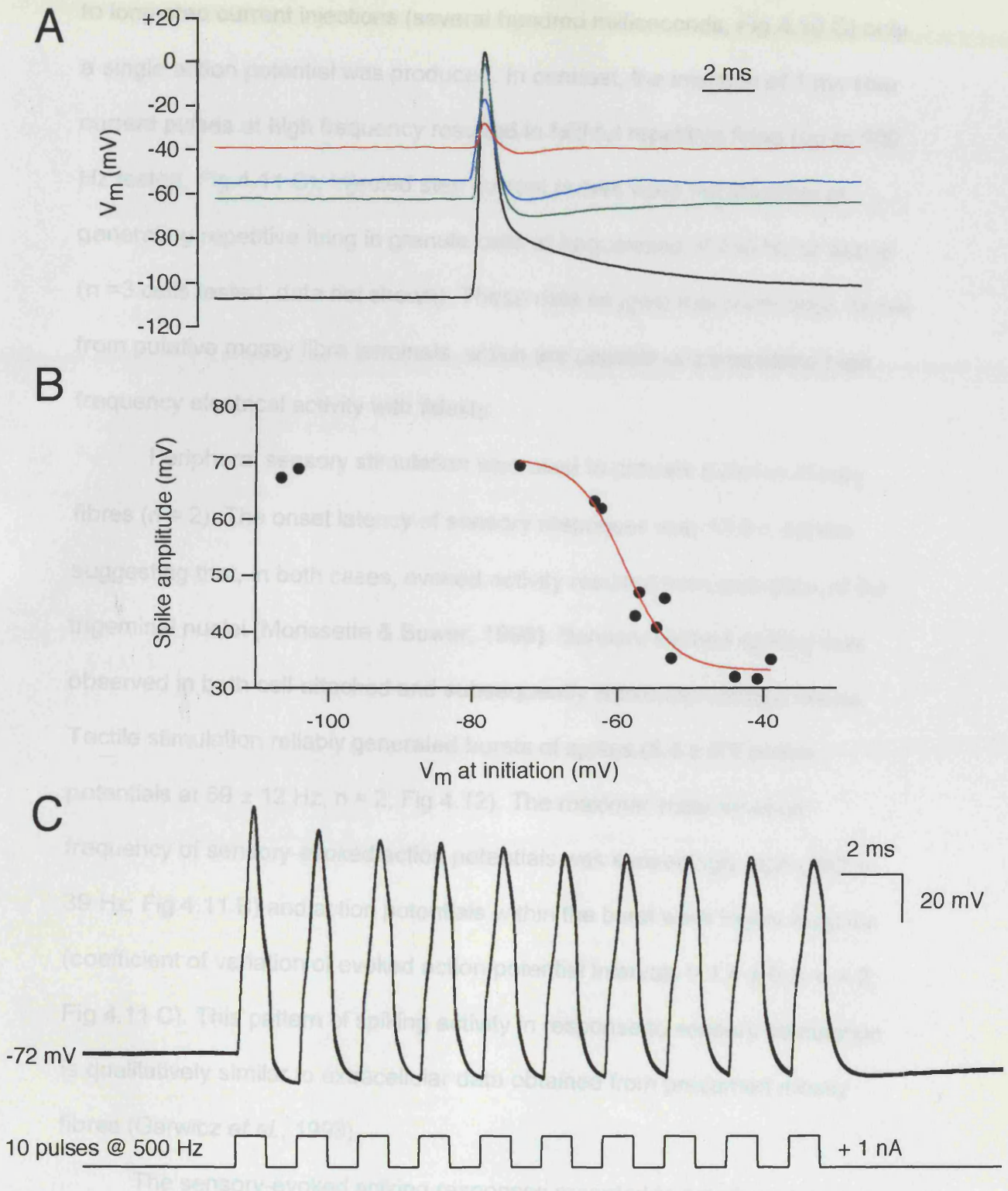

Figure 4.11

Spiking properties of putative mossy fibre terminals. **A** Representative action potentials recorded at different membrane potentials. **B** Action potential amplitude decreases in a sigmoidal manner at membrane potentials depolarised from rest (V_{rest} = -73 mV for this structure). **C** Putative mossy fibre terminals can be driven to fire action potentials at extremely high frequencies via pulsed current injections (Three consecutive trials, overlaid).

to long-step current injections (several hundred milliseconds, Fig 4.10 C) only a single action potential was produced. In contrast, the injection of 1 ms step current pulses at high frequency resulted in faithful repetitive firing (up to 500 Hz tested, Fig 4.11 C). Injected step current pulses were not effective at generating repetitive firing in granule cells at frequencies of 250 Hz or above (n =3 cells tested; data not shown). These data suggest that recordings derive from putative mossy fibre terminals, which are capable of transmitting high frequency electrical activity with fidelity.

Peripheral sensory stimulation was used to activate putative mossy fibres (n = 2). The onset latency of sensory responses was 12.0 ± 3.6 ms, suggesting that, in both cases, evoked activity resulted from activation of the trigeminal nuclei (Morissette & Bower, 1996). Sensory-evoked spiking was observed in both cell-attached and subsequently whole-cell configurations. Tactile stimulation reliably generated bursts of spikes (5.4 ± 0.3 action potentials at 69 ± 12 Hz, n = 2; Fig 4.12). The maximal instantaneous frequency of sensory-evoked action potentials was exceedingly high (742 ± 39 Hz; Fig 4.11 B) and action potentials within the burst were highly irregular (coefficient of variation of evoked action potential intervals = 1.4 ± 0.3, n = 2; Fig 4.11 C). This pattern of spiking activity in response to sensory stimulation is qualitatively similar to extracellular data obtained from presumed mossy fibres (Garwicz *et al.*, 1998).

The sensory-evoked spiking responses recorded in putative mossy fibres were compared with sensory-evoked mossy fibre EPSCs, recorded in cerebellar granule cells. Sensory-evoked EPSCs were also highly irregular (coefficient of variation of all evoked EPSC intervals = 0.82 ± 0.07, n = 5; Fig

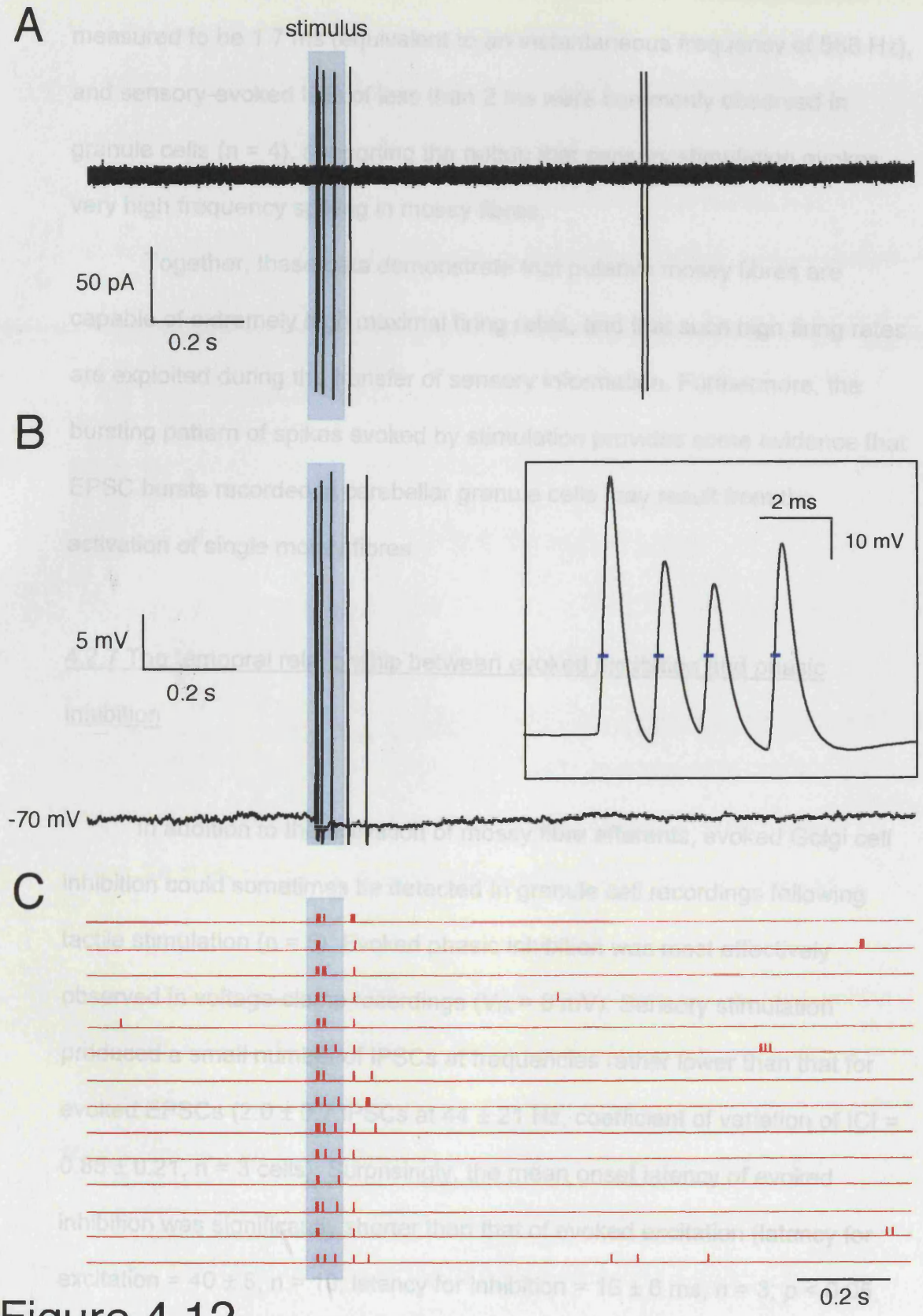

Figure 4.12

Recordings from putative mossy fibre terminals during sensory stimulation. **A** Cell-attached action currents evoked by whisker stimulation. **B** Whole-cell recording from the same structure during whisker stimulation. Panel: high frequency spike burst evoked by whisker stimulation (blue markers indicate time of spike detection). Interspike intervals of < 1.5 ms were observed. **C** Raster plot of spiking responses to whisker stimulation (14 consecutive trials).

4.4, Fig 4.5 A). Furthermore, the minimum ICI of mossy fibre EPSCs, was measured to be 1.7 ms (equivalent to an instantaneous frequency of 588 Hz), and sensory-evoked ICIs of less than 2 ms were commonly observed in granule cells (n = 4), supporting the notion that sensory stimulation evokes very high frequency spiking in mossy fibres.

Together, these data demonstrate that putative mossy fibres are capable of extremely high maximal firing rates, and that such high firing rates are exploited during the transfer of sensory information. Furthermore, the bursting pattern of spikes evoked by stimulation provides some evidence that EPSC bursts recorded in cerebellar granule cells may result from the activation of single mossy fibres.

4.2.7 The temporal relationship between evoked excitation and phasic inhibition

In addition to the activation of mossy fibre afferents, evoked Golgi cell inhibition could sometimes be detected in granule cell recordings following tactile stimulation (n = 5). Evoked phasic inhibition was most effectively observed in voltage-clamp recordings (V_m = 0 mV). Sensory stimulation produced a small number of IPSCs at frequencies rather lower than that for evoked EPSCs (2.0 ± 0.7 IPSCs at 44 ± 21 Hz, coefficient of variation of ICI = 0.85 ± 0.21, n = 3 cells). Surprisingly, the mean onset latency of evoked inhibition was significantly shorter than that of evoked excitation (latency for excitation = 40 ± 6, n = 10; latency for inhibition = 16 ± 6 ms, n = 3; $p < 0.05$, unpaired *t*-test). This pattern could be directly observed in one granule cell, in

which tactile stimulation evoked both mossy fibre EPSCs and Golgi cell IPSCs (Fig 4.13). Such a long delay (> 20 ms) between the onsets of excitatory and inhibitory activity cannot be explained through the connectivity of the granule cell layer. The precedence of inhibition over excitation is surprising, since afferent input to the granule cell layer of the cerebellum is exclusively excitatory. These findings suggest that, in these cases, Golgi cell activation may result from a separate subset of mossy fibres, conveying direct trigeminal nuclear input, rather than longer latency corticopontine inputs (Morissette & Bower, 1996).

4.2.8 Role of tonic inhibition in fidelity of the sensory signal

In the previous chapter, it was shown that a tonic GABAergic conductance plays a key role in regulating the transformation of mossy fibre input into granule cell output *in vivo*, specifically by dampening granule cell excitability. However, the role that tonic inhibition serves in granule cells during the processing of sensory-evoked activity has not been explored explicitly.

In one granule cell, it was possible to observe sensory-evoked spiking responses at rest, and following the blockade of $GABA_A$ receptors with gabazine (0.5 mM). Whisker stimulation evoked mossy fibre EPSPs in the absence of observable IPSPs, indicating that Golgi cell inputs were not concomitantly active. Under resting conditions, spontaneous firing rates remained extremely low, and stimulation trials generated one or two action potentials (Fig 4.14 A, B). Following block of inhibition, increases in both the

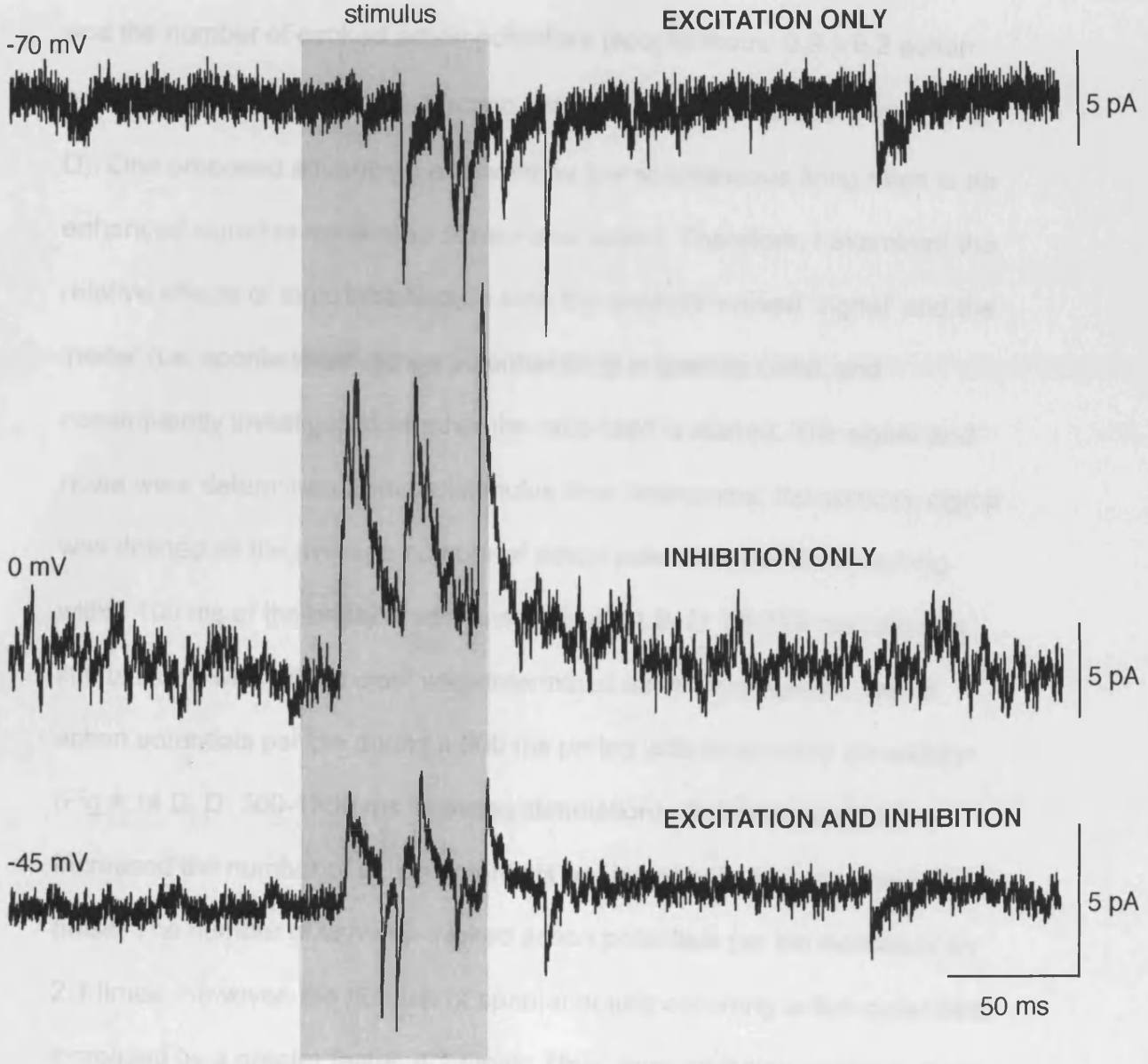

Figure 4.13

Excitation and inhibition evoked in a single granule cell following sensory stimulation. Top: Voltage clamp recording at -70 mV, resolving sensory-evoked mossy fibre EPSCs. Middle: Voltage clamp recording at 0 mV, resolving Golgi cell IPSCs. Bottom: Voltage clamp recording at -45 mV showing both inward (excitatory) and outward (inhibitory) synaptic currents. The onset latency of evoked inhibition was over 20 ms shorter than that of evoked excitation.

spontaneous firing rate (spontaneous: 0.9 ± 0.2 Hz, gabazine: 3.5 ± 0.4 Hz) and the number of evoked action potentials (spontaneous: 0.9 ± 0.2 action potentials, gabazine: 1.9 ± 0.1 action potentials) were observed (Fig 4.14 C, D). One proposed advantage endowed by low spontaneous firing rates is an enhanced signal-to-noise ratio of neuronal output. Therefore, I examined the relative effects of tonic inhibition on both the sensory-evoked 'signal' and the 'noise' (i.e. spontaneous action potential firing in granule cells), and consequently investigated whether the ratio itself is altered. The signal and noise were determined from peristimulus time histograms; the sensory-signal was defined as the average number of action potentials per bin occurring within 100 ms of the onset of response (Fig 4.14 B, D: 20-120 ms following stimulation), whilst the 'noise' was determined as the average number of action potentials per bin during a 800 ms period without sensory stimulation (Fig 4.14 B, D: 500-1300 ms following stimulation). Gabazine application increased the number of action potentials per bin of both the signal and the noise. The number of sensory-evoked action potentials per bin increased by 2.1 times. However, the number of spontaneously occurring action potentials increased by a greater factor, 4.1 times. Thus, tonic inhibition seems to have a greater impact upon the amplitude of the noise than the sensory signal. The signal-to-noise ratio was calculated directly as the average number of sensory-evoked action potentials per bin divided by the average number of action potentials per bin during spontaneous activity. Under control conditions at rest this value stood at 10.4, but, following block of inhibition, this value fell to 5.4, a 48% drop. Thus, tonic inhibition does serve to increase the signal-to-

noise ratio of sensory information transfer through the granule cell layer of the cerebellum.

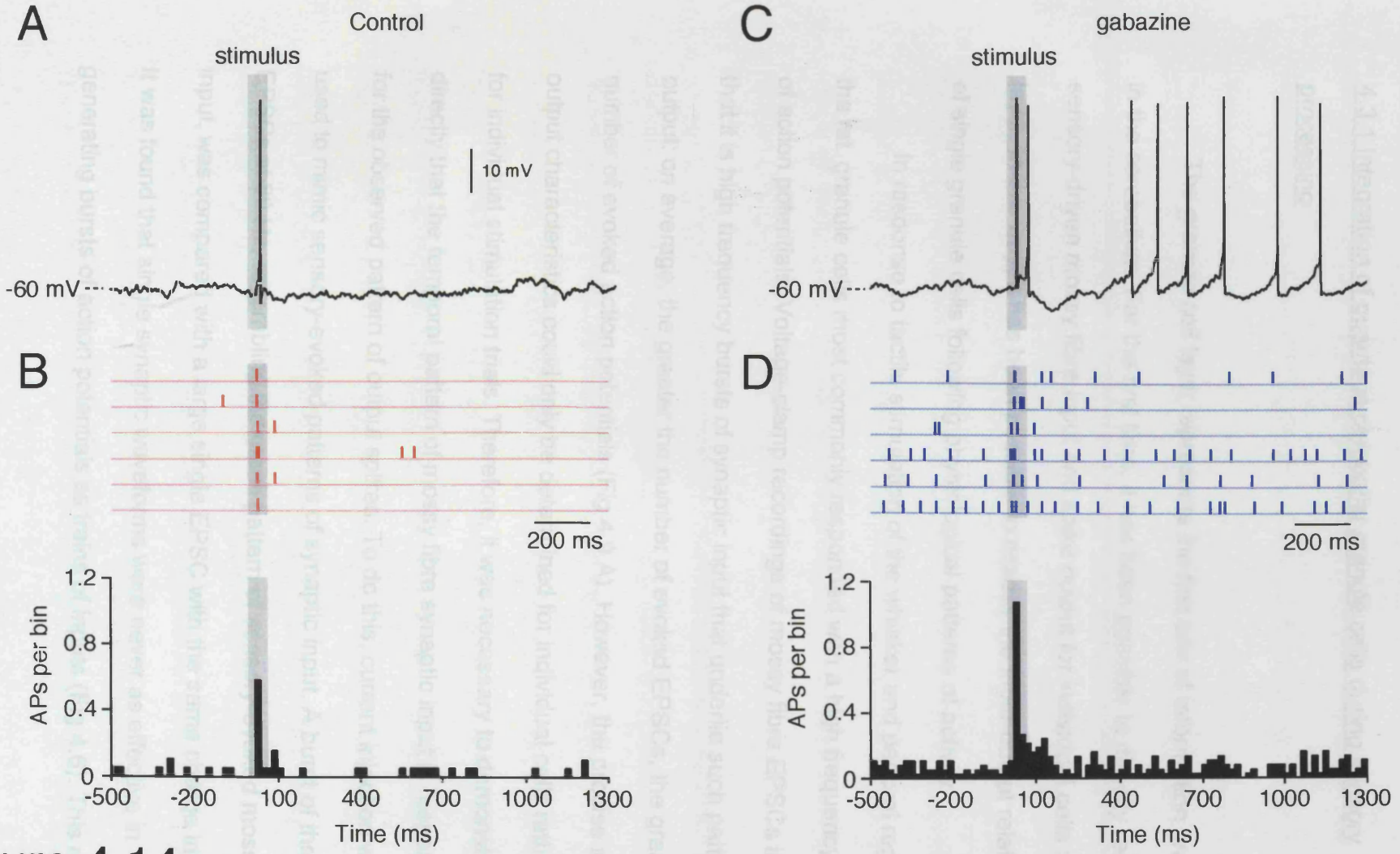

Figure 4.14

The contribution of tonic inhibition during sensory processing in cerebellar granule cells. **A** Sensory-evoked response in a single granule cell under resting conditions. **B** Representative raster plot (top) and peristimulus time histogram (bottom; 14 trials; bin size = 20 ms) from a single granule cell under conditions in which tonic inhibition is intact. **C** Sensory-evoked response in the same cell following the block of $GABA_A$-receptor mediated inhibition. **D** Representative raster plot (top) and peristimulus time histogram (bottom; 37 trials; bin size = 20 ms) from the same cell following block of $GABA_A$-receptor mediated inhibition. An increase in the spontaneous firing occludes the sensory-driven output. Thus tonic inhibition serves to enhance the signal-to-noise ratio during the transmission of sensory signals through the granule cell layer of the cerebellum.

4.3 DISCUSSION

4.3.1 Integration of quanta in cerebellar granule cells during sensory processing

The granule cell layer represents the first site of information processing in the cerebellum. For the first time, it has been possible to directly record sensory-driven mossy fibre input and spike output for individual cells in this layer. In this way, it has been possible to assess the input-output relationship of single granule cells following physiological patterns of activity.

In response to tactile stimulation of the whisker and perioral regions of the rat, granule cells most commonly responded with a high frequency burst of action potentials. Voltage-clamp recordings of mossy fibre EPSCs indicate that it is high frequency bursts of synaptic input that underlie such patterns of output: on average, the greater the number of evoked EPSCs, the greater the number of evoked action potentials (Fig 4.9 A). However, the precise input-output characteristics could only be determined for individual cells rather than for individual stimulation trials. Therefore, it was necessary to demonstrate directly that the temporal pattern of mossy fibre synaptic input is responsible for the observed pattern of output spikes. To do this, current injection was used to mimic sensory-evoked patterns of synaptic input. A burst of three EPSCs at 80 Hz, resembling the mean pattern of sensory-evoked mossy fibre input, was compared with a large single EPSC with the same charge integral. It was found that single synaptic waveforms were never as effective in generating bursts of action potentials as trains of inputs (Fig 4.6). This result

demonstrates that the short high frequency bursts of activity generated by granule cells during sensory stimulation are crucially dependent on the temporal pattern of mossy fibre synaptic input. In contrast, burst firing in other brain regions, such as the thalamus and hippocampus (Deschenes *et al.*, 1982; Deschenes *et al.*, 1984; Harris *et al.*, 2001), is known to be dependent upon intrinsic mechanisms, such as a T-type Ca^{2+} current (Suzuki & Rogawski, 1989). Thus, although granule cells respond to tactile stimulation with a brief burst of action potentials, these data also suggest that granule cells may faithfully represent ongoing high frequency mossy fibre activity. Indeed, *in vitro* studies suggest that intrinsic and synaptic mechanisms (e.g. persistent Na^{+} and NMDA-receptor mediated conductances) may play a key role in allowing granule cells to relay high frequency mossy fibre activity with fidelity (D'Angelo *et al.*, 1995, 1998).

This study has only investigated the sensory processing of one type of stimulus, namely brief tactile stimulation. It is possible that sensory signals derived from different sources, or modalities, will display different characteristics and representations within the cerebellar cortex. High tonic levels of mossy fibre activity, such as has been reported during graded limb movements of monkey forelimbs (van Kan *et al.*, 1993), may therefore be represented in the form of ongoing high frequency granule cell firing. At this stage, it is unclear whether granule cells would respond with a brief burst of activity or high ongoing firing rates under such conditions.

Careful analysis of mossy fibre EPSC amplitudes was performed in order to determine the source of sensory-evoked signals. The finding that the amplitude distributions of sensory-evoked and spontaneous EPSCs are

identical (Fig 4.7) indicates that, within a sensory-evoked burst of mossy fibre EPSCs, individual currents result from the activation of single mossy fibres. This rules out the possibility that single evoked EPSCs result from the synchronous activation of multiple mossy fibres. Therefore, sensory-evoked EPSC bursts either result from bursts within single mossy fibres (Eccles *et al.*, 1971; Garwicz *et al.*, 1998), or asynchronous activation of multiple mossy fibres. In the present experimental configuration, it was not possible to derive the precise number of mossy fibres active within sensory-evoked bursts of EPSCs. In order to address this question, it may be necessary to monitor both pre- and postsynaptic neurons in the same preparation, i.e. trigeminal/pontine neurons *and* granule cells during sensory stimulation. However, at present, the question remains open as to whether granule cell spiking is most commonly the result of single or multiple mossy fibre activation.

Quantal analysis of mossy fibre synaptic transmission was performed following the block of spike-driven transmitter release in the cerebellar cortex. The amplitude distribution of spontaneous and miniature EPSCs was again found to be very similar (Fig 4.8). On average, 70% of spontaneous, and hence sensory-evoked (Fig 4.7), mossy fibre EPSCs appear to result from the release of single quanta. This finding highlights the exquisite sensitivity of granule cells *in vivo*: when correlated by sensory input, the small number of quanta contained within EPSC bursts are sufficient to drive repetitive spiking in these neurons.

Additionally, this result suggests that release probability at the mossy fibre-granule cell synapse is likely to be low. This is in contrast with several *in vitro* studies, which report release probability at this synapse to be rather high

($P_r \geq 0.5$; Sargent *et al.*, 2003; Sola *et al.*, 2004). There are several possible explanations for this discrepancy between the *in vivo* and *in vitro* data. A reduced extracellular Ca^{2+} concentration *in vivo* would be expected to reduce release probability. Desensitisation of postsynaptic AMPA receptors *in vivo* could also account for a reduction in the amplitude spontaneous and sensory-evoked EPSCs (Xu-Friedman & Regehr, 2003). Alternatively, a high proportion of single-site mossy fibre-granule cell synapses could account for the observed low quantal content under conditions where release probability is high.

During sensory stimulation, the number of evoked EPSCs is critical in determining the resultant number of evoked action potentials. However, a one-to-one transformation of synaptic current to spike does not occur. Four out of five granule cells lay below the unity line, indicating a requirement for EPSP summation in spike generation (Fig 4.8). Such a finding is unsurprising considering the distance of granule cell resting membrane potential from threshold and the size of unitary EPSPs. The relationship between the number of evoked EPSCs and action potentials is approximately linear, suggesting that later EPSCs within evoked bursts can generate spikes in an 'one-to-one' manner. Such a transformation is supported by the finding that the input-output frequencies are very well matched for high-frequency, regularly-timed stimulations to granule cells *in vitro* (D'Angelo *et al.*, 1995). However, a similar correlation between input and output frequency was not observed in my results, and this is likely to be due high temporal irregularity observed in sensory-evoked EPSC bursts (Fig 4.5).

The precise degree of summation required to effect output in granule cells is likely to show a high degree of variability over both short and long time periods. Variations in quantal size, resting membrane potential, input resistance and inward rectification will all affect the degree of summation necessary to generate spiking, and hence alter the input-output relationship of cerebellar granule cells. All of these factors have been shown to be subject to modulatory control and will consequently alter the input-output relationship over different timescales. For example, phasic inhibition (milliseconds), tonic inhibition (seconds) and long-term plasticity at the mossy fibre-granule cell synapse (hours; Sola *et al.*, 2004) are all likely to interact to determine granule cell input-output transformation.

The burst-to-burst transformation of sensory-evoked activity performed by granule cells demonstrates that these neurons integrate sensory inputs over tens of milliseconds in order to generate spike output. Although simultaneous activation of multiple mossy fibres has been shown to generate granule cell output (D'Angelo *et al.*, 1995), single large-amplitude synaptic waveforms were observed to produce one, or at the most, two action potentials (Fig 4.5). It therefore appears that temporal integration of distributed synaptic inputs is extremely important in shaping sensory-evoked granule cell output patterns. In the previous chapter, it was seen that granule cells possess several intrinsic conductances that serve to broaden the time window of integration (Figs 3.5, 3.6). In particular, activation of NMDA receptors and 'spillover' activation of AMPA receptors within the glomerulus both produce a lengthening in the decay time of granule cell EPSPs (D'Angelo *et al.*, 1995; DiGregorio *et al.*, 2002). Furthermore, a persistent Na^+ current

also prolongs transient membrane depolarisations (D'Angelo *et al.*, 1998). Together these conductances extend the time window of granule cell integration beyond what would be expected from the passive membrane time constant and the kinetics of AMPA EPSC waveform, and facilitate granule cell spiking in response to mossy fibre inputs distributed over several tens of milliseconds.

4.3.2 Sensory-evoked bursting in putative mossy fibres

Patch clamp recordings were also made from putative mossy fibres within the granule cell layer of the cerebellum. Putative mossy fibres were classified as such on the basis of their characteristic electrophysiological properties. In all cases, synaptic activity was absent, and action potential occurrence was independent of membrane potential (Fig 4.10 A, B). Together, these features rule out a somatodendritic recording site, instead supporting an axonal recording location. Previously, patch clamp recordings have been made from mossy fibre nerve terminals in hippocampal slices (Geiger & Jonas, 2000) and neocortical synaptosomes (Smith *et al.*, 2004). Recordings have also been made from basket cell terminals in cerebellar slices (Southan & Robertson, 1998; Southan *et al.*, 2000). Qualitatively, putative mossy fibres in cerebellar granule cell layer share several features with these axonal recordings: in particular, the presence of an I_h current, as indicated by membrane potential sag, and outward rectification (Fig 4.10 C) (Southan & Robertson, 1998; Geiger & Jonas, 2000; Southan *et al.*, 2000). The precise role of I_h in synaptic terminals is unclear, although a resting I_h conductance in

mossy fibres will reduce the membrane time constant, favouring the rapid voltage fluctuations observed in response to brief current injections (Fig 4.11 C). The activation profile of I_h, increasing at hyperpolarising potentials (Southan *et al.*, 2000), may also serve a homeostatic function upon resting membrane potential.

Another characteristic feature of putative mossy fibres is their ability to fire action potentials at extremely high rates. This contrasts with granule cells, that were not observed to fire action potentials at frequencies above 250 Hz, and Golgi cells, not above 300 Hz (E D'Angelo; personal communication). Using pulsed current injection, putative mossy fibres could be reliably induced to fire at frequencies of up to 500 Hz and spontaneous action potentials were observed to occur at even higher frequencies. Extracellular recordings of putative mossy fibre activity (Eccles *et al.*, 1971; Garwicz *et al.*, 1998) and recordings made from neurons in the trigeminal and pontine nuclei, the origin of mossy fibres, report similarly high instantaneous firing rates.

Tactile stimulation reliably produced a high frequency burst of action potentials in mossy fibres (Fig 4.12). This pattern of response is potentially of great significance when one considers the observed pattern of sensory-evoked mossy fibre EPSCs recorded in granule cells. It has not been possible to determine the source of individual EPSCs within sensory-evoked bursts. However, since individual putative mossy fibres have been found to generate similar patterns of evoked activity, it seems likely that individual mossy fibres may be solely responsible for sensory responses observed in some granule cell recordings. Therefore, action potentials in granule cells may result from the activation of a single mossy fibre. The theoretical work of David Marr

(Marr, 1969), has suggested that such a scheme may be possible. However, to date, experimental evidence has been lacking on this matter. Previously, this issue has been investigated *in vitro*, using electrical stimulation of afferent fibres to recruit increasing numbers of mossy fibres to single granule cells. Coincident activation of three mossy fibres was necessary to trigger granule cell action potentials (D'Angelo *et al.*, 1995). However, it appears from my results that repetitive high frequency activity in single mossy fibres may also be sufficient to drive information transfer through the granule cell layer of the cerebellum.

Information transfer via single mossy fibres is especially surprising when considered from the perspective of the glomerulus. Within each glomerulus, a single mossy fibre makes synaptic contact with up to 50 individual granule cells (Hamori & Somogyi, 1983). If single mossy fibre activity drives spiking in single granule cells, then presumably mossy fibre activity can drive spiking activity in all of the granule cells of a given glomerulus. As such, high frequency, repetitive activation of single mossy fibres might be expected to drive synchronous firing in a great many granule cells. With 20-30 mossy fibre varicosities per folium (Palay & Chan-Palay, 1974), and 50 granule cell dendrites per varicosity, an expected 1000-1500 granule cells would be activated. The computational benefits of such a scheme are not clear: Albus's proposal that the granule cell layer serves as an 'expansion recoder' (Albus, 1971) does not seem compatible with this form of information transfer. However, without the capability to record from multiple granule cell units from same glomerulus during sensory stimulation, such discussion remains speculative.

4.3.3 Physiological significance of high frequency firing in granule cells

Somatosensory stimulation generated a characteristic burst of action potentials in cerebellar granule cells. There is considerable evidence to suggest that such patterns of output may have special implications for the downstream targets of granule cells through activation of a variety of frequency-dependent signalling pathways.

The parallel fibre-Purkinje cell synapse shows a marked frequency-dependent facilitation of transmitter release (Konnerth *et al.*, 1990; Perkel *et al.*, 1990; Atluri & Regehr, 1996), thus amplifying the contribution of repetitively-firing granule cells to synaptic integration within the Purkinje cell. Furthermore, glutamate diffusion from the synaptic cleft during high frequency parallel fibre stimulation is sufficient to activate extrasynaptic 'Type 1' metabotropic glutamate receptors (Finch & Augustine, 1998; Takechi *et al.*, 1998). Activation of such receptors has been shown to produce Ca^{2+} transients in Purkinje cell spines and dendrites via an IP_3-dependent pathway (Takechi *et al.*, 1998). Activation of mGluR1s has also been shown to mediate long-term synaptic changes at the parallel fibre-Purkinje cell synapse (Batchelor & Garthwaite, 1997; Wang *et al.*, 2000).

In addition, activation of NMDA receptors located at presynaptic terminals of parallel fibres is dependent upon high frequency repetitive firing. It has been shown that glutamate released at parallel fibre synapses will bind to presynaptic NMDA receptors, and that a subsequent depolarisation of the terminal is required for receptors to be activated (Casado *et al.*, 2000). Typically, when this phenomenon has been studied, activation of presynaptic

NMDA receptors has required at least two parallel fibre action potentials with an interspike interval of less than 50 ms (Casado *et al.*, 2000). This interspike interval corresponds to an instantaneous firing frequency of 20 Hz, and thus the frequency of sensory-evoked bursts in granule cells observed in this study (77 ± 12 Hz) is more than sufficient to activate these receptors. Activation of presynaptic NMDA receptors has been implicated in long-term depression of parallel fibre-Purkinje cell synapses when repetitive parallel activity is paired with postsynaptic depolarisation (Casado *et al.*, 2002).

Brief presynaptic bursts in parallel fibres have also been shown to activate an endocannabinoid-mediated signalling pathway that selectively reduces transmitter release at activated synapses for several seconds (Brown *et al.*, 2003; Brown *et al.*, 2004). Brown and colleagues demonstrated that 10 parallel fibre stimuli at 50 Hz could induce this suppression of excitation (Brown *et al.*, 2003), suggesting that sensory-evoked bursting may also activate this pathway.

Together, these studies highlight the sensitivity of the parallel fibre-Purkinje cell synapse to brief high frequency bursts of activity observed *in vivo*. It is not currently clear how the range of different frequency-dependent signalling pathways interact during synaptic integration in Purkinje cells. However, their effects over both short and long time scales suggests that high frequency firing in granule cells may be important in both information processing and memory storage in the cerebellum.

4.3.4 Sparse coding of sensory signals in the cerebellar cortex

It has been proposed that the cerebellar cortex serves the role of a pattern discriminator (Marr, 1969; Albus, 1971), and that the number of distinct distinguishable patterns is increased if parallel fibre activity is kept low. In other words, information provided to Purkinje cells via parallel fibres takes the form of a 'sparse code'. This study provides support the notion that the granule cell layer is a low-noise sparse coding system (Gibson *et al.*, 1991; Schweighofer *et al.*, 2001). The burst-to-burst transformation that occurs in individual granule cells ensures that granule cells reliably relay sensory-evoked mossy fibre signals, whereas events not associated with sensory stimulation are filtered out. It has previously been demonstrated that bursting further enhances the signal-to-noise ratio for transfer of sensory information in an input layer exhibiting low firing rates (Lisman, 1997; Harris *et al.*, 2001; Hahnloser *et al.*, 2002; Margrie *et al.*, 2002; Krahe & Gabbiani, 2004). One of the principal regulators of sparse coding in the granule cell layer would seem to be a tonic GABAergic inhibitory conductance (see chapter 3) (De Schutter, 2002; Hamann *et al.*, 2002). The influence of this conductance upon the transfer of sensory signals through the granule cell layer was investigated directly in this chapter (Fig 4.14). Under conditions where tonic inhibition was blocked, spontaneous and sensory-evoked spiking were both enhanced. However, the increase in spontaneous granule cell output was proportionately greater than the observed increase for sensory-evoked output. Thus if one considers sensory-evoked spiking as the 'signal' and spontaneous spiking as

the 'noise', their ratio is significantly improved by the presence of a tonic GABAergic conductance to cerebellar granule cells.

4.3.5 Temporal features of sensory-evoked Golgi cell input to granule cells

In addition to a tonic inhibitory conductance, phasic Golgi cell IPSCs were sometimes evoked during sensory stimulation (n = 3). Surprisingly, the onset latency of evoked phasic inhibition was over 20 ms shorter than the mean value for evoked mossy fibre excitation (Fig 4.13). In addition to feedback from parallel fibres, Golgi cells receive direct inputs from mossy fibres. The presence of an additional synaptic relay in the generation of mossy fibre-driven phasic inhibition to granule cells means that mossy fibre excitation should always precede inhibition. However, Golgi cells have a far larger dendritic arborisation than individual granule cells, and consequently receive inputs from many more mossy fibres. Therefore, one explanation for these results is that Golgi cells receive both fast and slow latency inputs (Morissette & Bower, 1996), and yet exert inhibitory control over granule cells receiving only one class of input. Such a scheme is plausible when one considers that both fast trigeminal, and longer latency corticopontine inputs arrive in approximately the same area of cerebellar cortex (Morissette & Bower, 1996), and that the majority of recorded sensory-evoked mossy fibre EPSCs in this study derive from a corticopontine origin.

This finding suggests some interesting functional implications for the role of sensory-evoked phasic inhibition in the granule cell layer. Although, fast trigeminal mossy fibres may only excite a small subset of granule cells,

their influence will be felt over a much larger population if the excitation is sufficient to activate Golgi cells. In this manner, all granule cells within the axonal plexus of a given Golgi cell will be influenced by the small number of short latency mossy fibres. Phasic inhibition has been shown to be crucial in regulating the timing of spike generation in neurons in many areas of the brain (Wehr & Zador, 2003; Mittmann *et al.*, 2004), and particularly in the establishment of rhythmic or synchronous firing in populations of neurons (Freund & Buzsaki, 1996; Maex & Schutter, 1998). Within the cerebellum, such fast, synchronous inhibition to a large population of granule cells could serve to enforce greater temporal precision upon spiking within the population, or act as to dampen granule cell activity prior to corticopontine sensory input.

4.3.6 Influence of the properties of the sensory stimulus on evoked responses in cerebellar granule cells

The evoked responses described in this thesis were produced using brief air puff stimulation to tactile surfaces of the face and vibrissae. All of the responses described in here, bar one, corresponded solely to the onset of the stimulus (i.e. a deflection of one or more whiskers, or pressure to a small area of skin), and the duration of the air puff itself did not alter the properties of the evoked response (Fig 4.3). Thus deflection (or in the case of the off response, presumably the relaxation following the deflection) is represented at the input layer of the cerebellum as a high frequency burst of activity. However, it is worth bearing in mind that in the current experimental configuration, the

animal is largely without sensory input except for the brief moments during which the stimulus is presented. In contrast, under awake conditions, rats typically exhibit spontaneous whisking (Kleinfeld *et al.*, 2002; Neimark *et al.*, 2003), and during certain behaviours, e.g. tactile exploration (Hartmann & Bower, 2001), it likely that sensory input will be, to some extent, 'ongoing'. In this case, it is difficult to say whether sensory information will be represented to the cerebellum as brief bursts of activity.

Chapter 5: PATTERNS OF PURKINJE CELL ACTIVITY *IN VIVO*

5.1 INTRODUCTION

Purkinje cells represent the final stage of information processing within the cerebellar cortex. In order to understand the cerebellum's role in sensory processing, it is therefore crucial to understand how sensory inputs shape the patterns of Purkinje cell output spikes. Purkinje cells integrate excitatory synaptic inputs from granule cells, made via axon ascending segments and parallel fibres (Llinas & Walton, 1998), and inhibitory synaptic inputs from molecular layer interneurons. In addition, each Purkinje cell receives a single excitatory climbing fibre input, which powerfully modulates activity. Together, synaptic inputs are integrated within Purkinje cells, and the resultant patterns of output spiking represent the sole cerebellar cortical output to the deep cerebellar nuclei.

Two discrete spike patterns are observed both intra- and extracellularly in Purkinje cells. They fire sodium action potentials, often referred to as simple spikes (SS), spontaneously *in vivo* and *in vitro*. Extracellular recordings from Purkinje cells in anaesthetised and awake animals at rest have reported mean SS firing rates of 40-50 Hz and 20-100 Hz respectively (Granit & Phillips, 1956; Eccles *et al.*, 1967a; Thach, 1968; Bell & Grimm, 1969; Armstrong & Rawson, 1979; Nitz & Tononi, 2002). Purkinje cells fire SS spontaneously *in vitro*, in the presence of synaptic blockers (Häusser & Clark, 1997), and as dissociated somata (Raman & Bean, 1997), suggesting that intrinsic conductances play an important role in establishing simple spike activity in these cells.

In response to climbing fibre activation, Purkinje cells generate a stereotyped burst discharge called a complex spike (CS), which can be distinguished from ongoing simple spikes both intra- and extracellularly (Ito, 1984). Complex spikes are most commonly observed to occur at low mean rates (0.5 - 2 Hz) in both anaesthetised and awake animals (Eccles *et al.*, 1967a; Thach, 1968; Bell & Grimm, 1969; Armstrong & Rawson, 1979). The importance of the climbing fibre input to Purkinje cells to overall cerebellar function is highlighted by the fact that destruction of climbing fibres produces behavioural effects similar to those of cerebellectomy (Armstrong, 1974; Sukin *et al.*, 1987). The work of Ito and his followers has revealed much about the dependence upon complex spike activity of some forms of parallel fibre synaptic plasticity (Ito, 2001), in a means consistent with Marr-Albus theories of cerebellar learning (Marr, 1969; Albus, 1971). Prior to, and following this work, considerable data has been gathered on the effects of CS firing on SS discharge. Classically, the CS has been described to cause a pause in SS firing (Armstrong, 1974). However, many studies have reported facilitation (Rawson & Tilokskulchai, 1981), or bidirectional effects on SS firing (Bell & Grimm, 1969; Murphy & Sabah, 1970; Armstrong & Rawson, 1979; McDevitt *et al.*, 1982). These effects upon simple spiking have been seen to persist over several hundred milliseconds (Armstrong & Rawson, 1979).

Granule cells provide the vast majority of excitatory synaptic input to Purkinje cells via ascending limb axons and parallel fibres. Parallel fibres span several millimetres of the cerebellar cortex and make synapses on at least every other Purkinje cell encountered along their course (Harvey & Napper, 1991). Thus, sensory inputs received by individual Purkinje cells are expected

to arise from large areas of the underlying granule cell layer. However, it has been shown that the cutaneous receptive fields of Purkinje cells are typically small (Ekerot & Jorntell, 2001), and that there exists a high degree of vertical congruence in the patterns of sensory activation in the cerebellar cortex (Bower & Woolston, 1983). Thus, it has been proposed that most parallel fibres are depressed or electrically silent (Isope & Barbour, 2002; Jorntell & Ekerot, 2002), or that parallel fibre activity provides a predominantly tonic source of excitation, serving to modulate Purkinje cell responses to powerful ascending limb inputs (Llinas, 1982).

In this chapter, I have investigated the spontaneous and sensory-evoked activity of Purkinje cells and interneurons from the cerebella of rats anaesthetised with ketamine / xylazine or urethane. By combining cell-attached and whole-cell recording, it has been possible to observe a profound and robust bistability of Purkinje cell spike output and membrane potential. This bistability is not exhibited by cerebellar interneurons, and is reflected in a bimodal pattern of Purkinje cell simple spiking. Spontaneous state transitions show a strong dependence upon climbing fibre input. Using peripheral sensory stimulation, it has been possible to evoke complex spikes, which, it will be shown, drive state transitions in both directions.

This work has been done in close collaboration with Dr. Severine Mahon, who has made quantitatively similar findings. As such, some values provided for sensory-evoked responses, described in the text, come from pooled data – these instances are indicated in the text. However, all data and traces presented in the figures derive from Purkinje cell recordings I have made.

5.2 RESULTS

5.2.1 Spontaneous membrane potential bistability in Purkinje cells *in vivo*

To investigate how physiological synaptic inputs interact to generate output in Purkinje cells, blind *in vivo* cell-attached and whole-cell patch clamp recordings were made in the lateral cerebellar hemispheres of anaesthetised rats. Purkinje cells were unequivocally identified according to the occurrence of complex spikes at a typical frequency (1.6 ± 0.5 Hz, range: 0.1 – 5.7 Hz; n = 10 cells). Previously, *in vitro* recordings targeted to Purkinje cell soma and dendrites have established that somatic Na^+ action potentials are initiated close to the soma and become strongly attenuated within Purkinje cell dendrites (Llinas & Sugimori, 1980c, b; Stuart & Hausser, 1994). Whole cell recordings in this study were classified as being made from a somatic location if fast, overshooting action potentials were observed (six out of ten recordings). In presumed dendritic recordings, simple spikes were always strongly attenuated (SS amplitudes < 5 mV; four out of ten recordings). Interestingly, in both somatic and dendritic recordings, discrete synaptic potentials were never observed (see records in Figs. 5.1, 5.2, 5.4, 5.5 and 5.7). As such, it was not possible to quantify the rate or amplitude of parallel fibre- and interneuron-driven synaptic inputs. Due to the large number of synaptic inputs to individual Purkinje cells (Harvey & Napper, 1988), this finding is likely to be due to dendritic filtering of ongoing inhibitory and excitatory synaptic inputs, rather than a complete lack of parallel fibre and interneuron activity.

In nine out of ten whole-cell recordings, Purkinje cells displayed step-like transitions in membrane potential between a hyperpolarised state (down state) and a depolarised spiking state (up state; Fig 5.1 A, B). Membrane potential up and down states were observed in both somatic (n = 5) and dendritic recordings (n = 4). The existence of two distinct states was apparent in the bimodal distribution of membrane potential (Fig 5.1 C). A dip test, which gives the likelihood of a sample being drawn from a unimodal distribution (Hartigan, 1985), was used to assess the statistical significance of this bimodality. In the nine cells in which bistable behaviour was observed, membrane potential was found to be significantly non-unimodal ($p < 0.001$).

The average values of membrane potential of non-spiking periods in down and up states were –62.2 ± 1.8 mV and –46.0 ± 2.3 mV respectively (n = 9 cells), leading to a voltage difference between the two states of 16.2 ± 2.7 mV (n = 9). The durations of up and down states were quantified using long periods of continuous recording. The time spent by a Purkinje cell in a given state could vary considerably between and within cells (Fig 5.1 A). The mean dwell times of the down and up states, calculated between averaged values of each cell, were 0.80 ± 0.24 sec (range: 0.61 – 2.29 sec) and 1.11 ± 0.35 sec (range: 0.36 – 1.32 sec) respectively (n = 5 cells). Corresponding coefficient of variance (CV) values were 0.66 ± 0.06 for down states and 0.57 ± 0.11 for up states. The mean duration between two successive down-to-up transitions was also examined, and found to be 1.80 ± 0.52 sec with a corresponding CV of 0.41 ± 0.05 (n = 5 cells). These results suggest that the up and down states in Purkinje cells are rather irregular and are thus unlikely to result from a simple underlying oscillatory process.

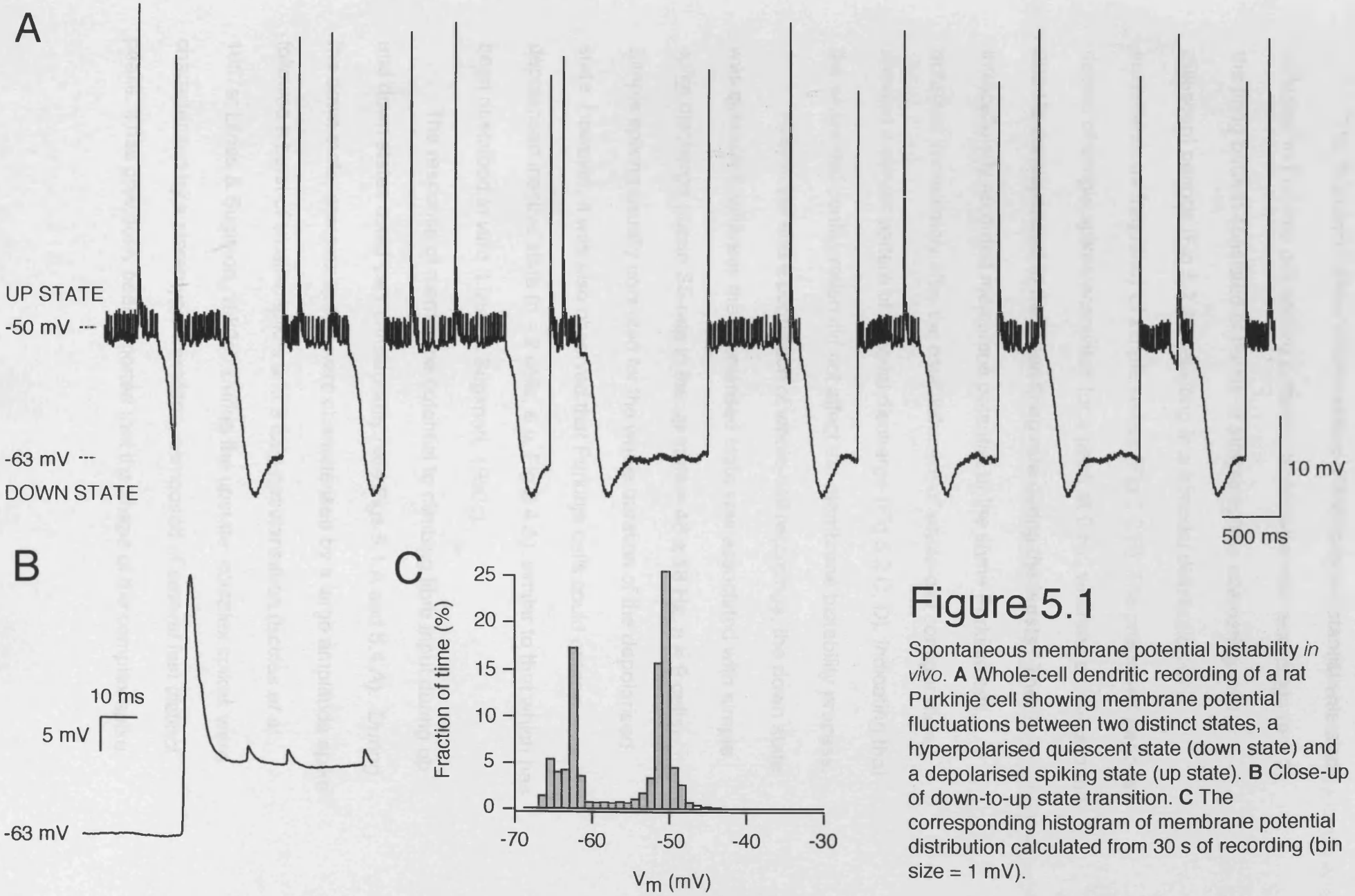

Figure 5.1

Spontaneous membrane potential bistability *in vivo*. **A** Whole-cell dendritic recording of a rat Purkinje cell showing membrane potential fluctuations between two distinct states, a hyperpolarised quiescent state (down state) and a depolarised spiking state (up state). **B** Close-up of down-to-up state transition. **C** The corresponding histogram of membrane potential distribution calculated from 30 s of recording (bin size = 1 mV).

The existence of two distinct states of membrane potential was also reflected in Purkinje cell spiking patterns. In cell-attached recordings (n = 3), the firing pattern consisted of bursts of simple spikes alternating with quiescent periods (Fig 5.2 A), resulting in a bimodal distribution of instantaneous frequency of simple spikes (Fig 5.2 B). The prolonged periods devoid of simple spikes accounted for a peak at 0 Hz, whereas a peak around 200 Hz corresponded to the mean firing rate during the bursts. The intracellularly recorded membrane potential of the same Purkinje cell, obtained immediately after the establishment of whole-cell configuration, showed a similar pattern of bimodal discharge (Fig 5.2 C, D), indicating that the whole-cell configuration did not affect the membrane bistability process.

Across the entire population of whole-cell recordings, the down state was quiescent, whereas the depolarised state was associated with simple spike discharge (mean SS rate in the up state = 46 ± 18 Hz, n = 9 cells). Simple spiking usually persisted for the whole duration of the depolarised state. However, it was also observed that Purkinje cells could enter a depolarised inactive state (n = 2 cells, e.g. Fig 5.4 A), similar to that which has been described *in vitro* (Llinas & Sugimori, 1980c).

The response of membrane potential to climbing fibre input during up and down states could vary considerably (see Figs 5.1 A and 5.4 A). During the down state, complex spikes were characterised by a large amplitude spike followed a burst of smaller spikes and a long depolarisation (Eccles *et al.*, 1967a; Llinas & Sugimori, 1980c). During the upstate, complex spikes were characterised by a stereotypic waveform, composed of several fast distinct peaks. It has previously been reported that the shape of the complex spike

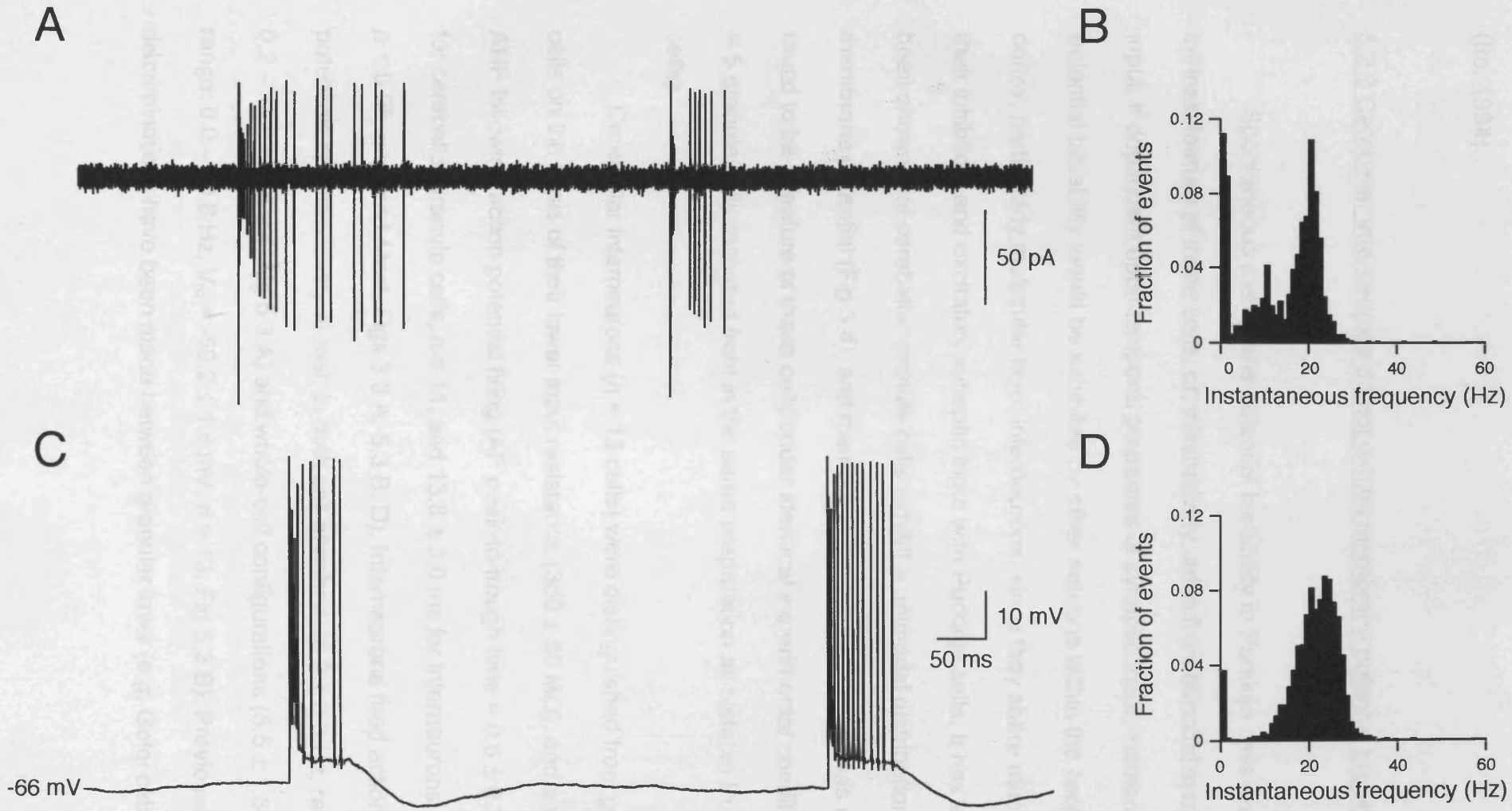

Figure 5.2

Membrane potential bistability is reflected in spike output pattern *in vivo*. **A** Cell-attached patch clamp recording showing the bimodal firing pattern of a Purkinje cell. **B** Bimodal distribution of the instantaneous frequency of simple spike calculated from 30 sec of cell-attached recording (bin size = 10 Hz). **C** Intracellular activity from the same Purkinje cell obtained immediately after the formation of whole-cell configuration. **D** Distribution of the instantaneous frequency of simple spikes calculated from 40 sec of whole-cell recording (bin size = 10 Hz).

following climbing fibre stimulation *in vitro* depends on membrane potential (Ito, 1984).

5.2.2 Cerebellar interneurons do not exhibit membrane potential bistability

Spontaneous membrane potential bistability in Purkinje cells may be an intrinsic feature of these cells, or, alternatively, arise from bimodal synaptic input. If dependent upon temporal properties of synaptic input, membrane potential bistability would be exhibited by other neurons within the cerebellar cortex, particularly molecular layer interneurons, since they share much of their inhibitory and excitatory synaptic input with Purkinje cells. It has already been shown that cerebellar granule cells exhibit a unimodal distribution of membrane potential (Fig 3.4), and membrane potential bistability was not found to be a feature of these cells under identical experimental conditions (n = 5 granule cells recorded from in the same preparation as bistable Purkinje cells).

Cerebellar interneurons (n = 13 cells) were distinguished from granule cells on the basis of their lower input resistance (360 ± 50 MΩ), and a slow AHP following action potential firing (AP peak-to-trough time = 0.6 ± 0.2 ms for cerebellar granule cells, n = 11, and 13.8 ± 3.0 ms for interneurons, n = 13; $p < 0.05$, unpaired *t*-test, Figs 3.3 A, 5.3 B, D). Interneurons fired action potentials spontaneously at rest, in both cell-attached (5.2 ± 3.3 Hz, range: 0.2 – 13.0 Hz, n = 4, Fig 5.3 A) and whole-cell configurations (5.5 ± 1.6 Hz, range: 0.0 – 20.8 Hz, V_m = -59.2 ± 1.8 mV, n = 13, Fig 5.3 B). Previously, discriminations have been made between granular layer (e.g. Golgi cells) and

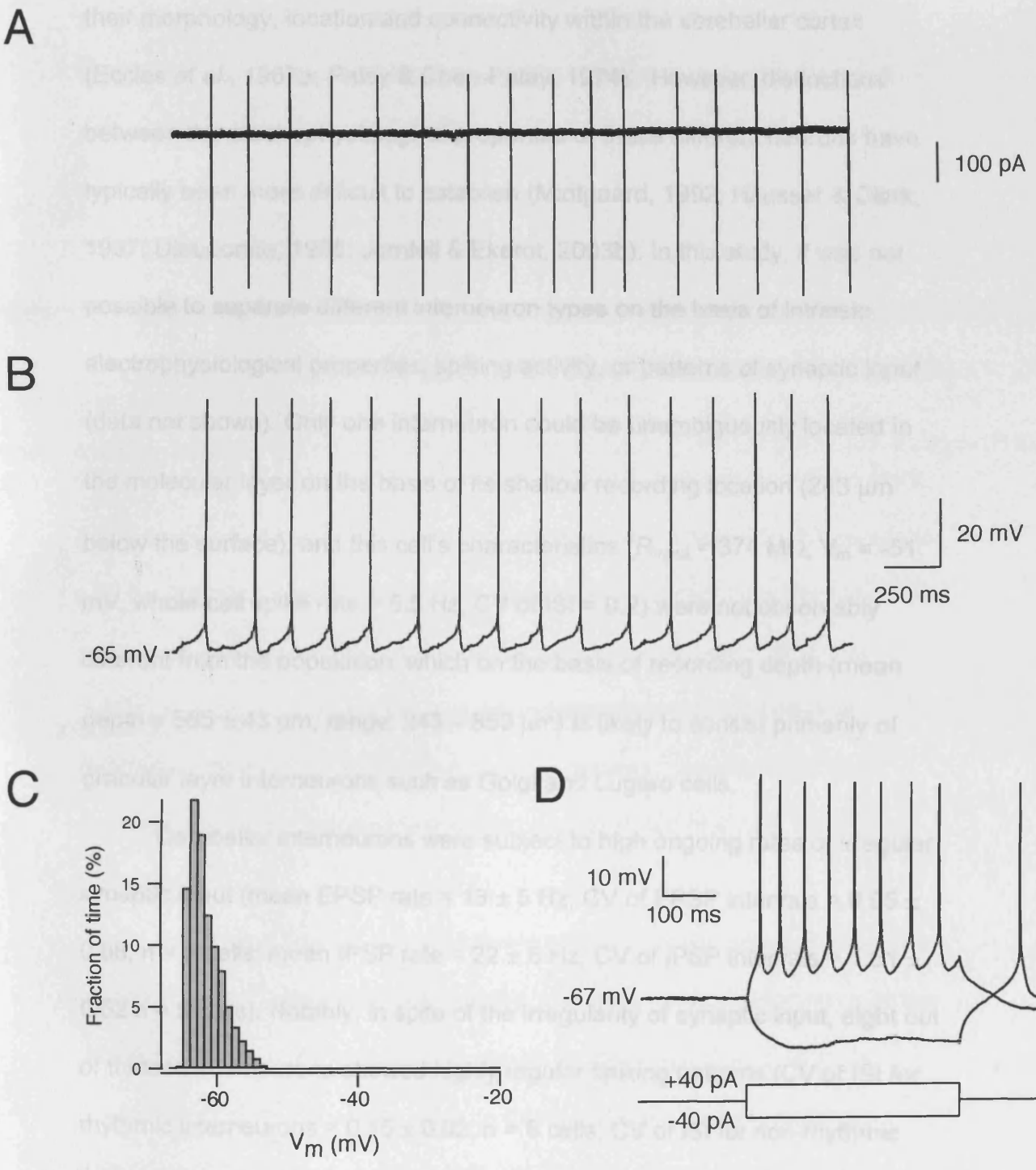

Figure 5.3

Cerebellar interneurons do not exhibit membrane potential bistability *in vivo*. **A** Interneuron firing recorded in cell-attached mode. **B** Voltage recording from the same cell in whole-cell mode in the absence of injected current. **C** Histogram of membrane potential (bin size = 1 mV) from the same cell. **D** Current-voltage relationships for a single cerebellar interneuron.

molecular layer interneurons (i.e. stellate and basket cells) on the basis of their morphology, location and connectivity within the cerebellar cortex (Eccles *et al.*, 1967a; Palay & Chan-Palay, 1974). However, distinctions between the electrophysiological properties of these different neurons have typically been more difficult to establish (Midtgaard, 1992; Häusser & Clark, 1997; Dieudonne, 1998; Jorntell & Ekerot, 2003b). In this study, it was not possible to separate different interneuron types on the basis of intrinsic electrophysiological properties, spiking activity, or patterns of synaptic input (data not shown). Only one interneuron could be unambiguously located in the molecular layer on the basis of its shallow recording location (243 μm below the surface), and this cell's characteristics (R_{input} = 374 MΩ, V_m = -51 mV, whole-cell spike rate = 5.5 Hz, CV of ISI = 0.2) were not observably different from the population, which on the basis of recording depth (mean depth = 565 ± 43 μm, range: 243 – 850 μm) is likely to consist primarily of granular layer interneurons such as Golgi and Lugaro cells.

Cerebellar interneurons were subject to high ongoing rates of irregular synaptic input (mean EPSP rate = 13 ± 5 Hz, CV of EPSP intervals = 0.95 ± 0.08, n = 6 cells; mean IPSP rate = 22 ± 6 Hz, CV of IPSP intervals = 1.61 ± 0.52 n = 5 cells). Notably, in spite of the irregularity of synaptic input, eight out of thirteen interneurons showed highly regular spiking patterns (CV of ISI for rhythmic interneurons = 0.15 ± 0.02, n = 8 cells; CV of ISI for non-rhythmic interneurons = 0.93 ± 0.19, n = 5 cells; Fig 5.3 A, B), indicating autorhythmicity. These cells did not show any detectable difference in their intrinsic properties (R_{input}, V_m, AHP, spike rate) compared with non-rhythmic interneurons (data not shown).

Nevertheless, it is important to note that all cerebellar interneurons lacked a bimodal distribution of membrane potential (Hartigan's dip test, $p > 0.05$; n = 9 cells tested), thus indicating that membrane potential bimodality is a specific property of Purkinje cells within the cerebellar cortex.

5.2.3 Synaptic control of intrinsic Purkinje cell bistability

To understand the origin of Purkinje cell membrane potential bistability, its voltage dependence was examined. Spontaneous up and down state transitions (Fig 5.4 A) could be abolished by injection of negative DC current (-530 ± 180 pA, 4 out of 4 cells tested), which hyperpolarized Purkinje cells to –76.8 ± 2.2 mV. When Purkinje cells were hyperpolarised, only complex spikes were recorded (Fig 5.4 B) and the membrane potential histogram displayed a bell-shaped distribution around the mean holding potential (Hartigan's dip test, $p > 0.05$; 4 out of 4 cells tested). Similarly, constant depolarising current resulted in a single up state (4 out of 4 cells tests; data not shown).

The finding that DC current injections can block Purkinje cell bistability *in vivo* provides further evidence that this phenomenon is dependent upon the intrinsic properties of these cells. However, further inspection of records revealed that state transitions were, in many cases, closely preceded by complex spikes. Indeed, it was found that 74 ± 9 % of state transitions were preceded by a complex spike, with a significantly lower ($p < 0.05$; n = 8 cells) number of transitions occurring apparently spontaneously in the absence of climbing fibre input (Fig 5.5 A-C). Across all Purkinje cells (n = 8), 62 ± 16 %

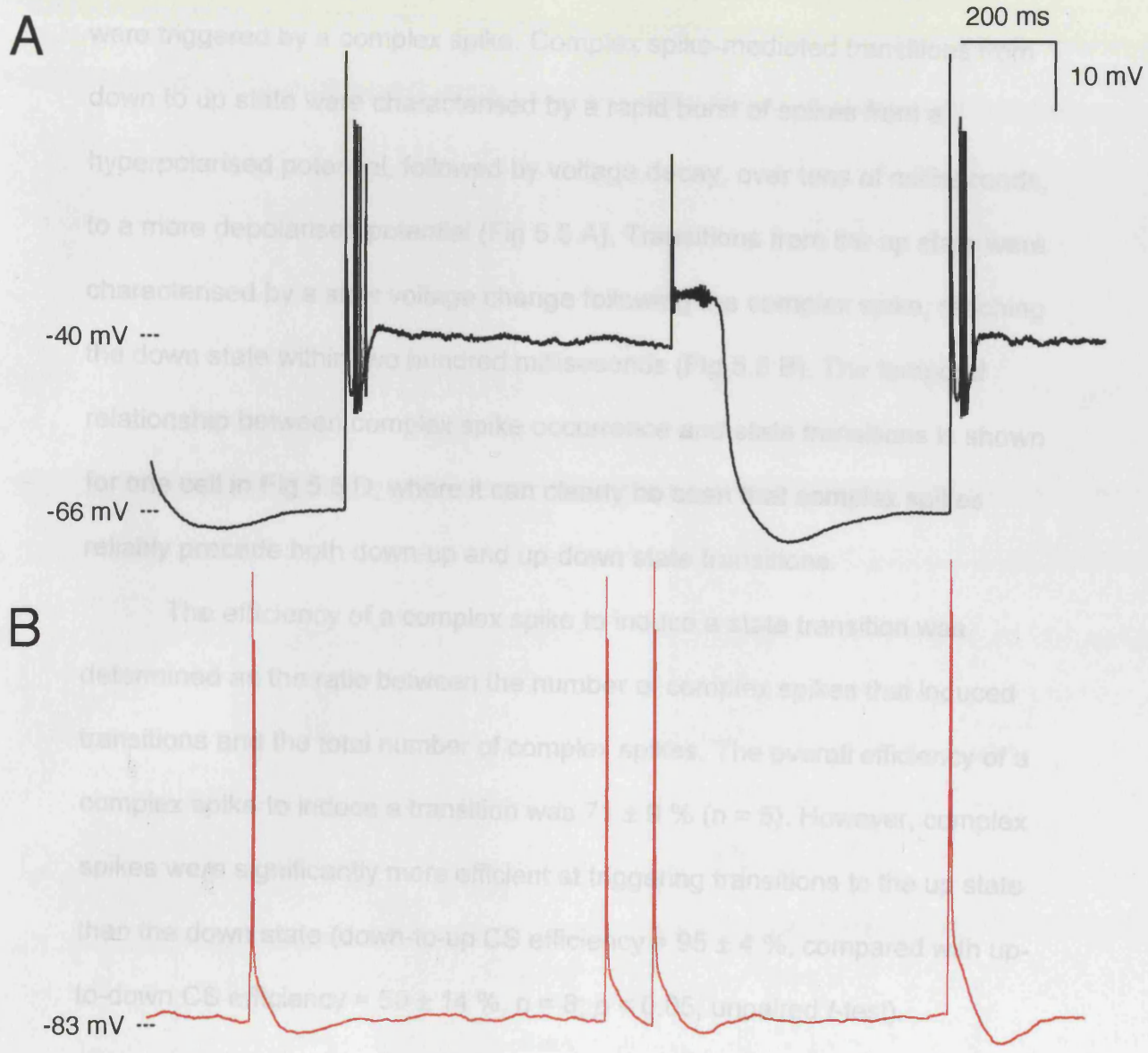

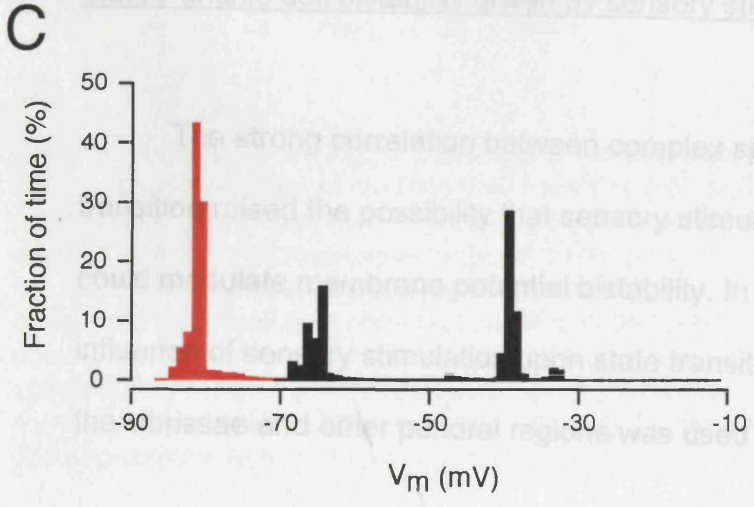

Figure 5.4

Contribution of intrinsic mechanisms to membrane potential bistability *in vivo*. **A** Whole-cell perisomatic recording of bistable behaviour in cerebellar Purkinje cell. **B** Bistability is abolished by injection of negative DC current (-800 pA). **C** Membrane potential histograms for a Purkinje cell in the absence of injected current (black) and during negative current injection (red; note unimodal distribution of membrane potential).

of transitions to the down state, and 95 ± 5 % of transitions to the up state were triggered by a complex spike. Complex spike-mediated transitions from down to up state were characterised by a rapid burst of spikes from a hyperpolarised potential, followed by voltage decay, over tens of milliseconds, to a more depolarised potential (Fig 5.5 A). Transitions from the up state were characterised by a slow voltage change following the complex spike, reaching the down state within two hundred milliseconds (Fig 5.5 B). The temporal relationship between complex spike occurrence and state transitions is shown for one cell in Fig 5.5 D, where it can clearly be seen that complex spikes reliably precede both down-up and up-down state transitions.

The efficiency of a complex spike to induce a state transition was determined as the ratio between the number of complex spikes that induced transitions and the total number of complex spikes. The overall efficiency of a complex spike to induce a transition was 71 ± 9 % (n = 8). However, complex spikes were significantly more efficient at triggering transitions to the up state than the down state (down-to-up CS efficiency = 95 ± 4 %, compared with up-to-down CS efficiency = 50 ± 14 %, n = 8; $p < 0.05$, unpaired *t*-test).

5.2.4 Purkinje cell bistability driven by sensory stimulation

The strong correlation between complex spike incidence and state transition raised the possibility that sensory stimuli that elicit complex spikes could modulate membrane potential bistability. In order to examine the influence of sensory stimulation upon state transition, air puff stimulation of the vibrissae and other perioral regions was used to activate climbing fibre

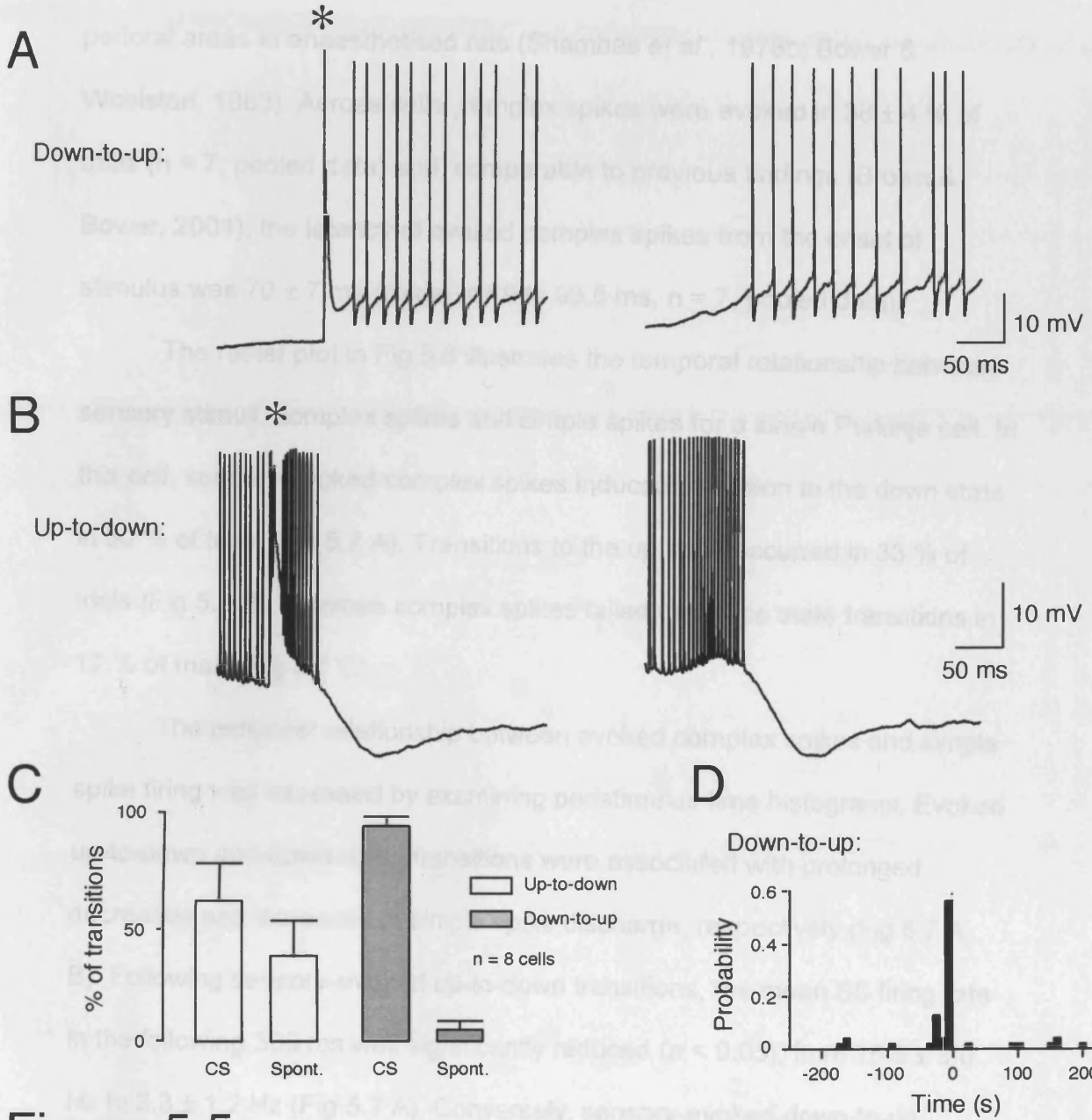

Figure 5.5

Climbing fibre inputs can trigger transitions between states. **A** Representative traces of climbing fibre-mediated (left) and spontaneous (right) transitions to the up state. (*) indicates complex spike. **B** Representative traces of climbing fibre-mediated (left) and spontaneous (right) transitions to the down state. **C** Pooled data showing the percentage of up-down and down-up transitions associated with complex spikes (CS) or occurring spontaneously (Spont.). **D** Cross-correlation of complex spike occurrence with state transitions; down-to-up state (top) and up-to-down (bottom).

inputs. Recordings were performed in folia Crus I and IIa of the cerebellar cortex, regions demonstrated to respond strongly to tactile stimulation of perioral areas in anaesthetised rats (Shambes *et al.*, 1978b; Bower & Woolston, 1983). Across cells, complex spikes were evoked in 38 ± 4 % of trials (n = 7; pooled data) and, comparable to previous findings (Brown & Bower, 2001), the latency of evoked complex spikes from the onset of stimulus was 70 ± 7 ms (range: 47.9 to 93.5 ms, n = 7; pooled data).

The raster plot in Fig 5.6 illustrates the temporal relationship between sensory stimuli, complex spikes and simple spikes for a single Purkinje cell. In this cell, sensory-evoked complex spikes induced transition to the down state in 50 % of trials (Fig 5.7 A). Transitions to the up state occurred in 33 % of trials (Fig 5.7 B), whereas complex spikes failed to induce state transitions in 17 % of trials (Fig 5.7 C).

The temporal relationship between evoked complex spikes and simple spike firing was assessed by examining peristimulus time histograms. Evoked up-to-down and down-to-up transitions were associated with prolonged decreases and increases in simple spike discharge, respectively (Fig 5.7 A, B). Following sensory-evoked up-to-down transitions, the mean SS firing rate in the following 300 ms was significantly reduced ($p < 0.05$), from 15.8 ± 3.0 Hz to 3.3 ± 1.2 Hz (Fig 5.7 A). Conversely, sensory-evoked down-to-up transitions were associated with an increase in SS discharge in the following 300 ms ($p < 0.05$), from 1.1 ± 0.8 Hz to 27.2 ± 4.1 Hz (Fig 5.7 B). When evoked complex spikes did not trigger state transitions, no significant change in simple spiking was observed (pre-CS simple spike rate = 20.8 ± 1.6 Hz, post-CS simple spike rate = 15.8 ± 2.0 Hz, $p > 0.05$; Fig 5.7 C). Similarly,

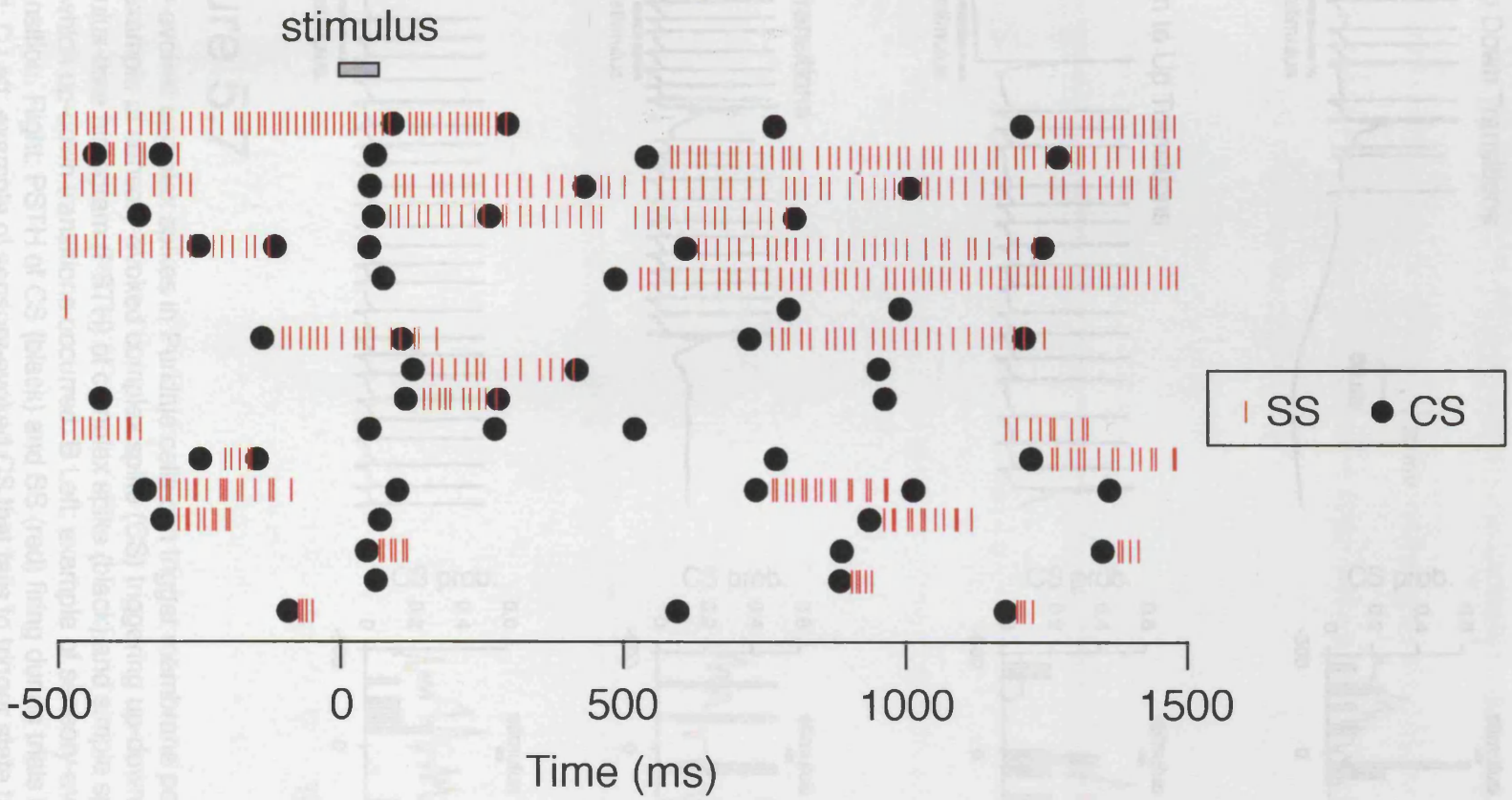

Figure 5.6

Sensory stimulation evokes complex spikes in Purkinje cells. Raster plot showing the temporal relationship between sensory stimulation (70 ms air puff to ipsilateral vibrissae), complex spikes (black circles) and simple spike firing (red lines). 17 consecutive trials are shown.

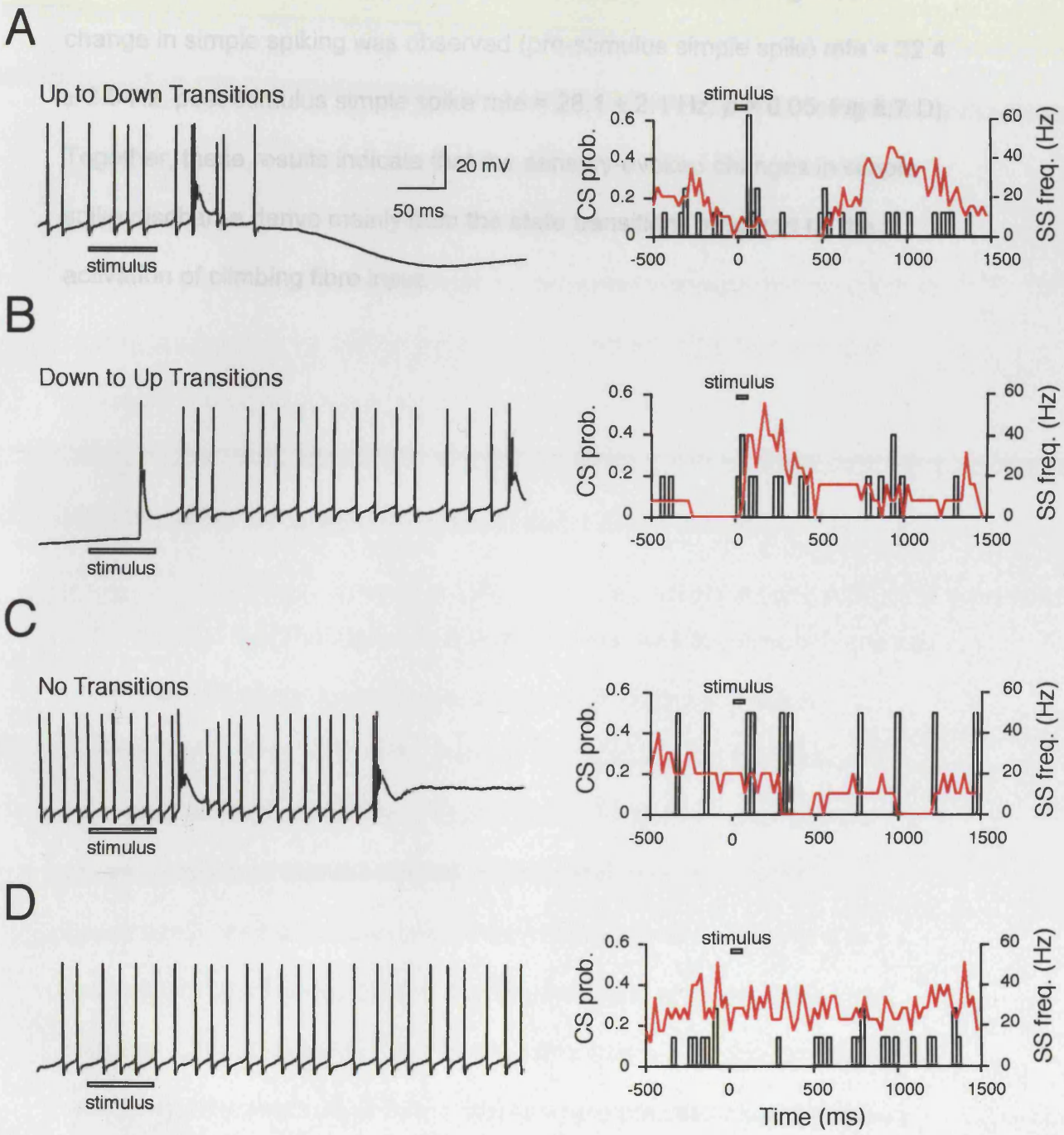

Figure 5.7

Sensory-evoked complex spikes in Purkinje cells can trigger membrane potential bistability *in vivo*. **A** Left: example of sensory-evoked complex spike (CS) triggering up-down state transition. Right: peristimulus-time histogram (PSTH) of complex spike (black) and simple spike firing (SS; red) during trials in which up-down transitions occurred. **B** Left: example of sensory-evoked CS triggering down-up state transition. Right: PSTH of CS (black) and SS (red) firing during trials in which down-up transition occurred. **C** Left: example of sensory-evoked CS that fails to trigger state transition. Right: PSTH of CS (black) and SS (red) firing for trials in which CS failed to trigger state transition. **D** Left: example of sensory stimulation failing to trigger a CS. Right: PSTH for CS (black) and SS (red) firing for trials in which sensory stimulation did not trigger CSs. Bin size = 25 ms in all cases.
Note the robust changes in SS rate seen when sensory-evoked CSs triggered state transitions.

when sensory stimulation failed to evoke a complex spike, no significant change in simple spiking was observed (pre-stimulus simple spike rate = 32.4 ± 3.0 Hz, post-stimulus simple spike rate = 28.1 ± 2.1 Hz, $p > 0.05$; Fig 5.7 D). Together, these results indicate that the sensory-evoked changes in simple spike discharge derive mainly from the state transitions triggered by the activation of climbing fibre input.

5.3 DISCUSSION

The work presented in this chapter demonstrates that Purkinje cells exhibit bistability of membrane potential and spike output *in vivo*, seemingly as a consequence of intrinsic membrane properties of Purkinje cells. This bistability can be bidirectionally triggered by sensory-driven input, suggesting that it may represent a cellular mechanism relevant for the processing of sensory information.

5.3.1 Bistability of Purkinje cell output *in vivo*

Bistability of Purkinje cells *in vitro* has been well documented, and has been observed to occur spontaneously (Llinas & Sugimori, 1980c; Hounsgaard & Midtgaard, 1988; Rapp *et al.*, 1994) or after modulation of intrinsic conductances (Williams *et al.*, 2002). The data presented in this chapter indicates that this bistability is retained *in vivo* under ketamine / xylazine and urethane anaesthesia. Bistability of membrane potential is manifested in two modes of firing activity: tonic firing of simple spikes and quiescent periods. Bistability of Purkinje cell output is supported by previous reports showing intermittent firing patterns where periods of high frequency simple spike firing are interspersed with periods of silence in anaesthetised (Bell & Grimm, 1969) and decerebrate animals (Granit & Phillips, 1956; McDevitt *et al.*, 1982). Irregular alternations between quiescence and high frequency simple spike activity have been observed in awake recordings from various animals (Armstrong & Rawson, 1979; Bauswein *et al.*, 1984).

Interestingly, recent recordings of deep cerebellar nucleus neurons reveal prolonged (up to 0.5 sec) inhibitory responses to brief sensory stimulation (Rowland & Jaeger, 2003), which may correspond to synchronised up states in presynaptic Purkinje cells activated by sensory stimulation.

However, other studies have not reported similar phenomena, and have tended to report continuous firing of Purkinje cells rather than bimodal discharge (Bower & Woolston, 1983; Ekerot & Jorntell, 2001). This suggests that expression of bistability may be rather heterogeneous. Work conducted *in vitro* suggests that the expression of bistability within a given cell is likely to depend upon on neuromodulation (Hounsgaard & Midtgaard, 1988; Lechner *et al.*, 1996; Williams *et al.*, 2002), and on the balance of excitation and inhibition in the local network.

The finding that complex spikes triggered by climbing fibre input can switch Purkinje cells between up and down states (Fig 5.5) goes some way towards resolving apparent discrepancies in the literature regarding the effect of complex spikes on simple spiking. It has been highlighted that complex spikes have been shown to be associated with both increases and decreases in simple spike activity (Bell & Grimm, 1969; Murphy & Sabah, 1970; Armstrong & Rawson, 1979; Rawson & Tilokskulchai, 1981; McDevitt *et al.*, 1982). The data presented in this chapter suggest that the effect of the complex spike on simple spiking depends on the state of the Purkinje cell occurring just before the complex spike. As such, Purkinje cells predominantly in the down state will tend to respond with an increase in simple spike activity associated with the complex spike, whereas Purkinje cells predominantly in an up state will tend to respond with a decrease.

5.3.2 Mechanisms underlying bistability

Bistability seems to be an intrinsic membrane property of Purkinje cells *in vivo* since it is abolished by strong negative or positive constant current injection (Fig 5.4). In addition, brief (≈ 10 ms) current pulses, either depolarising or hyperpolarising, can trigger state transitions (S Mahon; personal communication). Interneurons, which share many of the synaptic input received by Purkinje cells, and granule cells, did not exhibit membrane potential bistability (Figs 5.3, 3.4). Furthermore, interneurons typically expressed rhythmic firing patterns at around 5 Hz, whilst granule cells fired only rare irregular spikes in the absence of sensory input. Together this data provides strong evidence that bistability does not result from bimodal synaptic input. Bistability in Purkinje cells is thus very different from the up and down states described in many cortical and striatal neurons *in vivo.* In these neurons, the up state is thought to result mainly from a continuous barrage of synaptic excitation reflecting widespread activity across the network (Mahon *et al.*, 2001; Destexhe *et al.*, 2003; Shu *et al.*, 2003). In contrast, in Purkinje cells, the transition between states can be triggered by the activation of a single, large synaptic input (i.e. the climbing fibre synapse), whilst the persistence of a given state is maintained by intrinsic voltage-dependent mechanisms.

Previous *in vitro* studies have suggested that Purkinje cell bistability could result from interactions between non-inactivating sodium (Raman & Bean, 1997) and calcium conductances with potassium conductances (Llinas & Sugimori, 1980b, a). In addition, the voltage activation profile and reversal

potential of I_h, (increasing with activation with hyperpolarisation, and a depolarised reversal potential), makes it a candidate conductance in the establishment of stable membrane potential states (Loewenstein *et al.*, 2001). Currently, the role of I_h in Purkinje cell bistability is rather ambiguous. Some researchers have reported bistability in the presence of I_h (Llinas & Sugimori, 1980c; Rapp *et al.*, 1994), whereas other have shown that its downregulation, e.g. by serotonin, unmasks or enhances bistability (Williams *et al.*, 2002). These experiments presented in this chapter clearly show that I_h is present in bistable Purkinje cells *in vivo* (e.g. see depolarising 'sag' in Figs 5.1, 5.2, 5.4), although it is not clear from these experiments what contribution I_h makes towards the expression of bistability. The presence of bistability in the absence of I_h (Williams *et al.*, 2002), suggests that there may exist multiple routes towards bistable behaviour in Purkinje cells.

5.3.3 Computational implications of bistability

Traditionally, chemical synapses are classified as either excitatory or inhibitory according to their effect on the firing rate of the postsynaptic neuron. However, these data reveal that the same synapse can play both roles. Thus, the activation of climbing fibre synapses can either increase or decrease the firing rate of the Purkinje cell, depending on its initial state. In this manner, the climbing fibre input can be seen as a 'toggle switch'. It has been proposed that the ability of the same synapse to shift between the stable states in *both* directions may add computational powers to bistable neurons (Loewenstein *et al.*, 2001). Specifically, climbing fibre input has been suggested to represent

an error signal, such as unexpected sensory input (Andersson & Armstrong, 1987; Kim *et al.*, 1987; Lou & Bloedel, 1992). Climbing fibre-driven state transitions therefore offer a means to generate immediate and reflexive responses in cerebellar cortical output to the occurrence of an error by shifting Purkinje cell activity away from an erroneous operating state.

Membrane potential bistability is likely to exert profound effects upon the processing of parallel fibre activity in Purkinje cells. Purkinje cell simple spike output in response to the same set of active parallel fibre/interneuron synaptic inputs is likely to be different during the two states. It may be that the down state of Purkinje cells simply represents an inactive state for the neuron, i.e. sensory integration is prevented in Purkinje cells in the down state. However, this scenario has yet to be demonstrated. Although mechanistically different, it is work noting that spike output in neocortical pyramidal cells following sensory input is actually *increased* when coincident with the down state (Petersen *et al.*, 2003). It may also be the case that strong parallel fibre activity is sufficient to drive state transitions in one or both directions in the absence of climbing fibre activation: the presence of spontaneous state transitions (Fig 5.5 A, B) provides evidence that climbing fibre-mediated synaptic signals are not the sole means by which state transitions can occur *in vivo*.

Bistability is observed in both the soma and dendrite of Purkinje cells, and is therefore likely to affect a range of voltage-sensitive conductances across the neuron. In particular, Ca^{2+} spikes are all-or-none events that are nearly exclusively confined to the dendrite (Llinas & Sugimori, 1980c, b). Increases in dendritic Ca^{2+} have been linked to several forms of short-term

synaptic plasticity including depolarisation-induced suppression of excitation (DSE) (Kreitzer & Regehr, 2001; Brown *et al.*, 2003; Rancz & Hausser, 2004), and depolarisation-induced suppression, and potentiation, of inhibition (Duguid & Smart, 2004). It is likely that the membrane potential state of the Purkinje cell will profoundly affect the expression of these phenomena.

Bistability may also be relevant for the induction of long-term depression (LTD) at parallel fibre synapses, which is a prime cellular substrate for cerebellar learning (Ito, 2001). In experiments exploring the parallel fibre-Purkinje cell timing relationship required for LTD induction, a range of timing relationships have been reported (Ekerot & Kano, 1985; Chen & Thompson, 1995; Wang *et al.*, 2000). Given that strong depolarisation paired with parallel fibre activation has been shown to be sufficient for LTD induction (Crepel & Jaillard, 1991), Purkinje cell bistability may be an additional factor that shapes the time window for LTD induction. Thus, when there is a high probability that a climbing fibre will switch the neuron to the up state, activation of parallel fibres *after* a complex spike will be effective in generating LTD. In neurons in which there is a high probability that climbing fibre activation will generate the converse transition, LTD induction will be favoured when parallel fibres are activated *before* a complex spike. Consistent with this scenario, it has been suggested that the wide timing window observed in one study for parallel fibre LTD results from a long-lasting plateau depolarisation following climbing fibre activation (Ekerot & Oscarsson, 1981). It has subsequently been reported that LTD is abolished when plateau potentials are terminated by inhibition (Ekerot & Kano, 1985). Purkinje cell

bistability may therefore contribute to determining the rules for LTD induction in the intact cerebellar network.

5.3.4 Potential relevance of anaesthesia to the expression of Purkinje cell bistability *in vivo*

It is important to note that the Purkinje cell bistability described in this study was observed in the cerebella of rats under ketamine / xylazine and urethane anaesthesia. Recently, work performed in the laboratory of Chris De Zeeuw has suggested that Purkinje cell bistability is most commonly observed in deeply-anaesthetised animals, and that Purkinje cell simple spiking patterns become more unimodal under lightly-anaesthetised or awake conditions (M Schoneville and C I De Zeeuw, unpublished observations). This finding opens up the possibility that anaesthesia may promote bistability by favouring expression of a down state; under awake conditions, higher levels of cerebellar excitation may thus occlude expression of the down state.

Such data highlight the current difficulty in relating neuronal activity observed during anaesthesia and/or quiet wakefulness, and that present in actively behaving animals. However, the fact that Purkinje cell bistability is an intrinsic feature of these cells *in vivo* opens up the possibility that it is exploited in behavioural situations. As mentioned in the introduction, several studies have reported intermittent simple spiking activity in awake animals (Armstrong & Rawson, 1979; Rawson & Tilokskulchai, 1981; Nitz & Tononi, 2002). Conceptually, it seems unlikely that *every* Purkinje cell in the cerebellum exhibits high frequency simple spiking under all conditions. Due to

the high energetic cost of action potential firing (Laughlin *et al.*, 1998), such a scheme is extremely unfavourable (Attwell & Laughlin, 2001). The maintenance of a stable hyperpolarised membrane potential in the down state via intrinsic mechanisms affords an energetically efficient means of blocking spiking in Purkinje cells in the absence of ongoing inhibitory synaptic input (Attwell & Laughlin, 2001; Laughlin, 2001). It is also worth noting that climbing fibre input is most efficient at triggering transitions from down to up state (95 ± 4 %, Fig 5.5 D). On the basis of this result, it seems reasonable to hypothesise that climbing fibre activity, whether evoked in response to an external sensory- or internally generated 'attention signal', may favour rapid transitions to the up state in quiescent Purkinje cells of behaving animals.

Chapter 6: GENERAL DISCUSSION

The work presented in this thesis has focused upon the patterns of activity in cerebellar granule cells and Purkinje cells within the cerebellar cortex. By studying the synaptic input and spiking patterns of individual granule cells and Purkinje cells, it has been possible to gain insights into the function of the cerebellar network as a whole.

Intrinsic properties of cerebellar granule cells *in vivo*

The results presented in chapter 3 establish that cerebellar granule cells can be easily identified within the intact cerebellum through their characteristic electrophysiological properties. The passive properties of granule cells *in vivo* are generally in close agreement with those determined *in vitro*. Despite receiving ongoing mossy fibre synaptic inputs, and possessing several mechanisms that facilitate EPSP summation, resting firing rates are kept low. In particular, a shunting inhibition, in addition to hyperpolarisation, produced by tonic activation of $GABA_A$ receptors, are extremely important in decreasing granule cell excitability, and preventing the transformation of single mossy fibre inputs into granule cell action potentials. The resulting low firing rates act to increase the signal-to-noise ratio in the output of the granule cell layer by rejecting spontaneous mossy fibre inputs, thus potentially aiding the discrimination of sensory representations within the cerebellar cortex.

Presently, the factors that contribute to regulation of tonic GABAergic inhibition *in vivo* are not well established. In particular, it is not known to what

extent Golgi cell activity can modulate the amplitude of the tonic conductance. It has been shown that increased Golgi cell activity (and hence spike-triggered GABA release within individual glomeruli) enhances both phasic and tonic GABAergic currents in granule cells (Brickley *et al.*, 1996; Carta *et al.*, 2004). Given that such a relationship exists, the 'time constant' of Golgi cell-driven alterations in granule cell tonic inhibition could potentially be measured. Such an experiment could be feasibly conducted *in vitro*, by stimulating individual Golgi cells at variable frequencies and simultaneously measuring holding current in synaptically connected granule cells. Changes in the amplitude of the tonic conductance produce profound effects on the input-output relationship of individual granule cells (Figs 3.8, 3.9, 4.14). As such, it would be important to determine the time window during which Golgi cell-driven modulations in tonic conductance are effective, as information processing in the granule cell layer will be affected for the duration of this period.

Sensory integration in cerebellar granule cells

The means by which sensory signals may be represented and transformed at the input layer of the cerebellum have been discussed in chapter 4. Tactile stimulation of whisker and perioral regions of the anaesthetised rat generates brief high frequency bursts of action potentials in single cerebellar granule cells. These output bursts are dependent upon high frequency bursts of mossy fibre activity, which, it is suggested, may originate from high frequency repetitive activation of single mossy fibres or asynchronous activation of multiple fibres. The quantal content of sensory-

evoked EPSCs was found to be extremely low, highlighting the extreme sensitivity of information transfer at the mossy fibre-granule cell relay. The finding that sensory information is represented within granule cells through high frequency firing is in contrast with low resting activity rates in these neurons, and suggests that a high signal-to-noise ratio exists for the transfer of sensory signals.

However, the sensory stimuli used in this thesis typically caused the deflection of several whiskers. Therefore, it will be important to establish whether high frequency mossy fibre activity is also observed following single whisker stimulation. The use of more refined stimuli may help to establish the source of the small number of mossy fibres received by each granule cell, and thus provide investigators with a clearer idea of the information that is integrated by granule cells in order to generate output. It is possible that single granule cells integrate information pertaining to specific stimulus features, e.g. force and velocity, or that they instead integrate sensory afferents representing different peripheral locations, or even different sensory modalities. These data are likely to provide important clues to the function of the cerebellum.

The latency of sensory-evoked Golgi cell inhibition was typically found to precede that of evoked mossy fibre activation. In chapter 4, I raised the possibility that this was due to a mixed distribution of trigeminal and corticopontine afferents within the dendritic arborisation of individual Golgi cells. The role of these two distinct afferent pathways remains to be determined, and is of potential importance if we are to understand the role of the cerebellum in sensory processing and behaviour. Since the excitatory connectivity of the cerebellar cortex is purely feed-forward, inhibitory

interneurons activated by trigeminal inputs are unlikely to influence the processing of trigeminal inputs themselves in granule cells, and perhaps also Purkinje cells. However, trigeminal inputs are likely to influence the processing of subsequent corticopontine inputs, which are temporally more diffuse, and which presumably represent different information. One possibility is that the trigeminal input 'primes' the cerebellum for receipt of the larger corticopontine input by activating interneurons such as Golgi and Lugaro cells. One means of studying the relative contributions of these two sources of input would be to record sensory-evoked mossy fibre signals intracellularly from Golgi cells *in vivo*, and observe how short- and long-latency inputs contribute to sensory-evoked Golgi cell spiking. Although such an approach was attempted in the course of this study, the sparseness of Golgi cells within the granule cell layer has meant that it has been extremely difficult to reliably obtain whole-cell recordings from them. However, this problem may be tackled successfully in the future by combining 2-photon imaging of GFP-labelled Golgi cells with targeted patch clamp recording (Margrie *et al.* 2003). The size and distribution of Golgi cells makes them a good candidate for this new technique.

Patterns of Purkinje cell activity *in vivo*

The patterns of activity in the output neurons of the cerebellar cortex, Purkinje cells, were explored in chapter 5. Purkinje cells exhibit a profound and robust bistability of membrane potential, alternating between a hyperpolarised down state and a depolarised up state. This membrane

potential bistability is reflected in a bimodal pattern of simple spike output. Bistability is an intrinsic feature of Purkinje cells *in vivo*, and is not observed in other neurons of the cerebellar cortex. Transitions between the two states are reliably driven by climbing fibre activity. Sensory-evoked climbing fibre activation is capable of driving state transitions in *both* directions, thus altering the output of individual Purkinje cells over periods of several hundred milliseconds in a stimulus-dependent manner. These results indicate that the integration of granule cell and interneuron synaptic input is powerfully modulated by climbing fibre input and is likely to be highly dependent upon the intrinsic state of postsynaptic Purkinje cells.

In vivo whole-cell recordings are now necessary from the synaptic targets of Purkinje cells, deep cerebellar nuclear (DCN) neurons, to determine the contribution of Purkinje cell activity to the final output of the cerebellar circuit. Between 15 and 25 Purkinje cells converge upon each DCN neuron (Palkovits *et al.*, 1977), and is not clear how a convergence of bistable firing patterns will interact to affect DCN neuronal output. One possibility is that a synchronised up state in many converging Purkinje cells could produce prolonged hyperpolarisations in DCN neurons, which in turn could trigger rebound bursts in these cells (Aizenman & Linden, 1999).

Anaesthesia vs. awake cerebella

The recordings presented in this thesis have been made from deeply-anaesthetised rats. It will be necessary to repeat these experiments in awake animals in order to confirm that the patterns of sensory-evoked activity

described here, namely burst firing in cerebellar granule cells, and membrane potential bistability, are truly relevant. Technically, it is extremely difficult to make intracellular neuronal recordings from awake animals, and animals require considerable training to sit through recording sessions. However, such recordings have been performed in areas of neocortex (Margrie *et al.*, 2002; Brecht *et al.*, 2004), and inferior colliculi (Covey *et al.*, 1996). In addition, a first approximation to the awake state may be provided by alternative means. For example, the depth of anaesthesia provided by gas anaesthetics (e.g. halothane or isoflurane) can be modulated extremely rapidly by varying the concentration. In such a manner, it may be possible to 'lighten' anaesthesia during the course of whole-cell recording. Also, the μ-opiate receptor agonist, fentanyl, may be used to sedate, rather than anaesthetise animals. It is worth noting that the up and down states observed in neocortex under ketamine / xylazine anaesthesia appear to be absent in sedated animals (Bruno, 2003).

Sensory-evoked signals are also likely to be dependent upon the behavioural state of the animal. It has recently been shown that the evoked response within barrel cortex to whisker stimulation is highly dependent upon attention (Petersen *et al.*, 2003; Castro-Alamancos, 2004). Thus, it is also necessary to study the activity of individual cerebellar neurons whilst animals are engaged in specific behavioural tasks. Intracellular recordings may not be feasible under such conditions, and 2-photon imaging may then be a more effective means to study both single cell and population activity (Helmchen *et al.*, 2001).

Under awake or behaving conditions, it is likely that the granule cell layer of sensory areas of the cerebellum receives higher levels of afferent

input. It is therefore possible that information transfer through the granule layer will also be enhanced. However, since Golgi cell activity is driven by mossy and parallel fibre inputs, is likely that these cells provide enhanced inhibitory feedback onto granule cells under such conditions. Increased inhibitory input will raise the threshold for the conversion of mossy fibre synaptic input into granule cell spikes. Therefore, the net result may well be the maintenance of an approximately similar rate of granule cell spiking during periods of high-frequency afferent input (Marr 1969). If such a scheme does operate, the characteristics of mossy fibre synaptic integration in the granule cells of 'behaving cerebella' will differ from those observed in this study. Specifically, a greater number of excitatory synaptic inputs will be required to depolarise granule cells above threshold, and thus generate spiking. Furthermore, the properties of temporal integration will be affected, and the requirement for temporally coincident synaptic input will be enhanced. Thus, greater temporal precision of mossy fibre input may be a key difference between anaesthetised and awake cerebella.

Appendix A: Granule cell properties under different anaesthetics

A quantitative comparison was made between the intrinsic properties of granule cells recorded under ketamine / xylazine and urethane anaesthesia. No statistically significant difference was found between four key granule cell parameters obtained from rats using these two forms of anaesthesia (Table 1).

Table 1 Comparison of intrinsic properties of cerebellar granule cells *in vivo* under ketamine/xylazine and urethane anaesthesia

	Ketamine/Xylazine	Urethane	*P* value
V_{rest} (mV)	-64 ± 2 (22)	-66 ± 1 (42)	0.21
Whole-Cell Firing Rate (Hz)	0.7 ± 0.2 (23)	0.4 ± 0.4 (23)	0.40
R_{input} (GΩ)	1.3 ± 0.1 (18)	1.1 ± 0.1 (42)	0.58
ΔI_{hold} in gabazine (pA)	6.0 ± 1.1 (5)	6.3 ± 1.0 (6)	0.82

Ketamine has been reported to selectively inhibit NMDA receptor-mediated conductances (Anis *et al.*, 1983; Thomson *et al.*, 1985). Since NMDA receptors have been shown to contribute to granule cell EPSPs at depolarised potentials *in vitro* (D'Angelo *et al.*, 1995), the voltage-dependent enhancement of granule cell EPSP amplitude was compared between

ketamine / xylazine and urethane anaesthesia. Under urethane anaesthesia (n = 3), the granule cell EPSP integral was 46 ± 17 % larger at –50 mV than at –60 mV. Under ketamine / xylazine anaesthesia (n = 5), the granule cell EPSP integral was 96 ± 32 % larger at –50 mV than at –60 mV. Thus, voltage-dependent enhancement of EPSPs is observed under both anaesthetics (Fig A1), and the increases in EPSP area observed under ketamine / xylazine and urethane were not significantly different (p = 0.32). At –50 mV, EPSP half width was measured as 18.4 ± 3.7 ms (n =3) and 20.2 ± 3.0 ms for urethane and ketamine / xylazine anaesthesia respectively (p = 0.69).

These results indicate that granule cell depolarisation is associated with a broadening of the granule cell EPSPs, consistent with the contribution of NMDA receptors (Fig 3.6). Though both populations are admittedly rather small, the finding that there is no significant difference between ketamine / xylazine and urethane anaesthesia in the increase in the EPSP integral with depolarisation from –60 to –50 mV, suggests a similar contribution of NMDA receptors under the two conditions. However, in order to precisely determine the relative contribution of NMDA receptors and intrinsic conductances to EPSP shape *in vivo*, it will be necessary to examine the effect of APV on the voltage-dependence of the EPSP waveform under the two conditions.

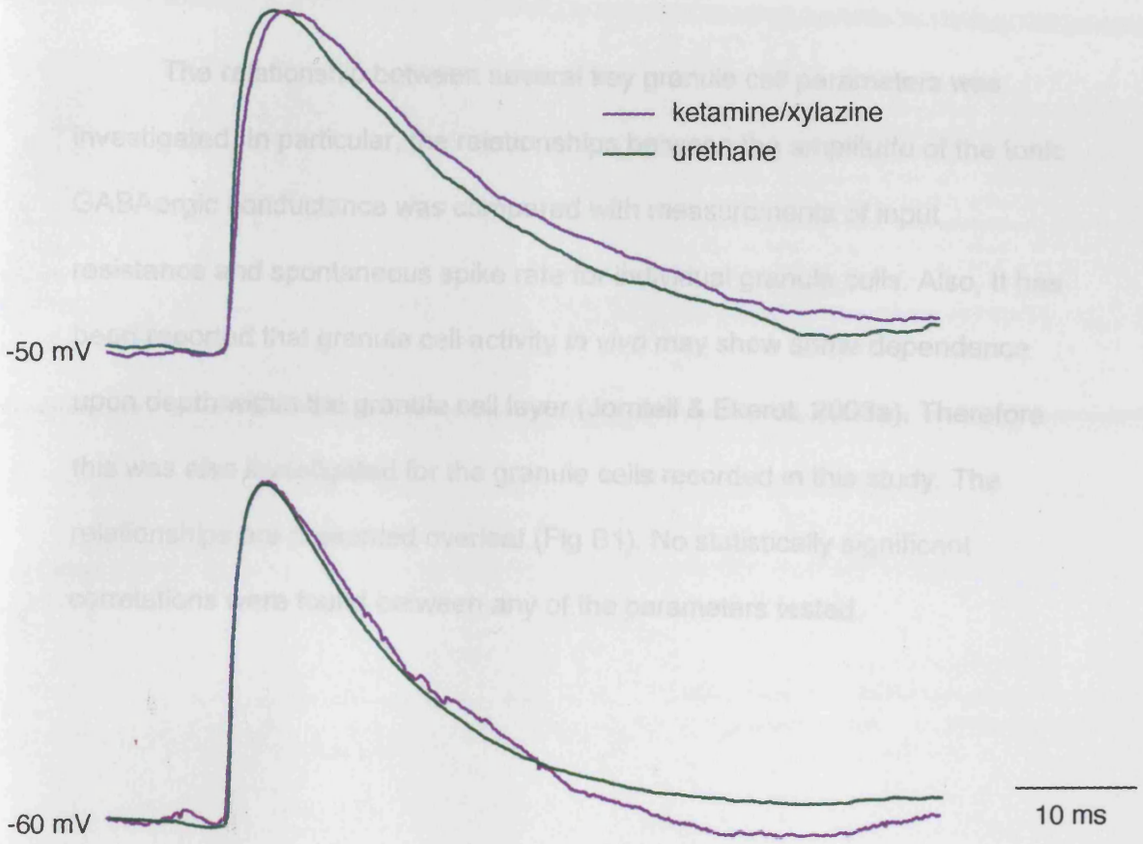

Figure A1

Comparison of normalised granule cell EPSP shapes at different membrane potentials recorded under ketamine/xylazine and urethane anaesthesia. Traces represent pooled averages from multiple cells (4 for ketamine/xylazine and 3 for urethane).

Appendix B: Relationships amongst granule cell intrinsic properties

The relationship between several key granule cell parameters was investigated. In particular, the relationships between the amplitude of the tonic GABAergic conductance was compared with measurements of input resistance and spontaneous spike rate for individual granule cells. Also, It has been reported that granule cell activity *in vivo* may show some dependence upon depth within the granule cell layer (Jorntell & Ekerot, 2003a). Therefore this was also investigated for the granule cells recorded in this study. The relationships are presented overleaf (Fig B1). No statistically significant correlations were found between any of the parameters tested.

Figure B1

Each point represents a single granule cell. The relationships between: **A** Input resistance and spontaneous firing rate. **B** Spontaneous IPSC rate and spontnaeous firing rate. **C** The gabazine-sensitive component of the tonic holding current and spontaneous IPSC rate. **D** The gabazine-sensitive component of the tonic holding current and input resistance. **E** Granule cell depth and spontaneous firing rate. **F** Membrane potential at break-in and spontaneous firing rate. **G** EPSP or EPSC rate and spontaneous firing rate.
No statistically significant correlations were found.

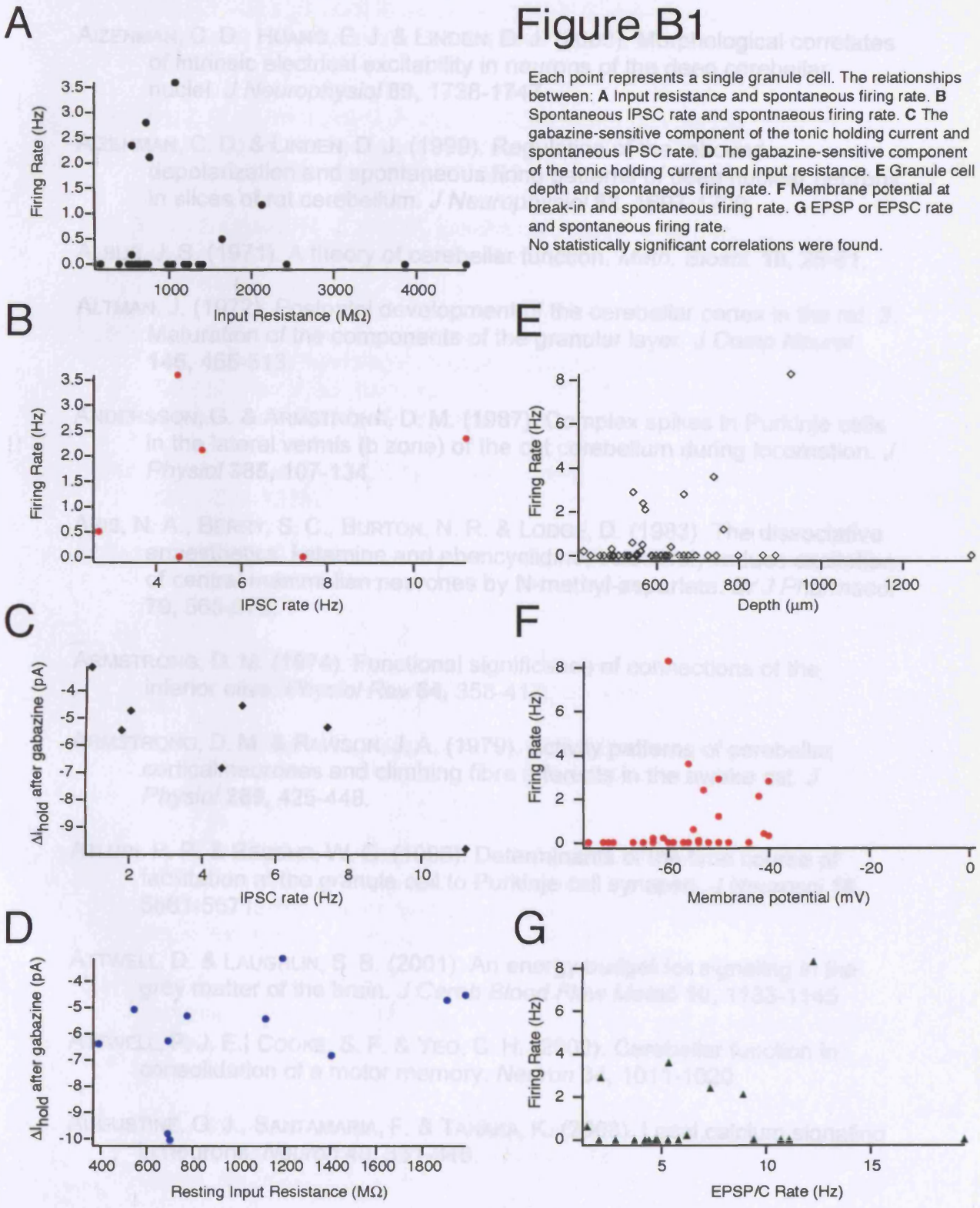

REFERENCES

ADRIAN, E. D. (1935). Discharge frequencies in the cerebral and cerebellar cortex. *J Physiol* **83,** 33.

AIZENMAN, C. D., HUANG, E. J. & LINDEN, D. J. (2003). Morphological correlates of intrinsic electrical excitability in neurons of the deep cerebellar nuclei. *J Neurophysiol* **89,** 1738-1747.

AIZENMAN, C. D. & LINDEN, D. J. (1999). Regulation of the rebound depolarization and spontaneous firing patterns of deep nuclear neurons in slices of rat cerebellum. *J Neurophysiol* **82,** 1697-1709.

ALBUS, J. S. (1971). A theory of cerebellar function. *Math. Biosci.* **10,** 25-61.

ALTMAN, J. (1972). Postnatal development of the cerebellar cortex in the rat. 3. Maturation of the components of the granular layer. *J Comp Neurol* **145,** 465-513.

ANDERSSON, G. & ARMSTRONG, D. M. (1987). Complex spikes in Purkinje cells in the lateral vermis (b zone) of the cat cerebellum during locomotion. *J Physiol* **385,** 107-134.

ANIS, N. A., BERRY, S. C., BURTON, N. R. & LODGE, D. (1983). The dissociative anaesthetics, ketamine and phencyclidine, selectively reduce excitation of central mammalian neurones by N-methyl-aspartate. *Br J Pharmacol* **79,** 565-575.

ARMSTRONG, D. M. (1974). Functional significance of connections of the inferior olive. *Physiol Rev* **54,** 358-417.

ARMSTRONG, D. M. & RAWSON, J. A. (1979). Activity patterns of cerebellar cortical neurones and climbing fibre afferents in the awake cat. *J Physiol* **289,** 425-448.

ATLURI, P. P. & REGEHR, W. G. (1996). Determinants of the time course of facilitation at the granule cell to Purkinje cell synapse. *J Neurosci* **16,** 5661-5671.

ATTWELL, D. & LAUGHLIN, S. B. (2001). An energy budget for signaling in the grey matter of the brain. *J Cereb Blood Flow Metab* **10,** 1133-1145.

ATTWELL, P. J. E., COOKE, S. F. & YEO, C. H. (2002). Cerebellar function in consolidation of a motor memory. *Neuron* **34,** 1011-1020.

AUGUSTINE, G. J., SANTAMARIA, F. & TANAKA, K. (2003). Local calcium signaling in neurons. *Neuron* **40,** 331-346.

BATCHELOR, A. M. & GARTHWAITE, J. (1997). Frequency detection and temporally dispersed synaptic signal association through a metabotropic glutamate receptor pathway. *Nature* **385,** 74-77.

BAUSWEIN, E., KOLB, F. P. & RUBIA, F. J. (1984). Cerebellar feedback signals of a passive hand movement in the awake monkey. *Pflugers Arch* **402,** 292-299.

BEKKERS, J. M. & STEVENS, C. F. (1989). NMDA and non-NMDA receptors are co-localized at individual excitatory synapses in cultured rat hippocampus. *Nature* **341,** 230-233.

BELL, C. C. & GRIMM, R. J. (1969). Discharge properties of Purkinje cells recorded on single and double microelectrodes. *J Neurophysiol* **32,** 1044-1055.

BLOEDEL, J. R. & COURVILLE, J. (1981). Cerebellar afferent systems. In *Handbook of Physiology, Section I: The Nervous System, Vol II: Motor Control, Part 2.* ed. BROOKS, V. B., pp. 735-829. American Physiological Society, Bethesda, MD.

BLOMFIELD, S. & MARR, D. (1970). How the cerebellum may be used. *Nature* **227,** 1224-1228.

BOWER, J. M. (1997). Is the cerebellum sensory for motor's sake, or motor for sensory's sake: the view from the whiskers of a rat? *Prog Brain Res* **114,** 463-496.

BOWER, J. M. (2002). The organization of cerebellar cortical circuitry revisited: implications for function. *Ann N Y Acad Sci* **978,** 135-155.

BOWER, J. M. & KASSEL, J. (1990). Variability in tactile projection patterns to cerebellar folia crus IIA of the Norway rat. *J Comp Neurol* **302,** 768-778.

BOWER, J. M. & WOOLSTON, D. C. (1983). Congruence of spatial organization of tactile projections to granule cell and Purkinje cell layers of cerebellar hemispheres of the albino rat: vertical organization of cerebellar cortex. *J Neurophysiol* **49,** 745-766.

BRECHT, M. & SAKMANN, B. (2002). Dynamic representation of whisker deflection by synaptic potentials in spiny stellate and pyramidal cells in the barrels and septa of layer 4 rat somatosensory cortex. *J Physiol* **543,** 49-70.

BRECHT, M., SCHNEIDER, M., SAKMANN, B. & MARGRIE, T. W. (2004). Whisker movements evoked by stimulation of single pyramidal cells in rat motor cortex. *Nature* **427,** 704-710.

BRICKLEY, S. G., CULL-CANDY, S. G. & FARRANT, M. (1996). Development of a tonic form of synaptic inhibition in rat cerebellar granule cells resulting from persistent activation of GABAA receptors. *J Physiol* **497 (Pt 3),** 753-759.

BRICKLEY, S. G., REVILLA, V., CULL-CANDY, S. G., WISDEN, W. & FARRANT, M. (2001). Adaptive regulation of neuronal excitability by a voltage-independent potassium conductance. *Nature* **409,** 88-92.

BROWN, I. E. & BOWER, J. M. (2001). Congruence of mossy fiber and climbing fiber tactile projections in the lateral hemispheres of the rat cerebellum. *J Comp Neurol* **429,** 59-70.

BROWN, S. P., BRENOWITZ, S. D. & REGEHR, W. G. (2003). Brief presynaptic bursts evoke synapse-specific retrograde inhibition mediated by endogenous cannabinoids. *Nat Neurosci* **6,** 1048-1057.

BROWN, S. P., SAFO, P. K. & REGEHR, W. G. (2004). Endocannabinoids inhibit transmission at granule cell to purkinje cell synapses by modulating three types of presynaptic calcium channels. *J Neurosci* **24,** 5623-5631.

BRUNO, R. M. (2003). Subthreshold cortical activation by individual thalamocortical neurons. Society for Neuroscience Abstracts, Program No. 58.10.

BUKOWSKA, D., ZGUCZYNSKI, L., MIERZEJEWSKA-KRZYZOWSKA, B. & SIKORA, E. (1998). Collateral projections of trigeminal sensory neurons to both cerebellar paramedian lobules in the rabbit: demonstration by fluorescent double labeling study. *Acta Neurobiol Exp (Wars)* **58,** 253-261.

BUZSAKI, G. (2002). Theta oscillations in the hippocampus. *Neuron* **33,** 325-340.

CARTA, M., MAMELI, M. & VALENZUELA, C. F. (2004). Alcohol enhances GABAergic transmission to cerebellar granule cells via an increase in Golgi cell excitability. *J Neurosci* **24,** 3746-3751.

CASADO, M., DIEUDONNE, S. & ASCHER, P. (2000). Presynaptic N-methyl-D-aspartate receptors at the parallel fiber-Purkinje cell synapse. *Proc Natl Acad Sci U S A* **97,** 11593-11597.

CASADO, M., ISOPE, P. & ASCHER, P. (2002). Involvement of presynaptic N-methyl-D-aspartate receptors in cerebellar long-term depression. *Neuron* **33,** 123-130.

CASTRO-ALAMANCOS, M. A. (2004). Absence of rapid sensory adaptation in neocortex during information processing states. *Neuron* **41,** 455-464.

CATHALA, L., BRICKLEY, S., CULL-CANDY, S. & FARRANT, M. (2003). Maturation of EPSCs and intrinsic membrane properties enhances precision at a cerebellar synapse. *J Neurosci* **23,** 6074-6085.

CHANCE, F. S., ABBOTT, L. F. & REYES, A. D. (2002). Gain modulation from background synaptic input. *Neuron* **35,** 773-782.

CHEN, C. & THOMPSON, R. F. (1995). Temporal specificity of long-term depression in parallel fiber--Purkinje synapses in rat cerebellar slice. *Learn Mem* **2,** 185-198.

CICIRATA, F., ANGAUT, P., SERIAPE, M. F., PANTO, M. R. & NICOTRA, G. (1992). Multiple representation in the nucleus lateralis of the cerebellum - an electrophysiologic study in the rat. *Exp Brain Res* **89,** 352-362.

CLARK, B. A., FARRANT, M. & CULL-CANDY, S. G. (1997). A direct comparison of the single-channel properties of synaptic and extrasynaptic NMDA receptors. *J Neurosci* **17,** 107-116.

COVEY, E., KAUER, J. A. & CASSEDAY, J. H. (1996). Whole-cell patch-clamp recording reveals subthreshold sound-evoked postsynaptic currents in the inferior colliculus of awake bats. *J Neurosci* **16,** 3009-3018.

CREPEL, F. & JAILLARD, D. (1991). Pairing of pre- and postsynaptic activities in cerebellar Purkinje cells induces long-term changes in synaptic efficacy in vitro. *J Physiol* **432,** 123-141.

CZUBAYKO, U., SULTAN, F., THIER, P. & SCHWARZ, C. (2001). Two types of neurons in the rat cerebellar nuclei as distinguished by membrane potentials and intracellular fillings. *J Neurophysiol* **85,** 2017-2029.

D'ANGELO, E., DE FILIPPI, G., ROSSI, P. & TAGLIETTI, V. (1995). Synaptic excitation of individual rat cerebellar granule cells in situ: evidence for the role of NMDA receptors. *J Physiol* **484,** 397-413.

D'ANGELO, E., DE FILIPPI, G., ROSSI, P. & TAGLIETTI, V. (1997). Synaptic activation of Ca2+ action potentials in immature rat cerebellar granule cells in situ. *J Neurophysiol* **78,** 1631-1642.

D'ANGELO, E., DE FILIPPI, G., ROSSI, P. & TAGLIETTI, V. (1998). Ionic mechanism of electroresponsiveness in cerebellar granule cells implicates the action of a persistent sodium current. *J Neurophysiol* **80,** 493-503.

D'ANGELO, E., NIEUS, T., MAFFEI, A., ARMANO, S., ROSSI, P., TAGLIETTI, V., FONTANA, A. & NALDI, G. (2001). Theta-frequency bursting and resonance in cerebellar granule cells: experimental evidence and modeling of a slow K^+-dependent mechanism. *J Neurosci* **21,** 759-770.

DE SCHUTTER, E. (2002). Cerebellar cortex: computation by extrasynaptic inhibition? *Curr Biol* **12,** R363-365.

DE SCHUTTER, E. & BOWER, J. M. (1994). Simulated responses of cerebellar Purkinje cells are independent of the dendritic location of granule cell synaptic inputs. *Proc Natl Acad Sci U S A* **91,** 4736-4740.

DE ZEEUW, C. I., HOLSTEGE, J. C., RUIGROK, T. J. & VOOGD, J. (1989). Ultrastructural study of the GABAergic, cerebellar, and mesodiencephalic innervation of the cat medial accessory olive: anterograde tracing combined with immunocytochemistry. *J Comp Neurol* **284,** 12-35.

DEBARBIEUX, F., BRUNTON, J. & CHARPAK, S. (1998). Effect of bicuculline on thalamic activity: a direct blockade of IAHP in reticularis neurons. *J Neurophysiol* **79,** 2911-2918.

DEL CASTILLO, J. & KATZ, B. (1954). Quantal components of the end-plate potential. *J Physiol* **124,** 560-573.

DENK, W., DELANEY, K. R., GELPERIN, A., KLEINFELD, D., STROWBRIDGE, B. W., TANK, D. W. & YUSTE, R. (1994). Anatomical and functional imaging of neurons using 2-photon laser scanning microscopy. *J Neurosci Methods* **54,** 151-162.

DESCHENES, M., PARADIS, M., ROY, J. P. & STERIADE, M. (1984). Electrophysiology of neurons of lateral thalamic nuclei in cat: resting properties and burst discharges. *J Neurophysiol* **51,** 1196-1219.

DESCHENES, M., ROY, J. P. & STERIADE, M. (1982). Thalamic bursting mechanism: an inward slow current revealed by membrane hyperpolarization. *Brain Res* **239,** 289-293.

DESTEXHE, A., RUDOLPH, M. & PARE, D. (2003). The high-conductance state of neocortical neurons in vivo. *Nat Rev Neurosci* **4,** 739-751.

DIEUDONNE, S. (1998). Submillisecond kinetics and low efficacy of parallel fibre-Golgi cell synaptic currents in the rat cerebellum. *J Physiol* **510,** 845-866.

DIEUDONNE, S. & DUMOULIN, A. (2000). Serotonin-driven long-range inhibitory connections in the cerebellar cortex. *J Neurosci* **20,** 1837-1848.

DIGREGORIO, D. A., NUSSER, Z. & SILVER, R. A. (2002). Spillover of glutamate onto synaptic AMPA receptors enhances fast transmission at a cerebellar synapse. *Neuron* **35,** 521-533.

DINO, M. R., SCHUERGER, R. J., LIU, Y., SLATER, N. T. & MUGNAINI, E. (2000). Unipolar brush cell: a potential feedforward excitatory interneuron of the cerebellum. *Neuroscience* **98,** 625-636.

DITTMAN, J. S., KREITZER, A. C. & REGEHR, W. G. (2000). Interplay between facilitation, depression, and residual calcium at three presynaptic terminals. *J Neurosci* **20,** 1374-1385.

DUGUID, I. C. & SMART, T. G. (2004). Retrograde activation of presynaptic NMDA receptors enhances GABA release at cerebellar interneuron-Purkinje cell synapses. *Nat Neurosci* **7,** 525-533.

ECCLES, J. C., FABER, D. S., MURPHY, J. T., SABAH, N. H. & TABORIKOVA, H. (1971). Afferent volleys in limb nerves influencing impulse discharges in cerebellar cortex. I. In mossy fibers and granule cells. *Exp Brain Res* **13,** 15-35.

ECCLES, J. C., ITO, M. & SZENTAGOTHAI, J. (1967a). *The Cerebellum as a Neuronal Machine*. Springer-Verlag, Berlin.

ECCLES, J. C., LLINÁS, R. & SASAKI, K. (1966). The mossy fibre-granule cell relay of the cerebellum and its inhibitory control by Golgi cells. *Exp Brain Res* **1,** 82-101.

ECCLES, J. C., SASAKI, K. & STRATA, P. (1967b). Interpretation of the potential fields generated in the cerebellar cortex by a mossy fibre volley. *Experimental Brain Research* **3,** 58-80.

EDGLEY, S. A. & LIDIERTH, M. (1987). The discharges of cerebellar Golgi cells during locomotion in the cat. *J Physiol* **392,** 315-332.

EKEROT, C. F. & JORNTELL, H. (2001). Parallel fibre receptive fields of Purkinje cells and interneurons are climbing fibre-specific. *Eur J Neurosci* **13,** 1303-1310.

EKEROT, C. F. & KANO, M. (1985). Long-term depression of parallel fibre synapses following stimulation of climbing fibres. *Brain Res* **342,** 357-360.

EKEROT, C. F. & OSCARSSON, O. (1981). Prolonged depolarization elicited in Purkinje cell dendrites by climbing fibre impulses in the cat. *J Physiol* **318,** 207-221.

FARRANT, M. & BRICKLEY, S. G. (2003). Properties of GABA(A) receptor-mediated transmission at newly formed Golgi-granule cell synapses in the cerebellum. *Neuropharmacology* **44,** 181-189.

FARRANT, M., FELDMEYER, D., TAKAHASHI, T. & CULL-CANDY, S. G. (1994). NMDA-receptor channel diversity in the developing cerebellum. *Nature* **368,** 335-339.

FATT, P. & KATZ, B. (1951). An analysis of the end-plate potential recorded with an intracellular electrode. *J Physiol* **115,** 320-370.

FERSTER, D. & JAGADEESH, B. (1992). EPSP-IPSP interactions in cat visual cortex studied with in vivo whole-cell patch recording. *J Neurosci* **12,** 1262-1274.

FINCH, E. A. & AUGUSTINE, G. J. (1998). Local calcium signalling by inositol-1,4,5-trisphosphate in Purkinje cell dendrites. *Nature* **396,** 753-756.

FLOURENS, P. (1824). Recherches experimentales sur les proprietes et les fonctions du systeme nerveux dans les animaux vertebres. *Arch Gen Med* **2,** 321-370.

FLUMERFELT, B. A. & HRYCYSHYN, A. W. (1985). Precerebellar nuclei and red nucleus. In *The Rat Nervous System*, vol. 2. ed. PAXINOS, G., pp. 221-250. Academic Press Australia.

FOX, F. A., HILLMAN, D. E., SUGESMUND, K. A. & DUTTA, C. R. (1967). The primate cerebellar cortex: A Golgi and electron microscope study. *Prog Brain Res* **25,** 174-225.

FREUND, T. F. & BUZSAKI, G. (1996). Interneurons of the hippocampus. *Hippocampus* **6,** 347-470.

FRITH, U. (1997). *Autism and Persuasive Developmental Disorders*. Blackwell Publishers Ltd, Oxford.

GABBIANI, F., MIDTGAARD, J. & KNOPFEL, T. (1994). Synaptic integration in a model of cerebellar granule cells. *J Neurophysiol* **72,** 999-1009.

GALL, D., ROUSSEL, C., SUSA, I., D'ANGELO, E., ROSSI, P., BEARZATTO, B., GALAS, M. C., BLUM, D., SCHURMANS, S. & SCHIFFMANN, S. N. (2003). Altered neuronal excitability in cerebellar granule cells of mice lacking calretinin. *J Neurosci* **23,** 9320-9327.

GAO, J.-H., PARSONS, L. M., BOWER, J. M., XIONG, J., LI, J. & FOX, P. T. (1996). Cerebellum implicated in sensory acquisition and discrimination rather than motor control. *Science* **272,** 545-547.

GARWICZ, M., JORNTELL, H. & EKEROT, C.-F. (1998). Cutaneous receptive fields and topography of mossy fibres and climbing fibres projecting to cat cerebellar C3 zone. *J Physiol* **512,** 277-293.

GEBHART, A. L., PETERSEN, S. E. & THACH, W. T. (2002). Role of the posterlateral cerebellum in language. *Ann N Y Acad Sci* **978,** 318-333.

GEIGER, J. R. & JONAS, P. (2000). Dynamic control of presynaptic Ca(2+) inflow by fast-inactivating K(+) channels in hippocampal mossy fiber boutons. *Neuron* **28,** 927-939.

GHELARDUCCI, B., ITO, M. & YAGI, N. (1975). Impulse discharges from flocculus Purkinje cells of alert rabbits during visual stimulation combined with horizontal head rotation. *Brain Res* **87,** 66-72.

GIBSON, W. G., ROBINSON, J. & BENNETT, M. R. (1991). Probabilistic secretion of quanta in the central nervous system: granule cell synaptic control of pattern separation and activity regulation. *Philos Trans R Soc Lond B Biol Sci* **332,** 199-220.

GILBERT, P. F. & THACH, W. T. (1977). Purkinje cell activity during motor learning. *Brain Res* **128,** 309-328.

GONZALEZ, L., SHUMWAY, C., MORISSETTE, J. & BOWER, J. M. (1993). Developmental plasticity in cerebellar tactile maps: fractured maps retain a fractured organization. *J Comp Neurol* **332,** 487-498.

GRANIT, R. & PHILLIPS, C. G. (1956). Excitatory and inhibitory processes acting upon individual Purkinje cells of the cerebellum in cats. *J Physiol* **133,** 520-547.

GRAY, C. M., KONIG, P., ENGEL, A. K. & SINGER, W. (1989). Oscillatory responses in cat visual cortex exhibit inter-columnar synchronization which reflects global stimulus properties. *Nature* **338,** 334-337.

GRUTZENDLER, J., KASTHURI, N. & GAN, W. B. (2002). Long-term dendritic spine stability in the adult cortex. *Nature* **420,** 812-816.

HAHNLOSER, R. H., KOZHEVNIKOV, A. A. & FEE, M. S. (2002). An ultra-sparse code underlies the generation of neural sequences in a songbird. *Nature* **419,** 65-70.

HAMANN, M., ROSSI, D. J. & ATTWELL, D. (2002). Tonic and spillover inhibition of granule cells control information flow through cerebellar cortex. *Neuron* **33,** 625-633.

HAMORI, J. & SOMOGYI, J. (1983). Differentiation of cerebellar mossy fibre synapses in the rat: a quantitative electron microscope study. *J Comp Neurol* **220,** 365-377.

HANSEL, C., LINDEN, D. J. & D'ANGELO, E. (2001). Beyond parallel fiber LTD: the diversity of synaptic and non-synaptic plasticity in the cerebellum. *Nat Neurosci* **4,** 467-475.

HARRIS, K. D., CSICSVARI, J., HIRASE, H., DRAGOI, G. & BUZSAKI, G. (2003). Organization of cell assemblies in the hippocampus. *Nature* **424,** 552-556.

HARRIS, K. D., HIRASE, H., LEINEKUGEL, X., HENZE, D. A. & BUZSAKI, G. (2001). Temporal interaction between single spikes and complex spike bursts in hippocampal pyramidal cells. *Neuron* **32,** 141-149.

HARSCH, A. & ROBINSON, H. P. (2000). Postsynaptic variability of firing in rat cortical neurons: the roles of input synchronization and synaptic NMDA receptor conductance. *J Neurosci* **20,** 6181-6192.

HARTELL, N. A. (1996). Strong activation of parallel fibers produces localized calcium transients and a form of LTD that spreads to distant synapses. *Neuron* **16,** 601-610.

HARTIGAN, P. M. (1985). Computation of the Dip Statistic to Test for Unimodality. *Applied Statistics* **34,** 320-325.

HARTMANN, M. J. & BOWER, J. M. (1998). Oscillatory activity in the cerebellar hemispheres of unrestrained rats. *J Neurophysiol* **80,** 1598-1604.

HARTMANN, M. J. & BOWER, J. M. (2001). Tactile responses in the granule cell layer of cerebellar folium crus IIa of freely behaving rats. *J Neurosci* **21,** 3549-3563.

HARVEY, R. J. & NAPPER, R. M. (1988). Quantitative study of granule and Purkinje cells in the cerebellar cortex of the rat. *J Comp Neurol* **274,** 151-157.

HARVEY, R. J. & NAPPER, R. M. (1991). Quantitative studies on the mammalian cerebellum. *Prog Neurobiol* **36,** 437-463.

HÄUSSER, M. & CLARK, B. A. (1997). Tonic synaptic inhibition modulates neuronal output pattern and spatiotemporal synaptic integration. *Neuron* **19,** 665-678.

HÄUSSER, M., MAJOR, G. & STUART, G. J. (2001). Differential shunting of EPSPs by action potentials. *Science* **291,** 138-141.

HAUSSER, M. & ROTH, A. (1997). Dendritic and somatic glutamate receptor channels in rat cerebellar Purkinje cells. *J Physiol* **501 (Pt 1),** 77-95.

HEBB, D. O. (1949). *The Organisation of Behavior.* Wiley, New York.

HELMCHEN, F., FEE, M. S., TANK, D. W. & DENK, W. (2001). A miniature head-mounted two-photon microscope. high-resolution brain imaging in freely moving animals. *Neuron* **31,** 903-912.

HESSLER, N. A., SHIRKE, A. M. & MALINOW, R. (1993). The probability of transmitter release at a mammalian central synapse. *Nature* **366,** 569-572.

HESSLOW, G., SVENSSON, P. & IVARSSON, M. (1999). Learned movements elicited by direct stimulation of cerebellar mossy fiber afferents. *Neuron* **24,** 179-185.

HILLE, B. (1992). *Ionic Channels of Excitable Membranes*. Sindauer, Sunderland.

HODGKIN, A. L. & HUXLEY, A. F. (1939). Action potentials recorded from inside a nerve fibre. *Nature* **144,** 710-712.

HODGKIN, A. L. & HUXLEY, A. F. (1952). A quantitative description of membrane current and its application to conduction and excitation in nerve. *J Physiol* **117,** 500-544.

HODGKIN, A. L. & KATZ, B. J. (1949). The effect of sodium ions on the electrical activity of the giant axon of the squid. *J Physiol* **108,** 37-77.

HOLMES, G. (1917). The symptoms of acute cerebellar injuries due to gunshot injuries. *Brain* **40,** 461-535.

HOLMES, G. (1939). The cerebellum of man. *Brain* **40,** 1-30.

HOLTZMAN, T., PHUAH, C. & EDGLEY, S. A. (2003). Oscillatory spike trains in the cerebellar cortex; a possible connection with Lugaro cells? Society for Neuroscience Abstracts, Program No. 75.7.

HORE, J., TIMMANN, D. & WATTS, S. (2002). Disorders in timing and force of finger opening in overarm throws made by cerebellar subjects. *Ann N Y Acad Sci* **978,** 1-15.

HOUNSGAARD, J. & MIDTGAARD, J. (1988). Intrinsic determinants of firing pattern in Purkinje cells of the turtle cerebellum in vitro. *J Physiol* **402,** 731-749.

HUANG, C., LIU, G. L., YANG, B. Y., MU, H. & HSIAO, C.-F. (1991). Auditory receptive area in the cerebellar hemisphere is surrounded by somatosensory areas. *Brain Res* **541,** 252-256.

HUBEL, D. H. & WIESEL, T. N. (1959). Receptive fields of single neurones in the cat's striate cortex. *J Physiol* **148,** 574-591.

HUBEL, D. H. & WIESEL, T. N. (1962). Receptive fields, binocular interaction and functional architecture in the cat's visual cortex. *J Physiol* **160,** 106-154.

ISOPE, P. & BARBOUR, B. (2002). Properties of unitary granule cell-->Purkinje cell synapses in adult rat cerebellar slices. *J Neurosci* **22,** 9668-9678.

ITO, M. (1982). Cerebellar control of the vestibulo-ocular reflex--around the flocculus hypothesis. *Annu Rev Neurosci* **5,** 275-296.

ITO, M. (1984). *The cerebellum and neural control.* Raven Press, New York.

ITO, M. (2001). Cerebellar long-term depression: characterization, signal transduction, and functional roles. *Physiol Rev* **81,** 1143-1195.

ITO, M., JASTREBOFF, P. J. & MIYASHITA, Y. (1982). Specific effects of unilateral lesions in the flocculus upon eye movements in albino rabbits. *Exp Brain Res* **45,** 233-242.

JAGADEESH, B., GRAY, C. M. & FERSTER, D. (1992). Visually evoked oscillations of membrane potential in cells of cat visual cortex. *Science* **257,** 552-554.

JAKAB, R. L. & HAMORI, J. (1988). Quantitative morphology and synaptology of cerebellar glomeruli in the rat. *Anat Embryol* **179,** 81-88.

JANSEN, J. & BRODAL, A. (1940). Experimental studies on the intrinsic fibers of the cerebellum. II. The cortico-nuclear projections. *J Comp Neurol* **73,** 267-321.

JOHNSON, J. W. & ASCHER, P. (1990). Voltage-dependent block by intracellular Mg2+ of N-methyl-D-aspartate-activated channels. *Biophys J* **57,** 1085-1090.

JONAS, P. & SAKMANN, B. (1992). Glutamate receptor channels in isolated patches from CA1 and CA3 pyramidal cells of rat hippocampal slices. *J Physiol* **455,** 143-171.

JORNTELL, H. & EKEROT, C. F. (2002). Reciprocal bidirectional plasticity of parallel fiber receptive fields in cerebellar Purkinje cells and their afferent interneurons. *Neuron* **34,** 797-806.

JORNTELL, H. & EKEROT, C. F. (2003a). Mossy fiber synaptic input to cerebellar granule cells in vivo. Society for Neuroscience Abstracts, Program No. 75.14.

JORNTELL, H. & EKEROT, C. F. (2003b). Receptive field plasticity profoundly alters the cutaneous parallel fiber synaptic input to cerebellar interneurons in vivo. *J Neurosci* **23,** 9620-9631.

KANEDA, M., FARRANT, M. & CULL-CANDY, S. G. (1995). Whole-cell and single-channel currents activated by GABA and glycine in granule cells of the rat cerebellum. *J Physiol* **485 (Pt 2),** 419-435.

KANG, D., HAN, J., TALLEY, E. M., BAYLISS, D. A. & KIM, D. (2003). Functional Expression of TASK-1/TASK-3 Heteromers in Cerebellar Granule Cells. *J Physiol.*

KASSEL, J., SHAMBES, G. M. & WELKER, W. (1984). Fractured cutaneous projections to the granule cell layer of the posterior cerebellar hemisphere of the domestic cat. *J Comp Neurol* **225,** 458-468.

KATZ, B. & MILEDI, R. (1965). The Effect of Calcium on Acetylcholine Release from Motor Nerve Terminals. *Proc R Soc Lond B Biol Sci* **161,** 496-503.

KERN, J. K. (2002). The possible role of the cerebellum in autism/PDD: disruption of a multisensory feedback loop. *Med Hypotheses* **59,** 255-260.

KETCHUM, K. L. & HABERLY, L. B. (1993). Membrane currents evoked by afferent fiber stimulation in rat piriform cortex. I. Current source-density analysis. *J Neurophysiol* **69,** 248-260.

KIM, J. H., WANG, J. J. & EBNER, T. J. (1987). Climbing fiber afferent modulation during treadmill locomotion in the cat. *J Neurophysiol* **57,** 787-802.

KLEINFELD, D., SACHDEV, R. N., MERCHANT, L. M., JARVIS, M. R. & EBNER, F. F. (2002). Adaptive filtering of vibrissa input in motor cortex of rat. *Neuron* **34,** 1021-1034.

KONNERTH, A., LLANO, I. & ARMSTRONG, C. M. (1990). Synaptic currents in cerebellar Purkinje cells. *Proc Natl Acad Sci U S A* **87,** 2662-2665.

KRAHE, R. & GABBIANI, F. (2004). Burst firing in sensory systems. *Nat Rev Neurosci* **5,** 13-23.

KREITZER, A. C. & REGEHR, W. G. (2001). Retrograde inhibition of presynaptic calcium influx by endogenous cannabinoids at excitatory synapses onto Purkinje cells. *Neuron* **29,** 717-727.

LAMPL, I., REICHOVA, I. & FERSTER, D. (1999). Synchronous membrane potential fluctuations in neurons of the cat visual cortex. *Neuron* **22,** 361-374.

LARKUM, M. E. & ZHU, J. J. (2002). Signaling of layer 1 and whisker-evoked Ca2+ and Na+ action potentials in distal and terminal dendrites of rat neocortical pyramidal neurons in vitro and in vivo. *J Neurosci* **22,** 6991-7005.

LAUGHLIN, S. B. (2001). Energy as a constraint on the coding and processing of sensory information. *Curr Opin Neurobiol* **4,** 475-480.

LAUGHLIN, S. B., DE RUYTER VAN STEVENINCK, R. R. & ANDERSON, J. C. (1998). The metabolic cost of neural information. *Nat Neurosci* **1,** 36-41.

LAVOND, D. G. & STEINMETZ, J. E. (1989). Acquisition of classical conditioning without cerebellar cortex. *Behav Brain Res* **33,** 113-164.

LAVOND, D. G., STEINMETZ, J. E., YOKAITIS, M. H. & THOMPSON, R. F. (1987). Reacquisition of classical conditioning after removal of cerebellar cortex. *Exp Brain Res* **67,** 569-593.

LECHNER, H. A., BAXTER, D. A., CLARK, J. W. & BYRNE, J. H. (1996). Bistability and its regulation by serotonin in the endogenously bursting neuron R15 in Aplysia. *J Neurophysiol* **75,** 957-962.

LEGER, J. F., STERN, E. A., AERTSEN, A. & HECK, D. (2004). Synaptic Integration in Rat Frontal Cortex Shaped by Network Activity. *J Neurophysiol.*

LEV-RAM, V., WONG, S. T., STORM, D. R. & TSIEN, R. Y. (2002). A new form of cerebellar long-term potentiation is postsynaptic and depends on nitric oxide but not cAMP. *Proc Natl Acad Sci U S A* **99,** 8389-8393.

LISBERGER, S. G. (1994). Neural basis for motor learning in the vestibuloocular reflex of primates. III. Computational and behavioral analysis of the sites of learning. *J Neurophysiol* **72,** 974-998.

LISMAN, J. E. (1997). Bursts as a unit of neural information: making unreliable synapses reliable. *Trends Neurosci* **20,** 38-43.

LLINAS, R. (1982). General discussion: radial connectivity in the cerebellar cortex: a novel view regarding the functional organisation of the molecular layer. In *The Cerebellum: New Vistas (Exp. Brain Res. Suppl. Vol 6)*. ed. PALAY, S. L. & CHAN-PALAY, V., pp. 189-194. Springer-Verlag, New York.

LLINAS, R. & SUGIMORI, M. (1980a). Calcium conductances in Purkinje cell dendrites: their role in development and integration. *Prog Brain Res* **51,** 323-334.

LLINAS, R. & SUGIMORI, M. (1980b). Electrophysiological properties of in vitro Purkinje cell dendrites in mammalian cerebellar slices. *J Physiol* **305,** 197-213.

LLINAS, R. & SUGIMORI, M. (1980c). Electrophysiological properties of in vitro Purkinje cell somata in mammalian cerebellar slices. *J Physiol* **305,** 171-195.

LLINAS, R. & WALTON, K. D. (1998). Cerebellum. In *The Synaptic Organisation of the Brain*. ed. SHEPHERD, G. M., pp. 255-288. Oxford University Press.

LOEWENSTEIN, Y., SOMPOLINSKY, H. & YAROM, Y. (2001). Complex spikes can toggle simple spikes bursting activity in cerebellar Purkinje cells, Program No. 294.4, Society for Neuroscience Abstracts.

LOU, J. S. & BLOEDEL, J. R. (1992). Responses of sagittally aligned Purkinje cells during perturbed locomotion: synchronous activation of climbing fiber inputs. *J Neurophysiol* **68,** 570-580.

MACDERMOTT, A. B., MAYER, M. L., WESTBROOK, G. L., SMITH, S. J. & BARKER, J. L. (1986). NMDA-receptor activation increases cytoplasmic calcium concentration in cultured spinal cord neurones. *Nature* **321,** 519-522.

MAEX, R. & SCHUTTER, E. D. (1998). Synchronization of golgi and granule cell firing in a detailed network model of the cerebellar granule cell layer. *J Neurophysiol* **80,** 2521-2537.

MAHON, S., DENIAU, J. M. & CHARPIER, S. (2001). Relationship between EEG potentials and intracellular activity of striatal and cortico-striatal neurons: an in vivo study under different anesthetics. *Cereb Cortex* **11,** 360-373.

MARGRIE, T. W., BRECHT, M. & SAKMANN, B. (2002). In vivo, low-resistance, whole-cell recordings from neurons in the anaesthetized and awake mammalian brain. *Pflügers Arch* **444,** 491-498.

MARGRIE, T. W., MEYER, A. H., CAPUTI, A., MONYER, H., HASAN, M. T., SCHAEFER, A. T., DENK, W. & BRECHT, M. (2003). Targeted whole-cell recordings in the mammalian brain in vivo. *Neuron* **39,** 911-918.

MARKRAM, H., LUBKE, J., FROTSCHER, M. & SAKMANN, B. (1997). Regulation of synaptic efficacy by coincidence of postsynaptic APs and EPSPs. *Science* **275,** 213-215.

MARR, D. (1969). A theory of cerebellar cortex. *J Physiol* **202,** 437-470.

MAYER, M. L., WESTBROOK, G. L. & GUTHRIE, P. B. (1984). Voltage-dependent block by Mg2+ of NMDA responses in spinal cord neurones. *Nature* **309,** 261-263.

MCCORMICK, D. A., GUYER, P. E. & THOMPSON, R. F. (1982). Superior cerebellar peduncle lesions selectively abolish the ipsilateral classically conditioned nictitating membrane/eyelid response of the rabbit. *Brain Res* **244,** 347-350.

MCDEVITT, C. J., EBNER, T. J. & BLOEDEL, J. R. (1982). The changes in Purkinje cell simple spike activity following spontaneous climbing fiber inputs. *Brain Res* **237,** 484-491.

MIDDLETON, F. A. & STRICK, P. L. (1994). Anatomical evidence for cerebellar and basal ganglia involvement in higher cognitive function. *Science* **266,** 458-461.

MIDDLETON, F. A. & STRICK, P. L. (2001). Cerebellar projections to the prefrontal cortex of the primate. *J Neurosci* **21,** 700-712.

MIDTGAARD, J. (1992). Membrane properties and synaptic responses of Golgi cells and stellate cells in the turtle cerebellum in vitro. *J Physiol* **457,** 329-354.

MILES, F. A. & LISBERGER, S. G. (1981). Plasticity in the vestibulo-ocular reflex: a new hypothesis. *Annu Rev Neurosci* **4,** 273-299.

MILLAR, J. A., BARRATT, L., SOUTHAN, A. P., PAGE, K. M., FYFFE, R. E., ROBERTSON, B. & MATHIE, A. (2000). A functional role for the two-pore domain potassium channel TASK-1 in cerebellar granule neurons. *Proc Natl Acad Sci U S A* **97,** 3614-3618.

MITCHELL, S. J. & SILVER, R. A. (2003). Shunting inhibition modulates neuronal gain during synaptic excitation. *Neuron* **38,** 433-445.

MITTMANN, W. M. O., KOCH, U. & HAUSSER, M. (2004). Feed-forward inhibition shapes the spike output of cerebellar Purkinje cells. *J Physiol* **in press**.

MORISSETTE, J. & BOWER, J. M. (1996). Contribution of somatosensory cortex to responses in the rat cerebellar granule cell layer following peripheral tactile stimulation. *Experimental Brain Research* **109,** 240-250.

MURPHY, J. T. & SABAH, N. H. (1970). Spontaneous firing of cerebellar Purkinje cells in decerebrate and barbiturate anesthetized cats. *Brain Res* **17,** 515-519.

NAPPER, R. M. & HARVEY, R. J. (1988). Number of parallel fiber synapses on an individual Purkinje cell in the cerebellum of the rat. *J Comp Neurol* **274,** 168-177.

NEHER, E. (1992). Correction for liquid junction potentials in patch clamp experiments. *Methods Enzymol* **207,** 123-131.

NEHER, E. & SAKMANN, B. (1975). Voltage-dependence of drug-induced conductance in frog neuromuscular junction. *Proc Natl Acad Sci U S A* **72,** 2140-2144.

NEHER, E. & SAKMANN, B. (1992). The patch clamp technique. *Sci Am* **266,** 28-35.

NEIMARK, M. A., ANDERMANN, M. L., HOPFIELD, J. J. & MOORE, C. I. (2003). Vibrissa resonance as a transduction mechanism for tactile encoding. *J Neurosci* **23,** 6499-6509.

NIELSEN, T. A., DIGREGORIO, D. A. & SILVER, R. A. (2004). Modulation of glutamate mobility reveals the mechanism underlying slow-rising AMPAR EPSCs and the diffusion coefficient in the synaptic cleft. *Neuron* **42,** 757-771.

NITZ, D. & TONONI, G. (2002). Tonic rhythmic activity of rat cerebellar neurons. *Exp Brain Res* **146,** 265-270.

O'KEEFE, J. & RECCE, M. L. (1993). Phase relationship between hippocampal place units and the EEG theta rhythm. *Hippocampus* **3,** 317-330.

O'KUSKY, J. & COLONNIER, M. (1982). A laminar analysis of the number of neurons, glia, and synapses in the adult cortex (area 17) of adult macaque monkeys. *J Comp Neurol* **210,** 278-290.

OHYAMA, T., NORES, W. L. & MAUK, M. D. (2003a). Stimulus generalization of conditioned eyelid responses produced without cerebellar cortex: implications for plasticity in the cerebellar nuclei. *Learn Mem* **10,** 346-354.

OHYAMA, T., NORES, W. L., MURPHY, M. & MAUK, M. D. (2003b). What the cerebellum computes. *Trends Neurosci* **26,** 222-227.

PALAY, S. L. & CHAN-PALAY, V. (1974). *Cerebellar Cortex - Cytology and Organization.* Springer, Berlin.

PALAY, S. L. & PALADE, G. E. (1955). The fine structure of neurons. *J Biophys Biochem Cytol* **1,** 69-88.

PALKOVITS, M., MEZEY, E., HAMORI, J. & SZENTAGOTHAI, J. (1977). Quantitative histological analysis of the cerebellar nuclei in the cat. I. Numerical data on cells and on synapses. *Exp Brain Res* **28,** 189-209.

PEI, X., VOLGUSHEV, M., VIDYASAGAR, T. R. & CREUTZFELDT, O. D. (1991). Whole cell recording and conductance measurements in cat visual cortex in-vivo. *Neuroreport* **2,** 485-488.

PERKEL, D. J., HESTRIN, S., SAH, P. & NICOLL, R. A. (1990). Excitatory synaptic currents in Purkinje cells. *Proc R Soc Lond B Biol Sci* **241,** 116-121.

PETERSEN, C. C., HAHN, T. T., MEHTA, M., GRINVALD, A. & SAKMANN, B. (2003). Interaction of sensory responses with spontaneous depolarization in layer 2/3 barrel cortex. *Proc Natl Acad Sci U S A* **100,** 13638-13643.

POIRAZI, P., BRANNON, T. & MEL, B. W. (2003a). Arithmetic of subthreshold synaptic summation in a model CA1 pyramidal cell. *Neuron* **37,** 977-987.

POIRAZI, P., BRANNON, T. & MEL, B. W. (2003b). Pyramidal neuron as two-layer neural network. *Neuron* **37,** 989-999.

POLSKY, A., MEL, B. W. & SCHILLER, J. (2004). Computational subunits in thin dendrites of pyramidal cells. *Nat Neurosci* **7,** 621-627.

POWELL, T. P. & MOUNTCASTLE, V. B. (1959). Some aspects of the functional organization of the cortex of the postcentral gyrus of the monkey: a correlation of findings obtained in a single unit analysis with cytoarchitecture. *Bull Johns Hopkins Hosp* **105,** 133-162.

RALL, W. (1962). Theory of physiological properties of dendrites. *Ann N Y Acad Sci* **96,** 1071-1092.

RAMACHANDRAN, R. & LISBERGER, S. G. (2005). Normal performance and expression of learning in the vestibulo-ocular reflex (VOR) at high frequencies. *J Neurophysiol* **93,** 2028-2038.

RAMAN, I. M. & BEAN, B. P. (1997). Resurgent sodium current and action potential formation in dissociated cerebellar Purkinje neurons. *J Neurosci* **17,** 4517-4526.

RAMÓN Y CAJAL, S. (1888). Estructura de los centros nerviosos de los aves. *Rev. Trimestr. Histol. Normal Patol.* **1,** 305-315.

RAMÓN Y CAJAL, S. (1904). *La Textura del Sistema Nerviosa del Hombre y los Vertebrados*. Moya, Madrid.

RANCZ, E. A. & HAUSSER, M. (2004). Dendritic calcium spikes trigger short- and long-term plasticity in cerebellar Purkinje cells. Society for Neuroscience Abstracts, Program No. 856.9.

RAPP, M., SEGEV, I. & YAROM, Y. (1994). Physiology, morphology and detailed passive models of guinea-pig cerebellar Purkinje cells. *J Physiol* **474,** 101-118.

RAUSCHECKER, J. P. (1991). Mechanisms of visual plasticity: Hebb synapses, NMDA receptors, and beyond. *Physiol Rev* **71,** 587-615.

RAWSON, J. A. & TILOKSKULCHAI, K. (1981). Repetitive firing of cerebellar Purkinje cells in response to impulse in climbing fibre afferents. *Neurosci Lett* **25,** 131-135.

REDIES, H., SIEBEN, U. & CREUTZFELDT, O. D. (1989). Functional subdivisions in the auditory cortex of the guinea pig. *J Comp Neurol* **282,** 473-488.

REGEHR, W. G. & STEVENS, C. S. (2001). Physiology of Synaptic Transmission and Short-Term Plasticity. In *Synapses*. ed. COWAN, W. M., SUDHOF, T. C. & STEVENS, C. S., pp. 135-176. John Hopkins University Press, Baltimore.

RIEHLE, A., GRUN, S., DIESMANN, M. & AERTSEN, A. (1997). Spike synchronization and rate modulation differentially involved in motor cortical function. *Science* **278,** 1950-1953.

RIEKE, F., WARLAND, D., DE RUYTER VAN STEVENINCK, R. & BIALEK, W. (1997). *Spikes: Exploring the neural code*. MIT Press, Cambridge.

ROGERS, J. H. & RESIBOIS, A. (1992). Calretinin and calbindin-D28k in rat brain: patterns of partial co-localization. *Neuroscience* **51,** 843-865.

ROLANDO, L. (1809). *Saggio Sopra la Vera Structtura Del Cervello Dell'uomo e Degli Animali Sopra le Funzioni del Sistema Nervoso*. Stamperia di S. S. R. M. Privilegiata, Sassari.

ROSSI, D. J., ALFORD, S., MUGNAINI, E. & SLATER, N. T. (1995). Properties of transmission at a giant glutamatergic synapse in cerebellum: the mossy fiber-unipolar brush cell synapse. *J Neurophysiol* **74,** 24-42.

ROSSI, D. J., HAMANN, M. & ATTWELL, D. (2003a). Multiple modes of GABAergic inhibition of rat cerebellar granule cells. *J Physiol* **548,** 97-110.

ROSSI, P., ROGGERI, L., PODDA, M. & D'ANGELO, E. (2003b). Persistent depression of inward rectifier currents following GABA-B receptor stimulation in cerebellar granule cells. Society for Neuroscience Abstracts, Program No. 53.5.

ROWLAND, N. C. & JAEGER, D. (2003). Somatosensory responses of neurons in deep cerebellar nuclei in ketamine-anesthetised rats show distinct temporal profiles but do not represent sensory stimulus parameters. Program No. 75.10 Society for Neuroscience Abstracts.

SABATINI, B. L. & SVOBODA, K. (2000). Analysis of calcium channels in single spines using optical fluctuation analysis. *Nature* **408,** 589-593.

SAKMANN, B. & NEHER, E. (1983). Geometric parameters of pipettes and membrane patches. In *Single channel recording*. ed. SAKMANN, B. & NEHER, E. Plenum Press, New York.

SARGENT, P. B., NIELSEN, T., DIGREGORIO, D. A. & SILVER, R. A. (2003). Time course of uniquantal release at the cerebellar mossy fiber-granule cell synapse. Society for Neuroscience Abstracts, Program No. 686.12.

SCHILLER, J., MAJOR, G., KOESTER, H. J. & SCHILLER, Y. (2000). NMDA spikes in basal dendrites of cortical pyramidal neurons. *Nature* **404,** 285-289.

SCHUETT, S., BONHOEFFER, T. & HUBENER, M. (2002). Mapping retinotopic structure in mouse visual cortex with optical imaging. *J Neurosci* **22,** 6549-6559.

SCHWEIGHOFER, N., DOYA, K. & LAY, F. (2001). Unsupervised learning of granule cell sparse codes enhances cerebellar adaptive control. *Neuroscience* **103,** 35-50.

SEMYANOV, A., WALKER, M. C., KULLMANN, D. M. & SILVER, R. A. (2004). Tonically active GABA A receptors: modulating gain and maintaining the tone. *Trends Neurosci* **27,** 262-269.

SEUTIN, V., SCUVEE-MOREAU, J. & DRESSE, A. (1997). Evidence for a non-GABAergic action of quaternary salts of bicuculline on dopaminergic neurones. *Neuropharmacology* **36,** 1653-1657.

SHADLEN, M. N. & NEWSOME, W. T. (1994). Noise, neural codes and cortical organization. *Curr Opin Neurobiol* **4,** 569-579.

SHADLEN, M. N. & NEWSOME, W. T. (1998). The variable discharge of cortical neurons: implications for connectivity, computation, and information coding. *J Neurosci* **18,** 3870-3896.

SHAMBES, G. M., BEERMANN, D. H. & WELKER, W. (1978a). Multiple tactile areas in cerebellar cortex: another patchy cutaneous projection to granule cell columns in rats. *Brain Res* **157,** 123-128.

SHAMBES, G. M., GIBSON, J. M. & WELKER, W. (1978b). Fractured somatotopy in granule cell tactile areas of rat cerebellar hemispheres revealed by micromapping. *Brain Behav Evol* **15,** 94-140.

SHEPHERD, G. M. & COREY, D. P. (1992). Sensational science. Sensory Transduction: 45th Annual Symposium of the Society of General Physiologists, Marine Biological Laboratory, Woods Hole, MA, USA, September 5-8, 1991. *New Biol* **4,** 48-52.

SHOHAM, S. & NAGARAN, S. (2004). Chapter 2.4: The theory of nervous system recording. In *Neuroprosthetics: Theory and Practice*, vol. 2. ed. HORCH, K. W. & DHILLON, G. World Scientific Publishing Co Inc.

SHU, Y., HASENSTAUB, A., BADOUAL, M., BAL, T. & MCCORMICK, D. A. (2003). Barrages of synaptic activity control the gain and sensitivity of cortical neurons. *J Neurosci* **23,** 10388-10401.

SILVER, R. A., TRAYNELIS, S. F. & CULL-CANDY, S. G. (1992). Rapid-time-course miniature and evoked excitatory currents at cerebellar synapses in situ. *Nature* **355,** 163-166.

SIMONS, D. J. & WOOLSEY, T. A. (1979). Functional organization in mouse barrel cortex. *Brain Res* **165,** 327-332.

SIMPSON, J. I. & ALLEY, K. E. (1974). Visual climbing fiber input to rabbit vestibulo-cerebellum: a source of direction-specific information. *Brain Res* **82,** 302-308.

SINGER, W. (1999). Neuronal synchrony: a versatile code for the definition of relations? *Neuron* **24,** 49-65, 111-125.

SINGER, W. & GRAY, C. M. (1995). Visual feature integration and the temporal correlation hypothesis. *Annu Rev Neurosci* **18,** 555-586.

SMITH, S. M., BERGSMAN, J. B., HARATA, N. C., SCHELLER, R. H. & TSIEN, R. W. (2004). Recordings from single neocortical nerve terminals reveal a nonselective cation channel activated by decreases in extracellular calcium. *Neuron* **41,** 243-256.

SOLA, E., PRESTORI, F., ROSSI, P., TAGLIETTI, V. & D'ANGELO, E. (2004). Increased Neurotransmitter Release During Long-Term Potentiation at Mossy Fibre-Granule Cell Synapses in Rat Cerebellum. *J Physiol.*

SOUTHAN, A. P., MORRIS, N. P., STEPHENS, G. J. & ROBERTSON, B. (2000). Hyperpolarization-activated currents in presynaptic terminals of mouse cerebellar basket cells. *J Physiol* **526 Pt 1,** 91-97.

SOUTHAN, A. P. & ROBERTSON, B. (1998). Patch-clamp recordings from cerebellar basket cell bodies and their presynaptic terminals reveal an asymmetric distribution of voltage-gated potassium channels. *J Neurosci* **18,** 948-955.

STEINMETZ, P. N., ROY, A., FITZGERALD, P. J., HSIAO, S. S., JOHNSON, K. O. & NIEBUR, E. (2000). Attention modulates synchronized neuronal firing in primate somatosensory cortex. *Nature* **404,** 187-190.

STELL, B. M., BRICKLEY, S. G., TANG, C. Y., FARRANT, M. & MODY, I. (2003). Neuroactive steroids reduce neuronal excitability by selectively enhancing tonic inhibition mediated by delta subunit-containing GABAA receptors. *Proc Natl Acad Sci U S A* **100,** 14439-14444.

STOSIEK, C., GARASCHUK, O., HOLTHOFF, K. & KONNERTH, A. (2003). In vivo two-photon calcium imaging of neuronal networks. *Proc Natl Acad Sci U S A* **100,** 7319-7324.

STUART, G. & HAUSSER, M. (1994). Initiation and spread of sodium action potentials in cerebellar Purkinje cells. *Neuron* **13,** 703-712.

STUART, G. J. & SAKMANN, B. (1994). Active propagation of somatic action potentials into neocortical pyramidal cell dendrites. *Nature* **367,** 69-72.

SUKIN, D., SKEDROS, D. G., BEALES, M., STRATTON, S. E., LORDEN, J. F. & OLTMANS, G. A. (1987). Temporal sequence of motor disturbances and increased cerebellar glutamic acid decarboxylase activity following 3-acetylpyridine lesions in adult rats. *Brain Res* **426,** 82-92.

SUZUKI, S. & ROGAWSKI, M. A. (1989). T-type calcium channels mediate the transition between tonic and phasic firing in thalamic neurons. *Proc Natl Acad Sci U S A* **86,** 7228-7232.

TAKECHI, H., EILERS, J. & KONNERTH, A. (1998). A new class of synaptic response involving calcium release in dendritic spines. *Nature* **396,** 757-760.

THACH, W. T. (1968). Discharge of Purkinje and cerebellar nuclear neurons during rapidly alternating arm movements in the monkey. *J Neurophysiol* **31,** 785-797.

THOMSON, A. M., WEST, D. C. & LODGE, D. (1985). An N-methylaspartate receptor-mediated synapse in rat cerebral cortex: a site of action of ketamine? *Nature* **313,** 479-481.

TRACHTENBERG, J. T., CHEN, B. E., KNOTT, G. W., FENG, G., SANES, J. R., WELKER, E. & SVOBODA, K. (2002). Long-term in vivo imaging of experience-dependent synaptic plasticity in adult cortex. *Nature* **420,** 788-794.

TRAYNELIS, S. F., SILVER, R. A. & CULL-CANDY, S. G. (1993). Estimated conductance of glutamate receptor channels activated during EPSCs at the cerebellar mossy fiber-granule cell synapse. *Neuron* **11,** 279-289.

TYRRELL, T. & WILLSHAW, D. (1992). Cerebellar cortex: its simulation and the relevance of Marr's theory. *Philos Trans R Soc Lond B Biol Sci* **336,** 239-257.

VAN KAN, P. L., GIBSON, A. R. & HOUK, J. C. (1993). Movement-related inputs to intermediate cerebellum of the monkey. *J Neurophysiol* **69,** 74-94.

VOLNY-LURAGHI, A., MAEX, R., VOSDAGGER, B. & DE SCHUTTER, E. (2002). Peripheral stimuli excite coronal beams of Golgi cells in rat cerebellar cortex. *Neuroscience* **113,** 363-373.

VOOGD, J. & GLICKSTEIN, M. (1998). The anatomy of the cerebellum. *Trends Neurosci* **21,** 370-375.

VOS, B. P., VOLNY-LURAGHI, A., MAEX, R. & DE SCHUTTER, E. (2000). Precise spike timing of tactile-evoked cerebellar Golgi cell responses: a reflection of combined mossy fiber and parallel fiber activation? *Prog Brain Res* **124,** 95-106.

WALL, M. J. (2003). Endogenous nitric oxide modulates GABAergic transmission to granule cells in adult rat cerebellum. *Eur J Neurosci* **18,** 869-878.

WALL, M. J. & USOWICZ, M. M. (1997). Development of action potential-dependent and independent spontaneous GABAA receptor-mediated currents in granule cells of postnatal rat cerebellum. *Eur J Neurosci* **9,** 533-548.

WALLNER, M., HANCHAR, H. J. & OLSEN, R. W. (2003). Ethanol enhances alpha 4 beta 3 delta and alpha 6 beta 3 delta gamma-aminobutyric acid type A receptors at low concentrations known to affect humans. *Proc Natl Acad Sci U S A* **100,** 15218-15223.

WANG, S. S., DENK, W. & HÄUSSER, M. (2000). Coincidence detection in single dendritic spines mediated by calcium release. *Nat Neurosci* **3,** 1266-1273.

WATERS, J., LARKUM, M., SAKMANN, B. & HELMCHEN, F. (2003). Supralinear Ca2+ influx into dendritic tufts of layer 2/3 neocortical pyramidal neurons in vitro and in vivo. *J Neurosci* **23,** 8558-8567.

WEHR, M. & ZADOR, A. M. (2003). Balanced inhibition underlies tuning and sharpens spike timing in auditory cortex. *Nature* **426,** 442-446.

WELKER, C. (1976). Receptive fields of barrels in the somatosensory neocortex of the rat. *J Comp Neurol* **166,** 173-189.

WELKER, W., BLAIR, C. & SHAMBES, G. M. (1988). Somatosensory projections of cerebellar granule cell layer of giant bushbaby, Galago crassicaudatus. *Brain Behav Evol* **31,** 150-160.

WILLIAMS, S. R., CHRISTENSEN, S. R., STUART, G. J. & HAUSSER, M. (2002). Membrane potential bistability is controlled by the hyperpolarization-activated current I(H) in rat cerebellar Purkinje neurons in vitro. *J Physiol* **539,** 469-483.

WILSON, M. A. & MCNAUGHTON, B. L. (1993). Dynamics of the hippocampal ensemble code for space. *Science* **261,** 1055-1058.

WOODIN, M. A., GANGULY, K. & POO, M. M. (2003). Coincident pre- and postsynaptic activity modifies GABAergic synapses by postsynaptic changes in Cl- transporter activity. *Neuron* **39,** 807-820.

WOOLSEY, T. A. & VAN DER LOOS, H. (1970). The structural organization of layer IV in the somatosensory region (SI) of mouse cerebral cortex. The description of a cortical field composed of discrete cytoarchitectonic units. *Brain Res* **17,** 205-242.

XU-FRIEDMAN, M. A. & REGEHR, W. G. (2003). Ultrastructural contributions to desensitization at cerebellar mossy fiber to granule cell synapses. *J Neurosci* **23,** 2182-2192.

YASUDA, R., SABATINI, B. L. & SVOBODA, K. (2003). Plasticity of calcium channels in dendritic spines. *Nat Neurosci* **6,** 948-955.